

General Disclaimer

One or more of the Following Statements may affect this Document

- This document has been reproduced from the best copy furnished by the organizational source. It is being released in the interest of making available as much information as possible.
- This document may contain data, which exceeds the sheet parameters. It was furnished in this condition by the organizational source and is the best copy available.
- This document may contain tone-on-tone or color graphs, charts and/or pictures, which have been reproduced in black and white.
- This document is paginated as submitted by the original source.
- Portions of this document are not fully legible due to the historical nature of some of the material. However, it is the best reproduction available from the original submission.



Technical Memorandum 85038

Experiments Using Atmospheric Forcing From a FGGE Analysis to Drive an Upper Ocean Model

Alejandro Camerlengo

June 1983

Laboratory for Atmospheric Sciences
Global Modeling and Simulation Branch

National Aeronautics and
Space Administration

Goddard Space Flight Center
Greenbelt, Maryland 20771



(NASA-TM-85038) EXPERIMENTS USING
ATMOSPHERIC FORCING FROM A FGGE ANALYSIS TO
DRIVE AN UPPER OCEAN MODEL (NASA) 88 p
HC A05/MF A01

CSC 03B

N83-29156

Unclas
G3/91 28021

TECH. MEMO 85038

Experiments Using Atmospheric Forcing From A FGGE Analysis
to Drive an Upper Ocean Model

Alejandro Camerlengo
M/A Com Sigma Data Inc.
Laboratory for Atmospheric Sciences
NASA/Goddard Space Flight Center
Greenbelt, Md. 20771

June 1983

Table of Contents

Acknowledgements	11
1. Introduction	1
2. The ocean model and atmospheric analysis	3
3. Description of the experiments	4
4. Results	21
5. Conclusions	76
Appendix	77
Figure Captions:	78
References	82

ACKNOWLEDGEMENTS

I would like express my appreciation to Dr. Eugenia Kalnay, who originally suggested this study and whose support is gratefully acknowledged. I have benefitted from helpful discussions with Paul Schopf. Steve Stalos provided me with the ocean model code, and J. Susskind with averaged January and February 1979 sea surface temperature fields.

The manuscript was prepared by M. A. Wells and J. Wentz and edited by C. Lipsey. The figures were expertly drafted by L. Rumburg.

1. Introduction

In this study we present results of a series of numerical experiments in which an upper ocean model is driven by surface heat fluxes and stress fields derived from the FGGE SOP-1 GLAS analysis/forecast system (Halem et al., 1982).

The ocean model is essentially an oceanic boundary layer coupled with a dynamic model of the upper ocean currents (Schopf and Cane, 1983). The oceanic boundary layer can be viewed as an intermediary zone between the deep ocean circulation and the atmosphere, extending from the surface to a depth of about 10-150 meters. In this layer both the temperature and the salinity fields are almost constant in the vertical. This vertical constancy is due to mixing which is caused by turbulence. The turbulence is in turn caused by breaking waves, shear instabilities, etc.

The aim of this study is to seek a better understanding of the model ocean boundary layer response to various forms of atmospheric forcings and the associated time and space scales involved. It is known that the time scales of the atmospheric flow are smaller than those of the oceanic flow even for an upper ocean model like ours. On the other hand, the space scales for the baroclinic motion in the ocean are considerably less than in the atmosphere. The grid being used is of 4° by 5° of latitude and longitude, respectively and was chosen to coincide with that of the atmospheric analysis. However, an accurate description of the oceanic synoptic scales requires a much finer horizontal resolution, on the order of 10-50 kilometers. The coarseness of the grid is very significant limitation of our experiments.

Although the distributions of atmospheric wind forcings are very similar in summer and in winter, their intensity is greater in winter (Elsberry and Camp, 1978; Elsberry and Raney, 1978). The source of mechanical energy is

proportional to u_x^3 . Thus, during the passage of a winter storm, there is an upward heat flux and the mechanical mixing is enhanced by the strengthening of the wind forcing. As a result of the upward heat flux, the bottom of the mixed layer deepens. After the storm's passage, the cooling effect continues, due to entrainment. In summer, the winds are weaker. Consequently, the entrainment at the base of the oceanic boundary layer is almost nonexistent. As a direct consequence of the stabilizing effect of the surface heating, the oceanic boundary layer becomes shallower. (Elsberry and Camp, 1978; Elsberry and Raney, 1978).

One of the problems faced in this kind of study is the initialization of the ocean model. A solution may be available in the near future: according to Levoy (1981), it is expected that global SST distributions with higher resolution will be possible to get from satellite radiances. Also, accurate estimates of the surface wind field may be obtained using data from the radar Scatterometer (O'Brien, 1981). However, in the present study somewhat arbitrary initial conditions are used for the mixed layer depth and deep temperature fields. The initial currents were assumed to be zero and the initial SST's were obtained from the GLAS/temperature retrieval system for January 1979 (Susskind et al., 1982). It is very possible that the results may have been dependent on such a choice.

Another characteristic of these experiments is that we have used a one-way coupling mechanism, in which the atmospheric parameters derived from the GLAS analysis/forecast system were used to drive the ocean model. It should be noted that the atmospheric analysis was performed assuming climatological SST's, and that the coupling did not allow any feedback from the ocean model's predicted SST to the atmosphere. The lack of feedback may also be a serious deficiency of our experiments.

2. The ocean model and atmospheric analysis

The mixed-layer ocean model used in this study is the one developed by Schopf and Cane (1983). Following Kasahara (1974), the model equations of momentum, temperature, continuity and the hydrostatic relation are as follows:

$$\frac{\partial(hV)}{\partial t} + \nabla \cdot (\tilde{V}hV) + \frac{\partial(w_e V)}{\partial s} - [f + u/a \tan \theta] \tilde{k} \times hV = -h \{Vp + b \nabla z\} + \frac{\partial \tau}{\partial s} + h F_H(V), \quad (1)$$

$$\frac{\partial(hT)}{\partial t} + \nabla \cdot (\tilde{V}hT) + \frac{\partial(w_e T)}{\partial s} = -\frac{\partial Q}{\partial s} - \frac{\partial D_V}{\partial s} + h D_H(T) \quad (2)$$

$$\frac{\partial h}{\partial t} + \nabla \cdot (\tilde{V}h) + \frac{\partial w_e}{\partial s} = 0 \quad (3)$$

$$\frac{\partial P}{\partial s} = bh. \quad (4)$$

where s is a generalized vertical coordinate. The bouyancy, b , is calculated via a linear expression:

$$b = b(T) = g\alpha(T - T_r). \quad (5)$$

Following Niiler and Krauss (1977) and Kim (1976) the equation of entrainment, w_e , needed to close the system is:

$$w_e H(w_e) \{h_1(b_1 - b_e) + q^2 - m_e |\Delta V|^2\} = 2 m_s u_x^3 - 2 \epsilon_0 h_1 + h_1 B_0 [1 - m_b H(B_0)] + B_1(h). \quad (6)$$

For a more detailed explanation about the model and the symbolism being used, the reader is referred to the original paper (Schopf and Cane, 1983).

In these experiments the model has been used in a global configuration with a resolution of 4° of latitude by 5° of longitude. While no slip conditions are used at the coastal boundaries, no flux of temperature is allowed through these same boundaries. The time step used is of three hours.

Because salinity is not predicted in the model, and in order to avoid complications associated with ice generation, artificial boundaries have been arbitrarily placed at $70^\circ N$ and $58^\circ S$.

3. Description of the experiments

The parameters that drive the ocean model are: the surface heat budget, the wind stress and the friction velocity. The components of the surface heat budget include the latent and sensible heat fluxes and the incoming and outgoing radiative fluxes. Thus, the surface heat balance, Q , is computed as:

$$Q = (S_w - X_w - E_v - S_H)/\rho \quad (7)$$

where S_w , X_w , E_v and S_H represent the solar radiation at ground level, the long wave radiation at ground level, the latent heat, and the sensible heat flux, respectively. A reference sea density is represented by ρ .

The surface wind stress, τ , is computed as in the atmospheric model while the friction velocity, u_x , is calculated as usual (Sommerville et al., 1974).

Both Q , u_x and τ from the 6 hour cycle global analysis produced by the GLAS analysis/forecast system (Halem et al., 1982).

The geopotential height, horizontal wind, and relative humidity are analyzed at mandatory pressure levels in the GLAS objective analysis scheme (Baker, 1983). The 6-hour model forecast supplies a first-guess for the above fields at 300 mb and sea level. The assimilation/forecast model is a fourth-order global atmospheric model which is based on an energy-conserving scheme with all horizontal differences computed with fourth-order accuracy (Kalnay-Rivas et al., 1977; Kalnay-Rivas and Hoitsma, 1979).

Five experiments to study the result of using the FGGE GLAS analysis/forecast system to drive (without feedback) a global upper ocean model, were performed for the period 5 January to 9 February, 1979 (FGGE first special observing period).

Preliminary experiments coupling the atmospheric forcing from the GLAS FGGE analysis showed unrealistic large changes in the sea surface temperature

(SST). In order to understand the causes of these unrealistic variations, a series of simpler idealized experiments were conducted. The main objectives in setting up these experiments were to study the time evolution and seek a better understanding of the time scales involved in the development of asymmetric oceanic features.

In the first three idealized experiments, the oceanic initial conditions were zonally averaged (Figures 3.1 and 3.2). In addition, in the first experiment, all the external atmospheric forcings were obtained from the January 1979 analysis and zonally averaged; i.e., the surface heat balance, the friction velocity, were assumed to be constant in time and independent of longitude (Figures 3.3, 3.4, and 3.5).

In the second experiment, the wind stress and friction velocities were zonally averaged throughout the entire time integration. For the surface heat balance, however we used the January 1979 average value (Figure 3.6) as obtained from the GLAS analysis.

In the third experiment, the only forcing parameter that was zonally averaged was the surface heat balance. On the other hand, for the other two atmospheric parameters--friction velocity and wind stress--their respective January 1979 average values were used during the five week integration.

In the last two experiments (fourth and fifth), the initial condition for the mixed layer depth is depicted in Figure 3.7. In the fourth experiment, all the atmospheric forcing parameters were the time average values corresponding to January 1979 (Figures 3.6, 3.9, 3.10, and 3.11).

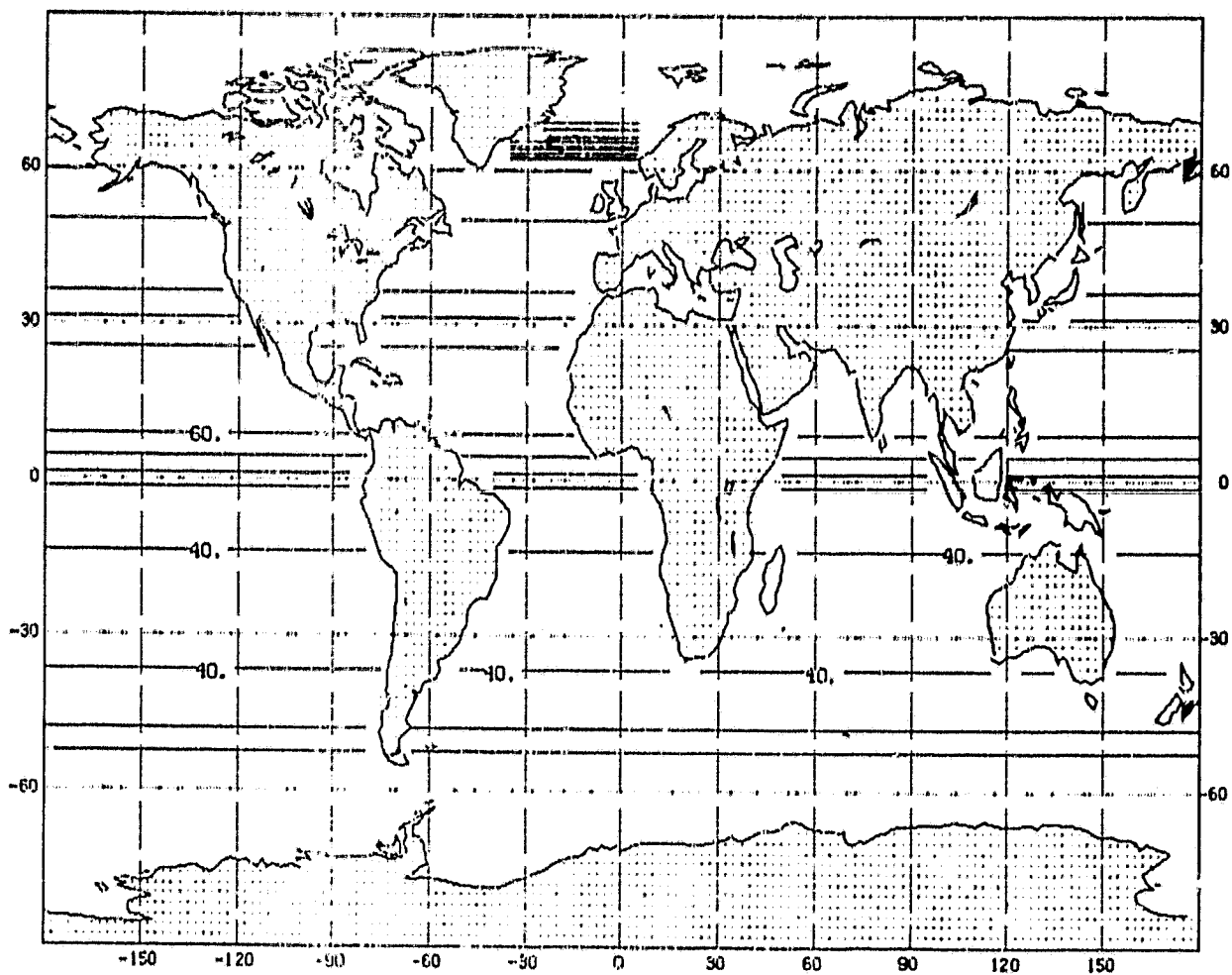
Finally, in the last experiment the instantaneous values of all the externally atmospheric forcings were used in the time integration.

The initial SST conditions were the January time averaged SST obtained by

Susskind et al. (1982) and is shown in Fig. 3.8. For comparison with the numerical results we also present the averaged February SST (Fig. 3.12) and the difference between the two fields (Fig. 3.13). Also, for the sake of completeness, the climatological difference between February and January is depicted in Fig. (3.14).

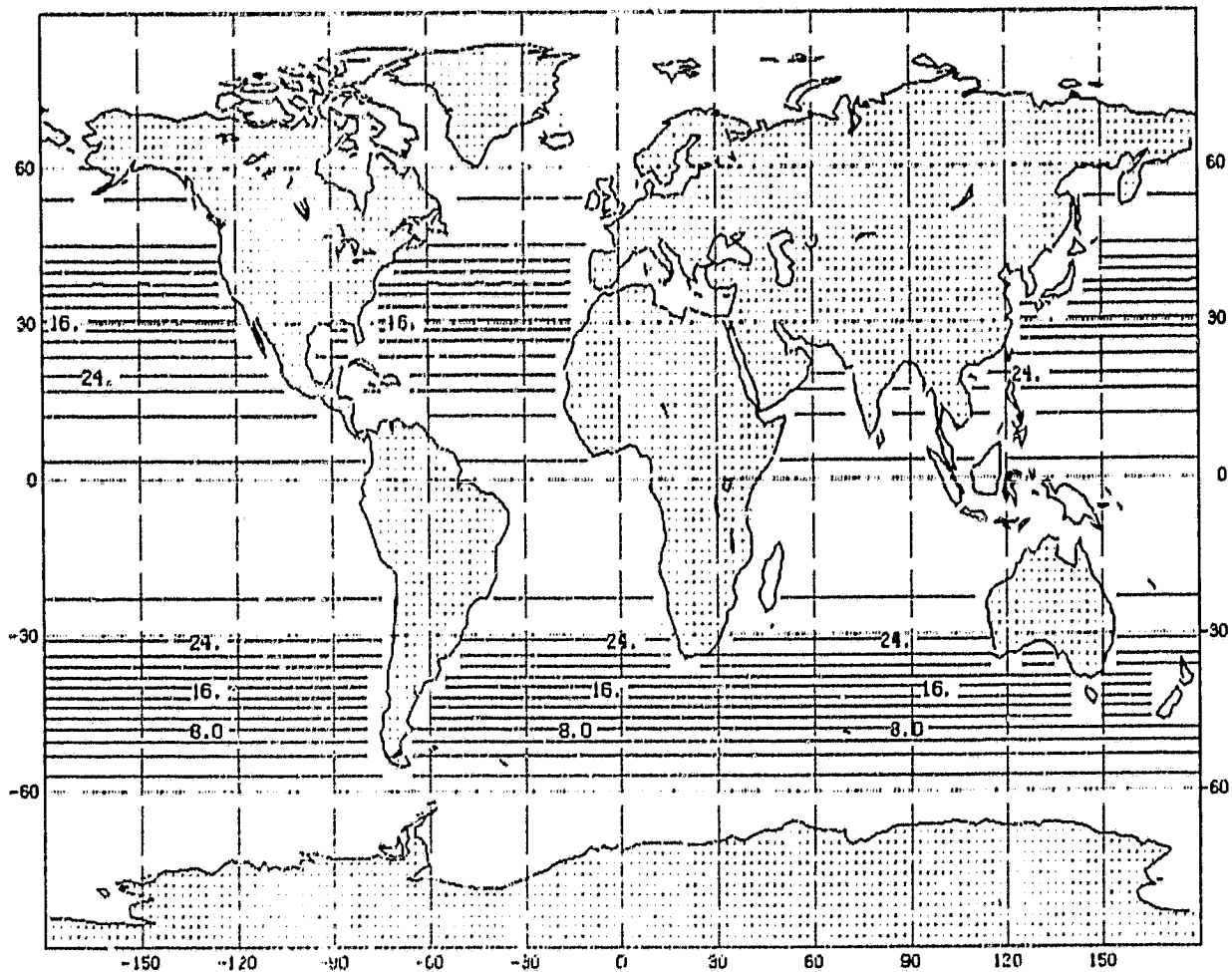
In all five experiments, the ocean model was started from rest.

ORIGINAL PAGE IS
OF POOR QUALITY



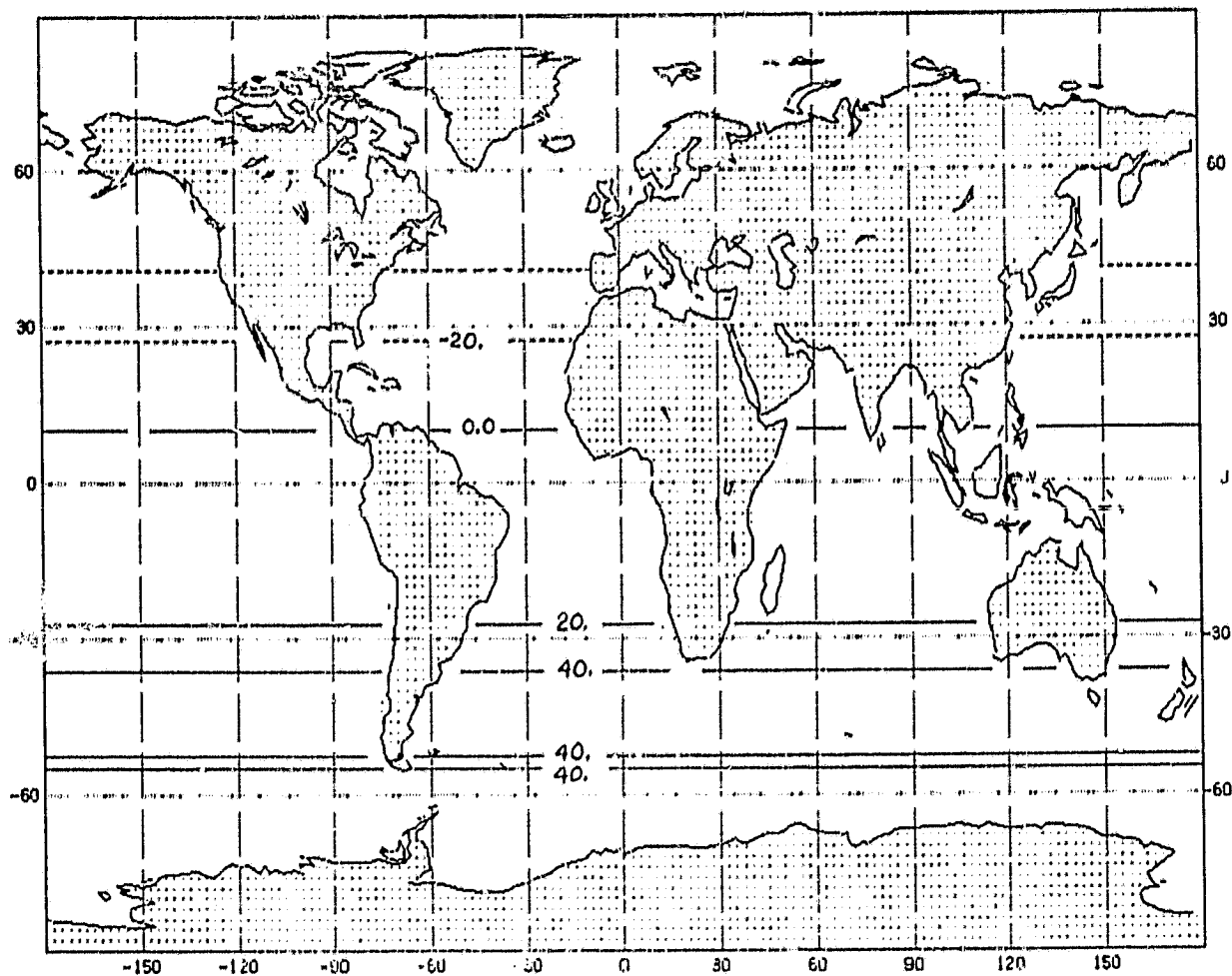
3.1 Zonally averaged ML depth
Contour interval of 5 m

ORIGINAL PAGE IS
OF POOR QUALITY



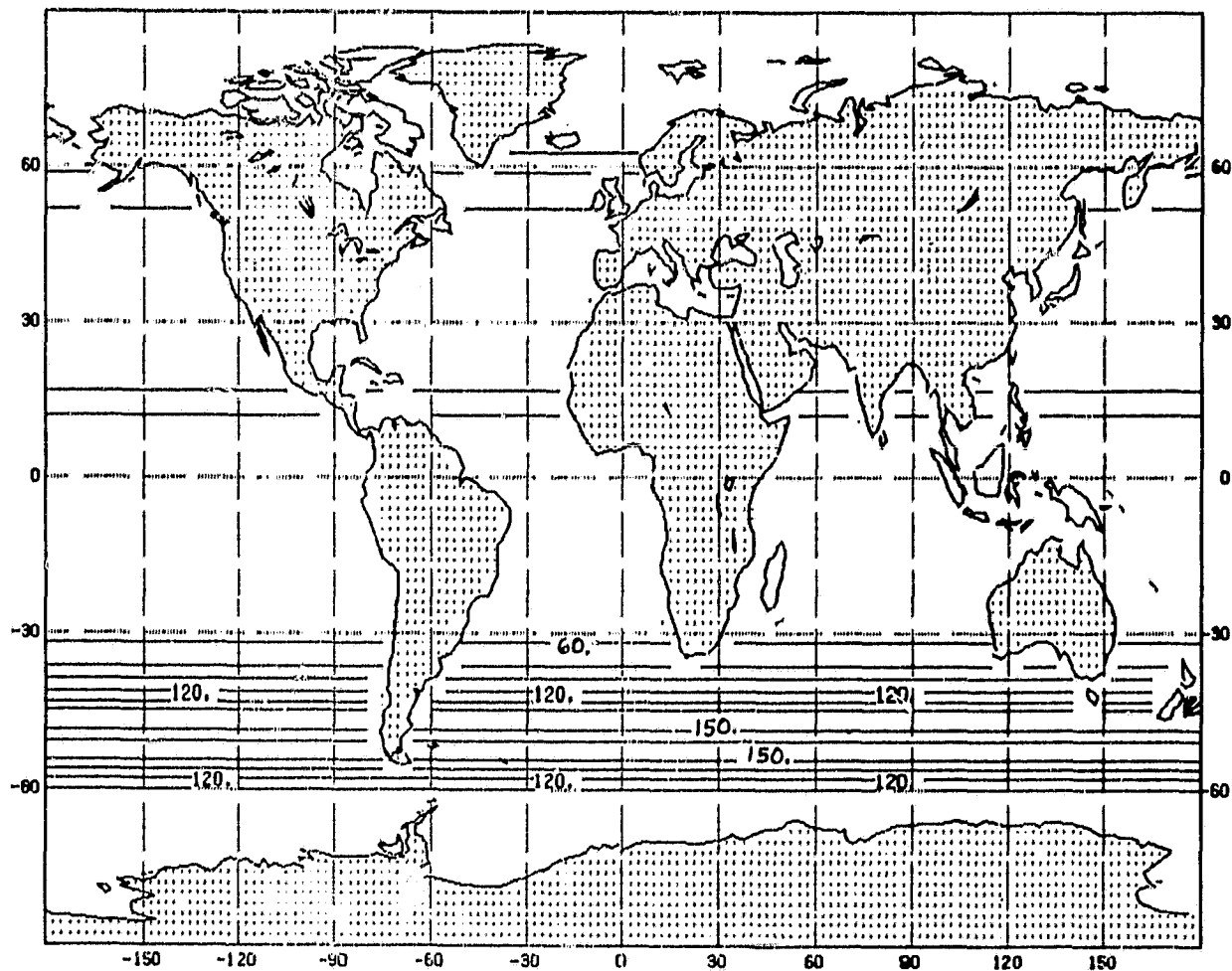
3.2 Zonally averaged temperature
Contour interval of 2°C

ORIGINAL PAGE IS
OF POOR QUALITY



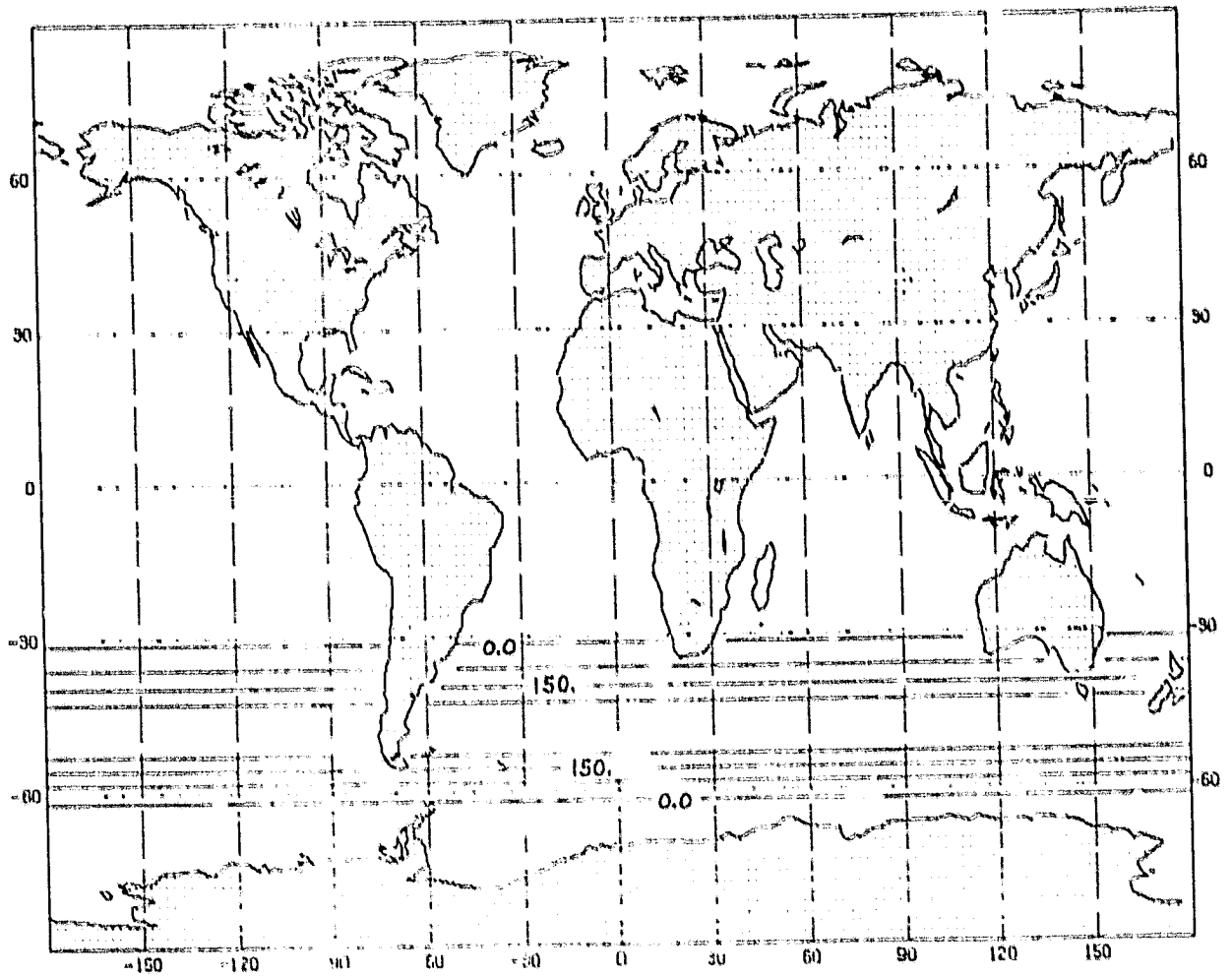
3.3 Zonally averaged surface heat balance
Contour interval of 20 Watts/m²

ORIGINAL PAGE IS
OF POOR QUALITY



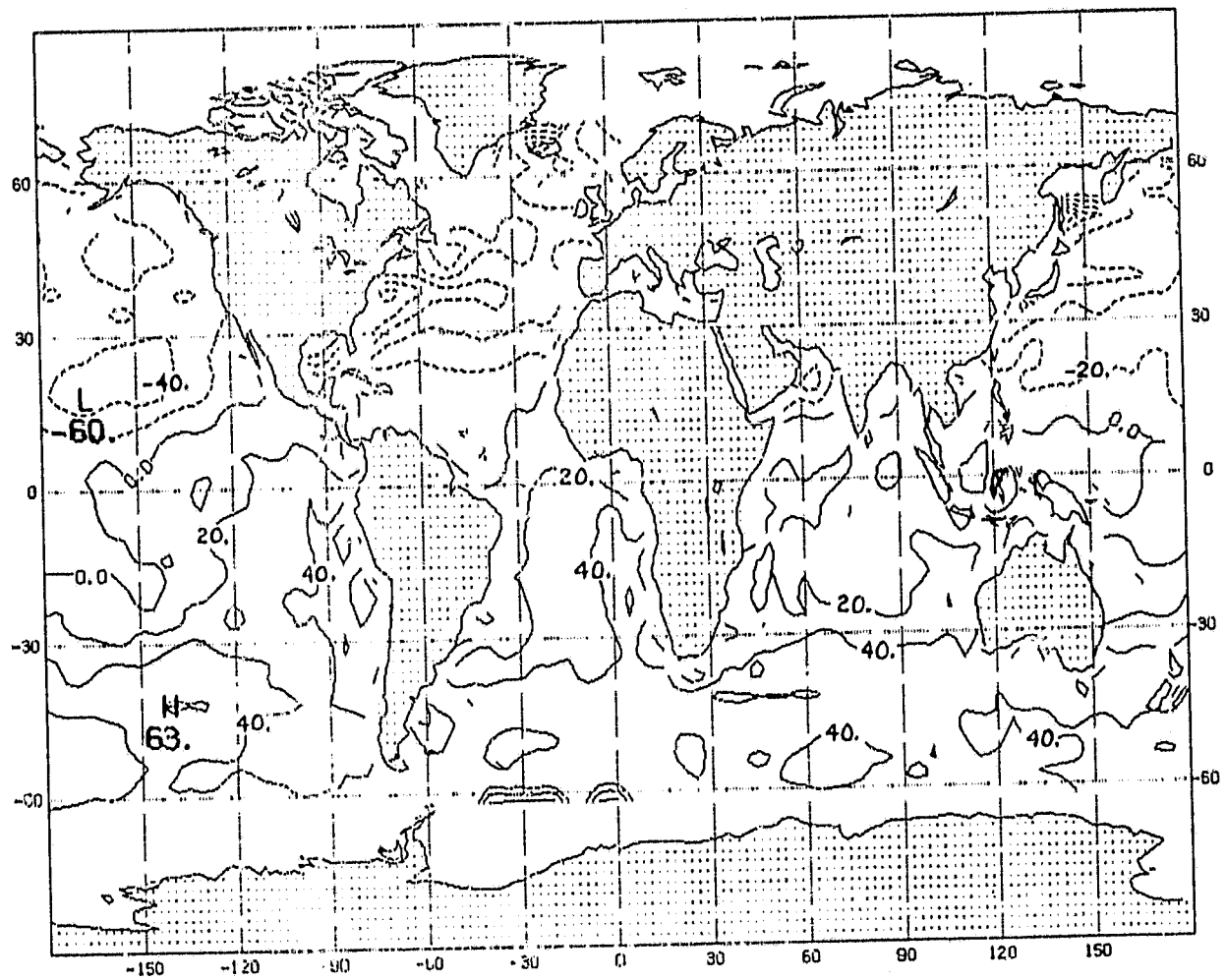
3.4 Zonally averaged friction velocity
Contour interval of $15 \cdot 10^{-1} \text{ mm/s}$

ORIGINAL PAGE IS
OF POOR QUALITY



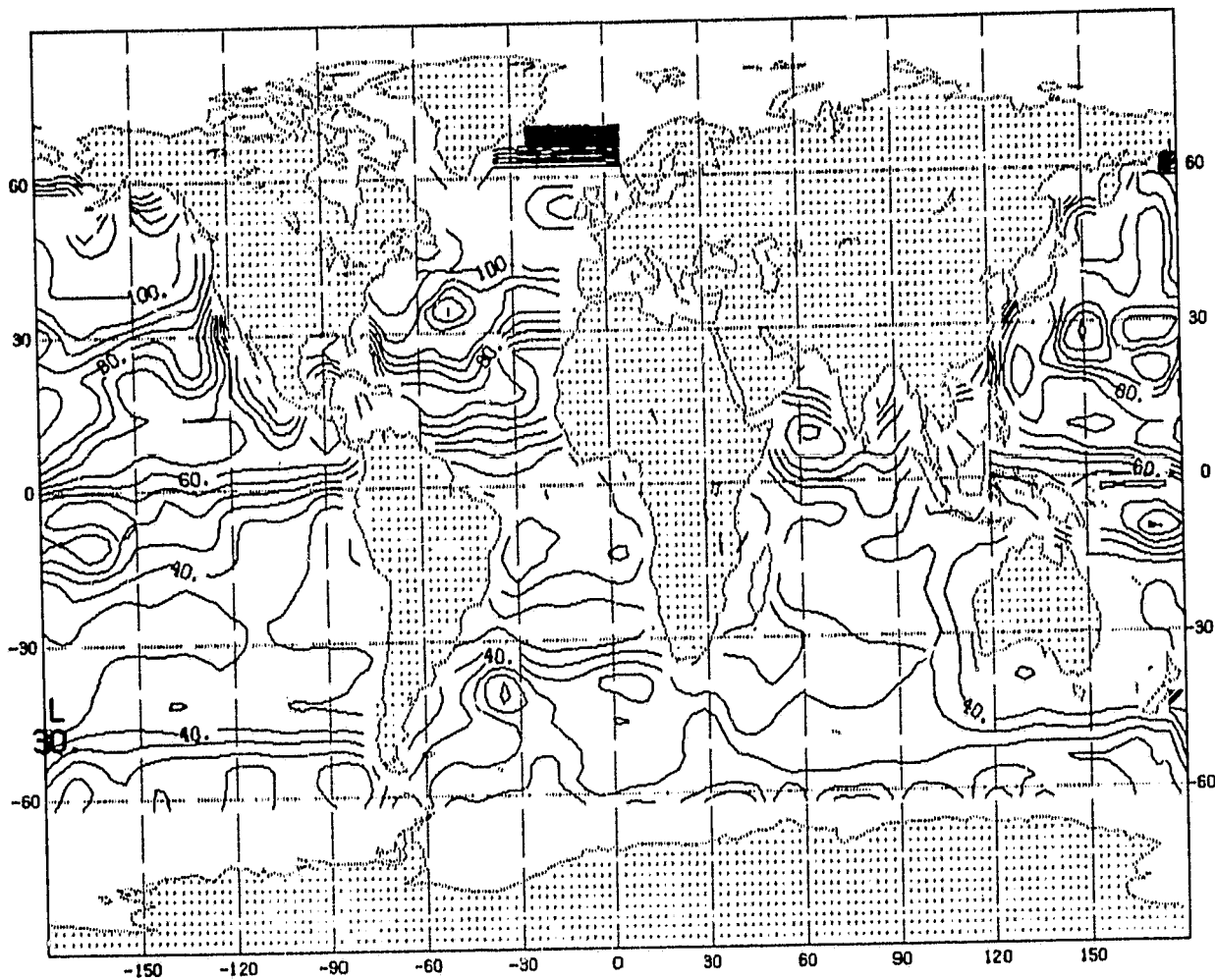
3.5 Zonally averaged wind stress in the x direction
Contour interval of $75 \times 10^{-3} \text{ N/m}^2$

ORIGINAL PAGE IS
OF POOR QUALITY



3.6 January 1979 average value of the surface heat balance
Contour interval of 20 Watts/m²

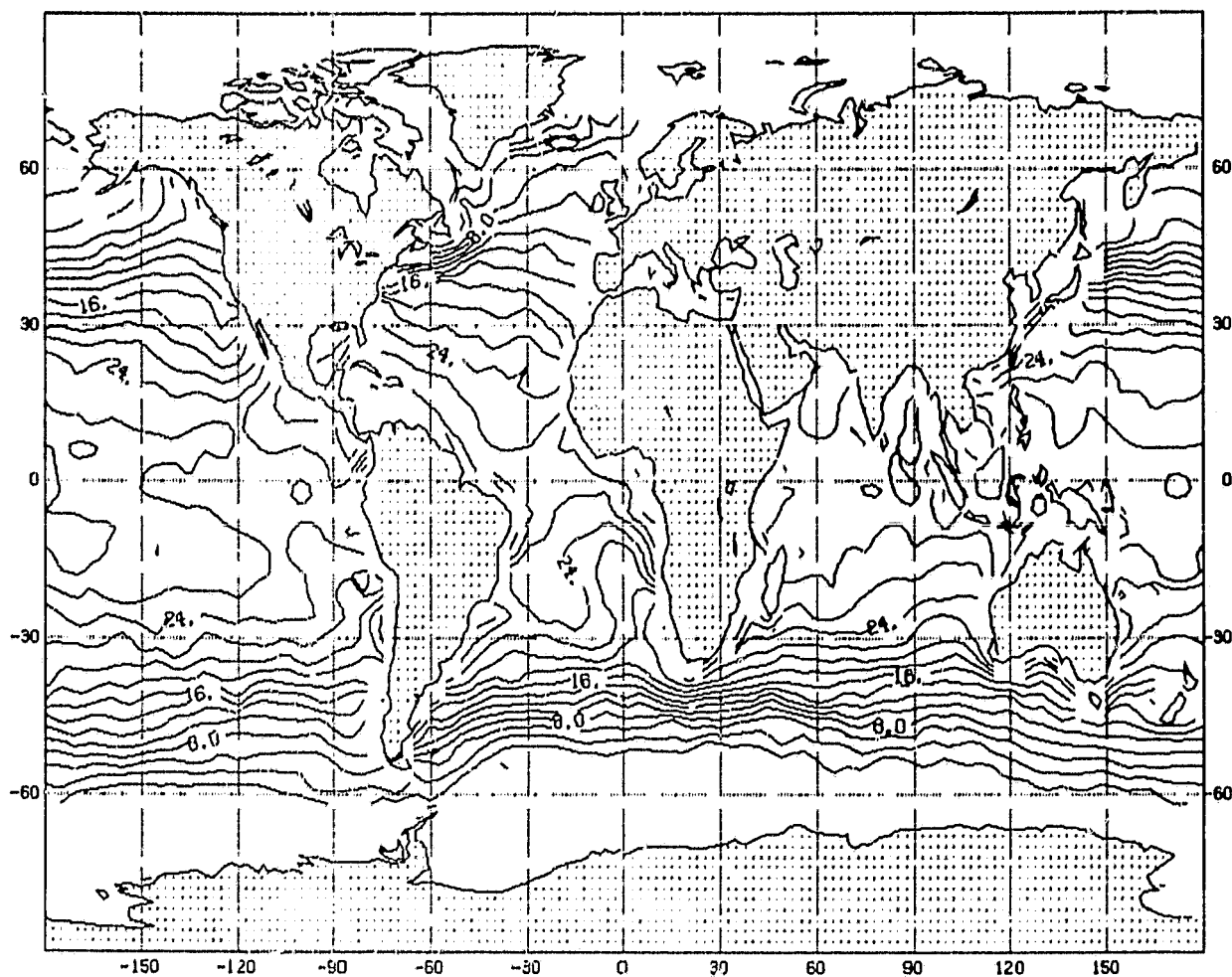
ORIGINAL PAGE IS
OF POOR QUALITY



3.7

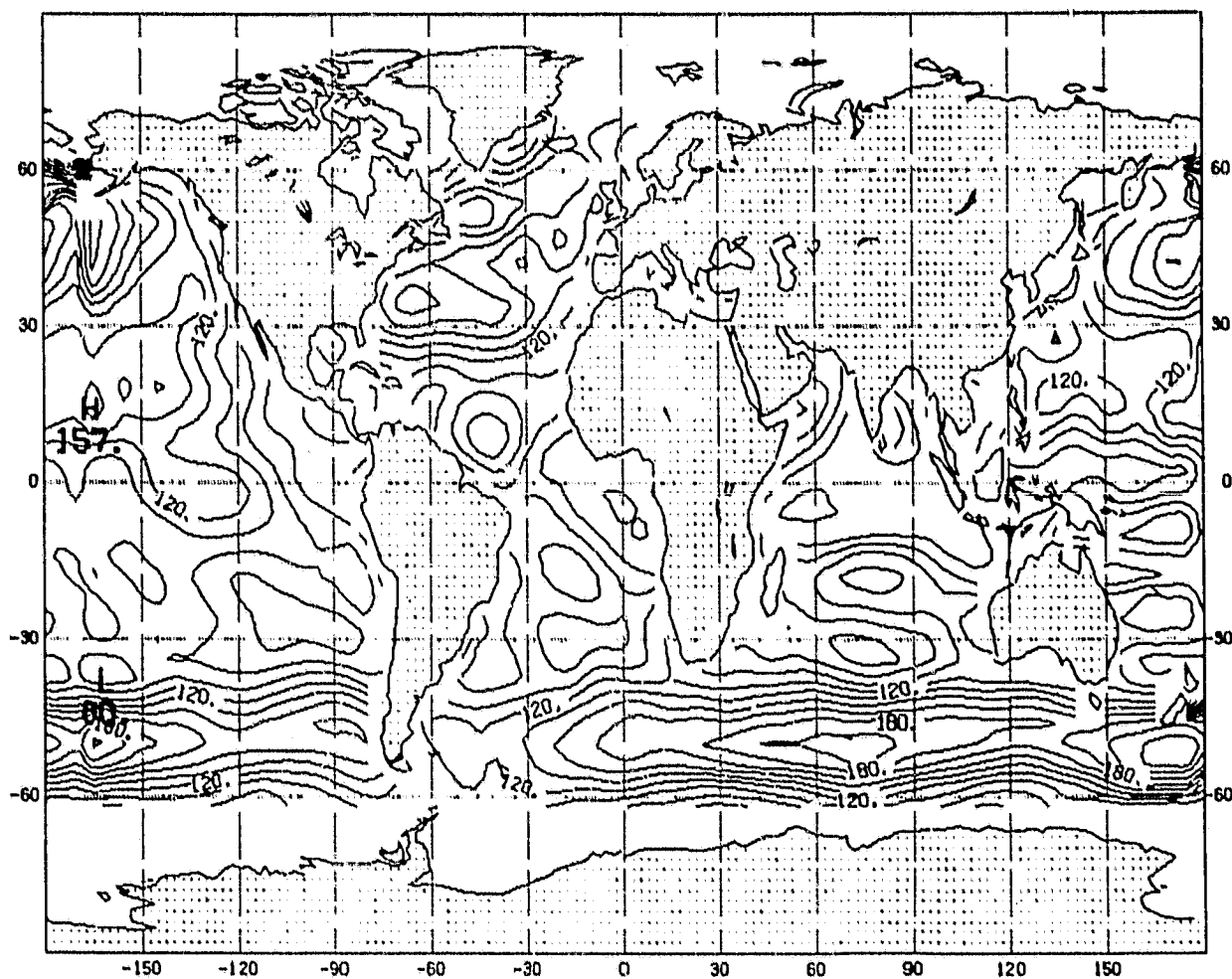
Initial condition of ML depth (not zonally averaged)
Contour interval of 5 m

ORIGINAL PAGE IS
OF POOR QUALITY



3.8 Initial condition of ML temperature (not zonally averaged)
(Susskind et al. 1982) Contour interval of 2° C

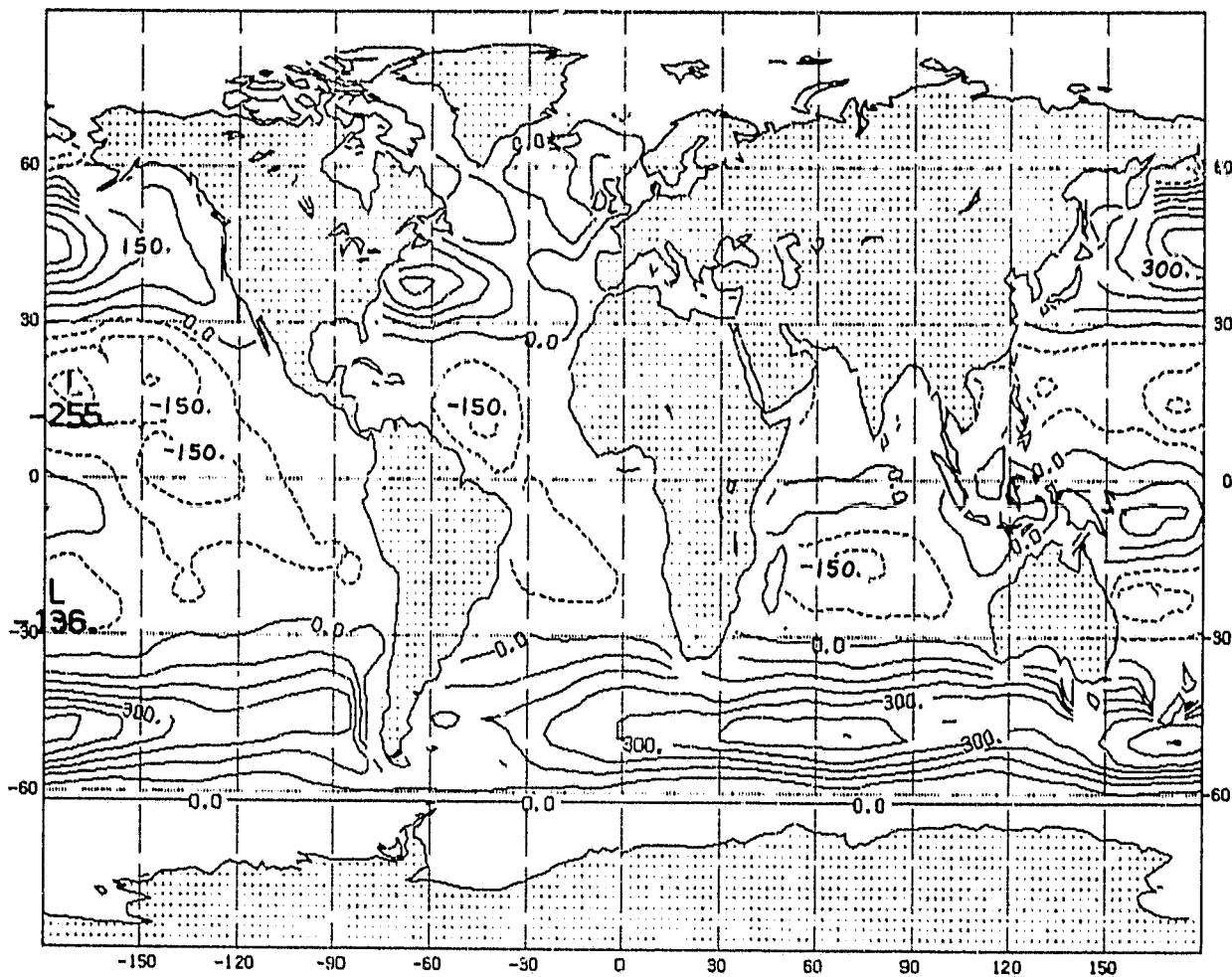
ORIGINAL PAGE IS
OF POOR QUALITY



3.9

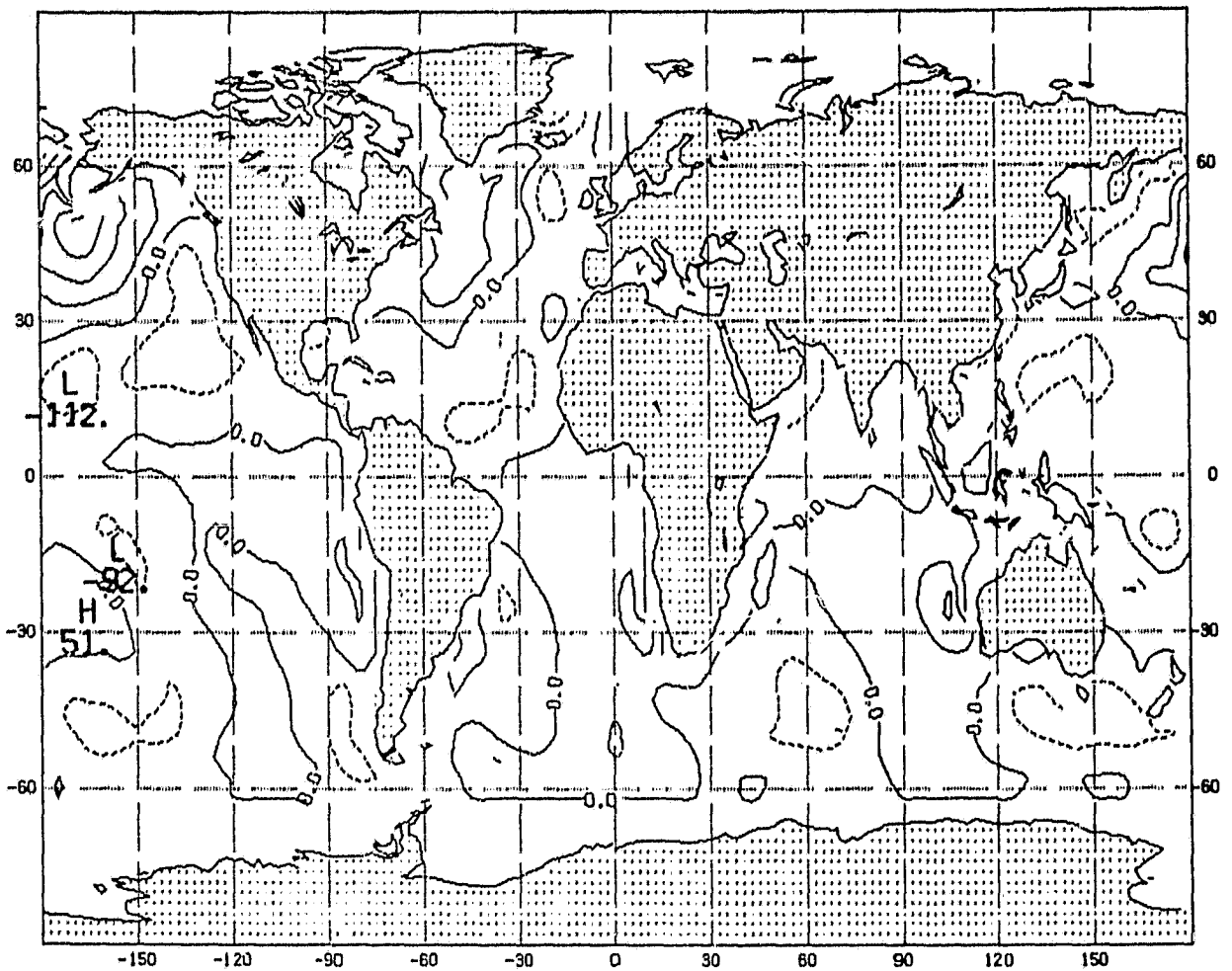
January 1979 average value of the friction velocity
Contour interval of $15 \cdot 10^{-1} \text{ mm/s}$

ORIGINAL PAGE IS
OF POOR QUALITY



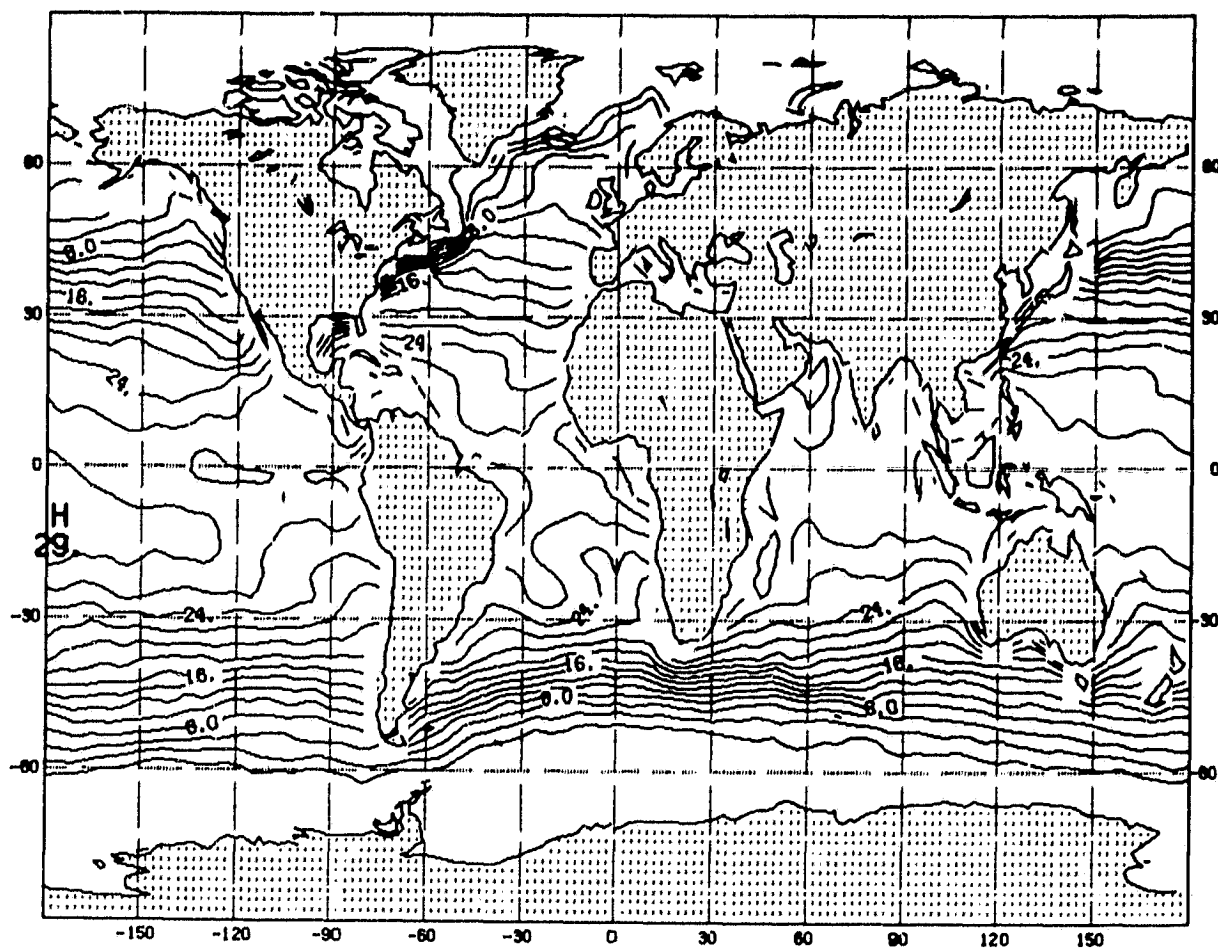
3.10 January 1979 average value of the wind stress in the x direction
Contour interval of $75 \cdot 10^{-3} \text{N/m}^2$

ORIGINAL PAGE IS
OF POOR QUALITY



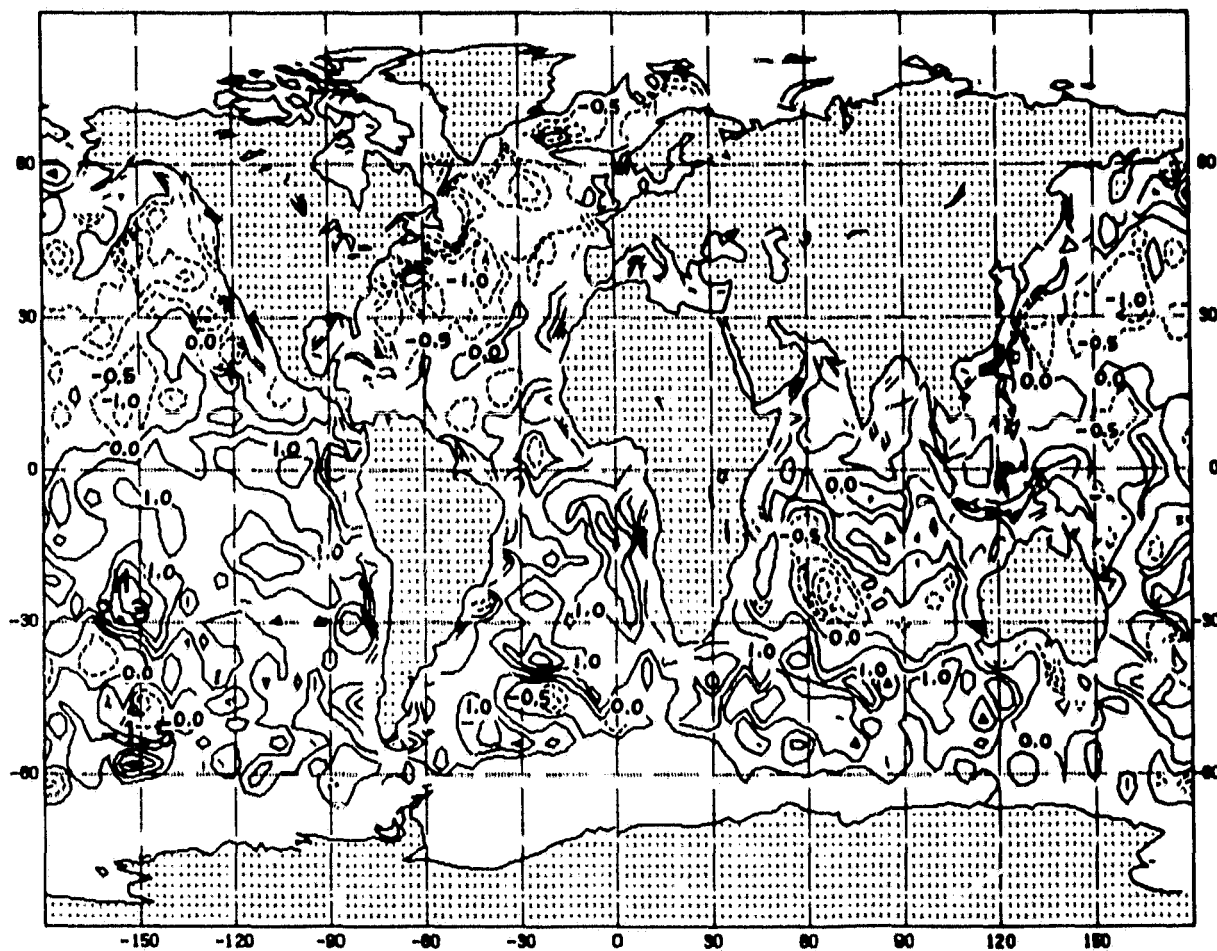
3.11 January 1979 average value of the wind stress in the y direction
Contour interval of $75 \cdot 10^{-3} \text{N/m}^2$

ORIGINAL PAGE IS
OF POOR QUALITY



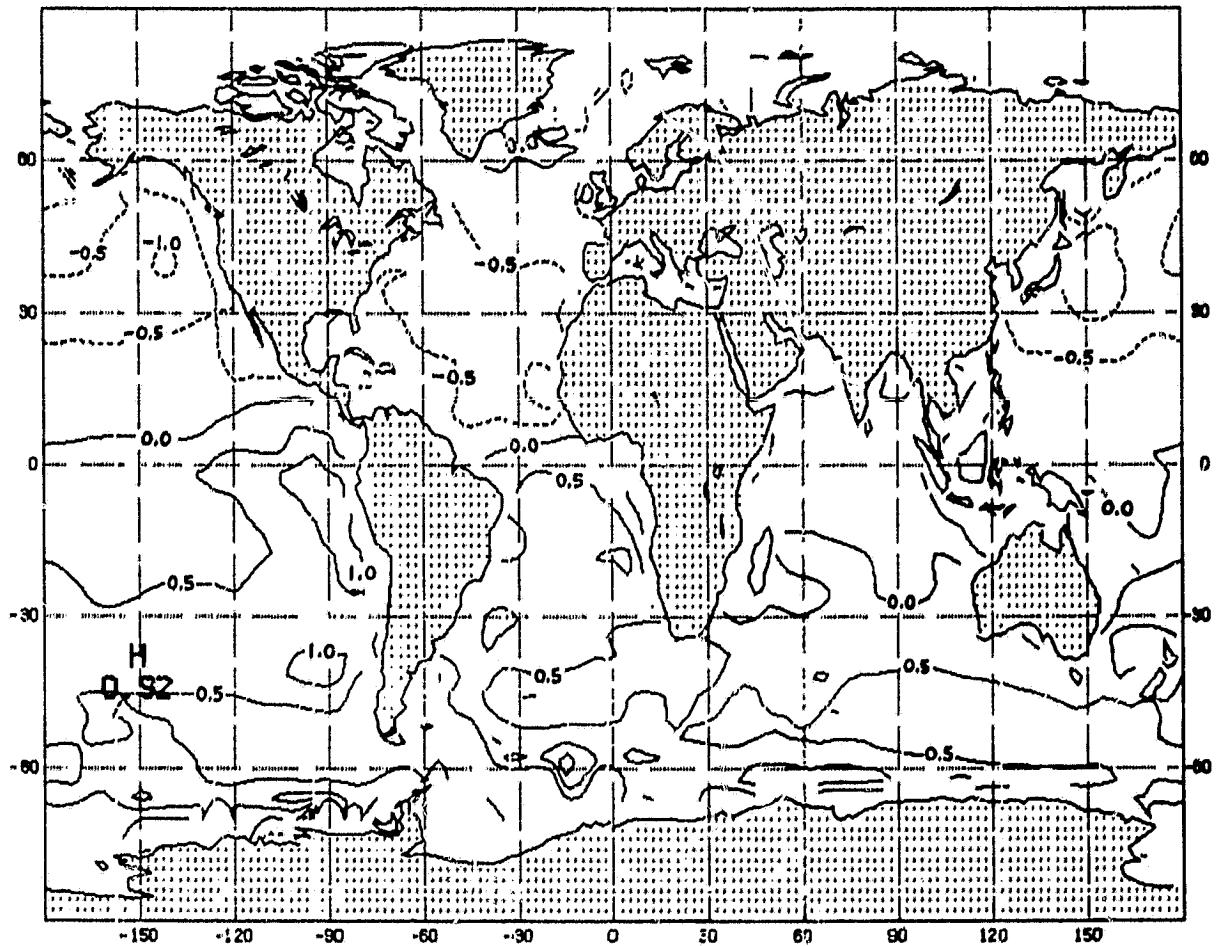
3.12 February 1979 average sea surface temperature (Susskind et al. 1982)
Contour interval of 2° C

ORIGINAL PAGE IS
OF POOR QUALITY



3.13 Observed sea surface temperature difference between February and January 1979 (Susskind et al. 1982) Contour interval of 0.5° C

ORIGINAL PAGE IS
OF POOR QUALITY



3.14 Climatological sea surface temperature difference between February and January. Contour interval of 0.5° C.

4. Results

The discussions of these experiments will be limited to the open ocean regimes. Thus, I will avoid the study of the especially complex circulations in coastal regions, where the lack of boundary currents in the initial conditions and the coarseness of the grid, make the model particularly unrealistic.

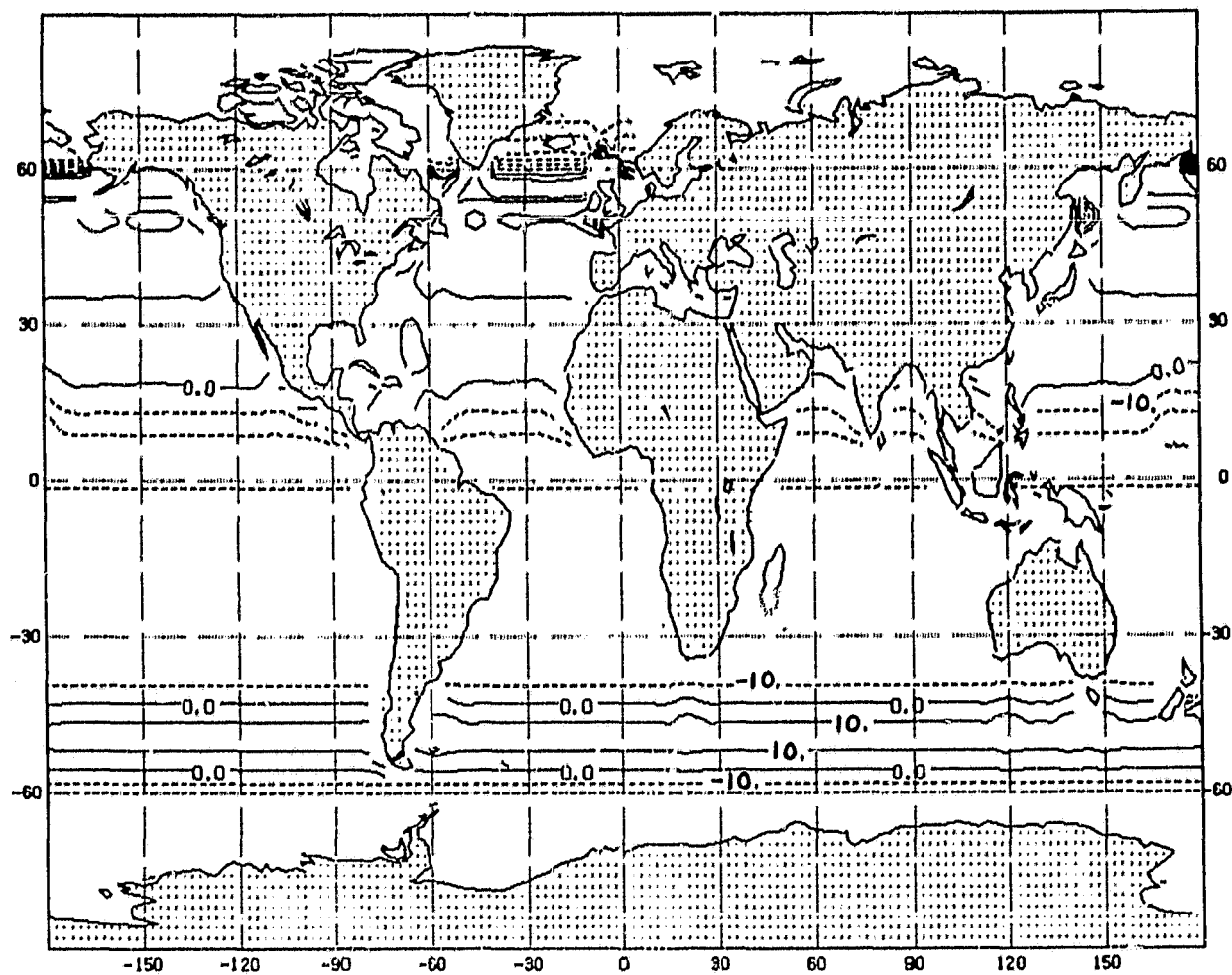
First Case: (zonally averaged initial conditions, zonally averaged surface heat flux, wind stress and friction velocity)

The analysis of Figures 4.1.1 and 4.1.5 shows that most of the changes in the ML depth occurs in the first ten days. The same feature is observed for the horizontal velocity (Figures 4.1.3, 4.1.4, 4.1.7 and 4.1.8). However, the changes in the temperature field do occur in a much longer time (Figures 4.1.2 and 4.1.6). More specifically, no net change of temperature is observed after one week.

Since the results show that the principal changes after one week in depth, and velocity field are essentially retained after five weeks for the first three cases, to avoid redundancy we will limit our discussion to an examination and description of the fifth week's results.

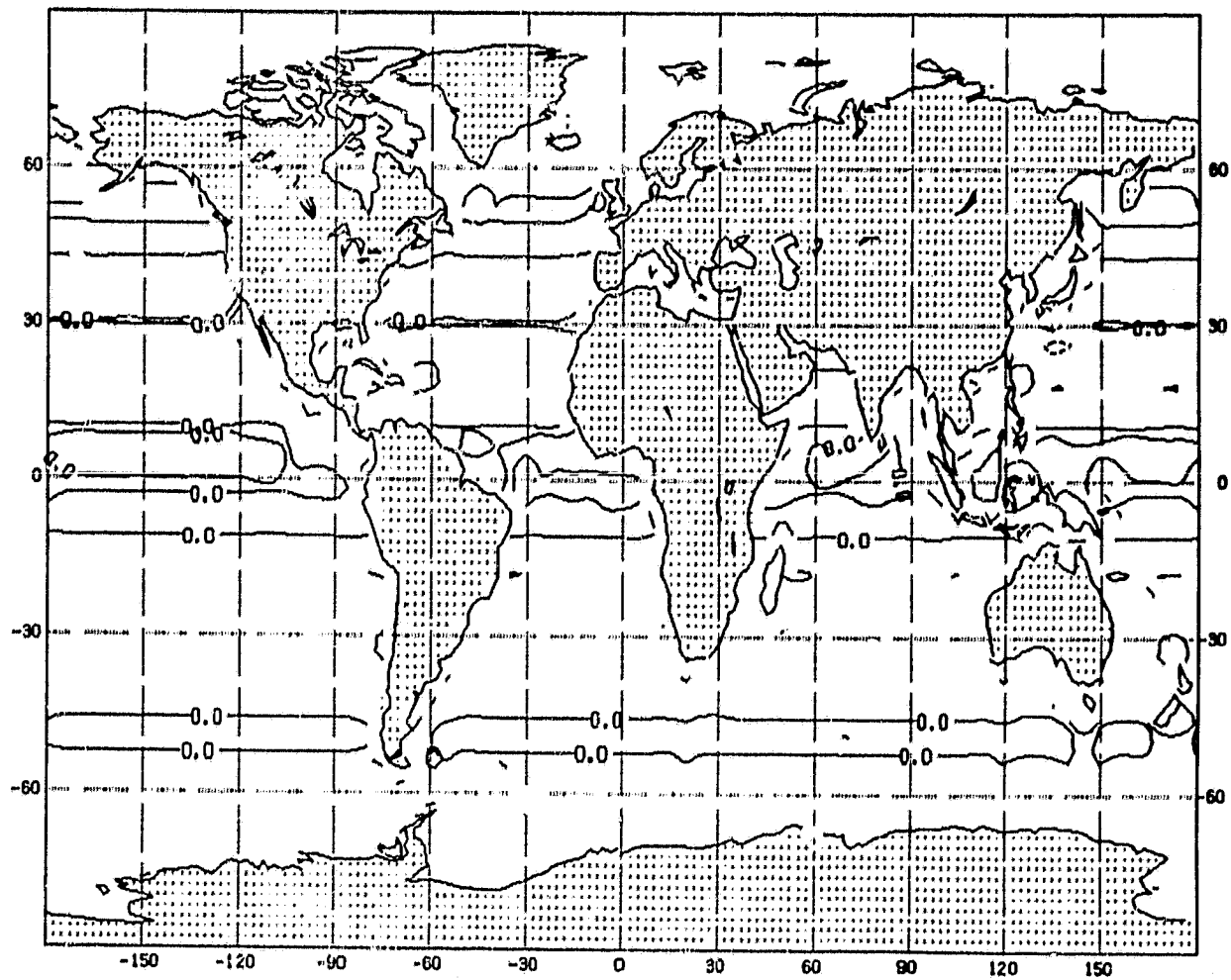
In Figure 4.1.6 we observe a decrease in temperature north of 10°S up to 45°N . This can be attributed to two factors: the deficit of surface heat balance north of 10°N (Figure 3.3), combined with equatorial upwelling (notice the divergence implied by $\partial v / \partial y$ in Fig. 4.1.8). Conversely, the increase in temperature south of 10°S should be attributed to the surplus of surface heat balance; north of 50°N the winds and heat balance are very weak, and so is the change in temperature.

ORIGINAL PAGE IS
OF POOR QUALITY



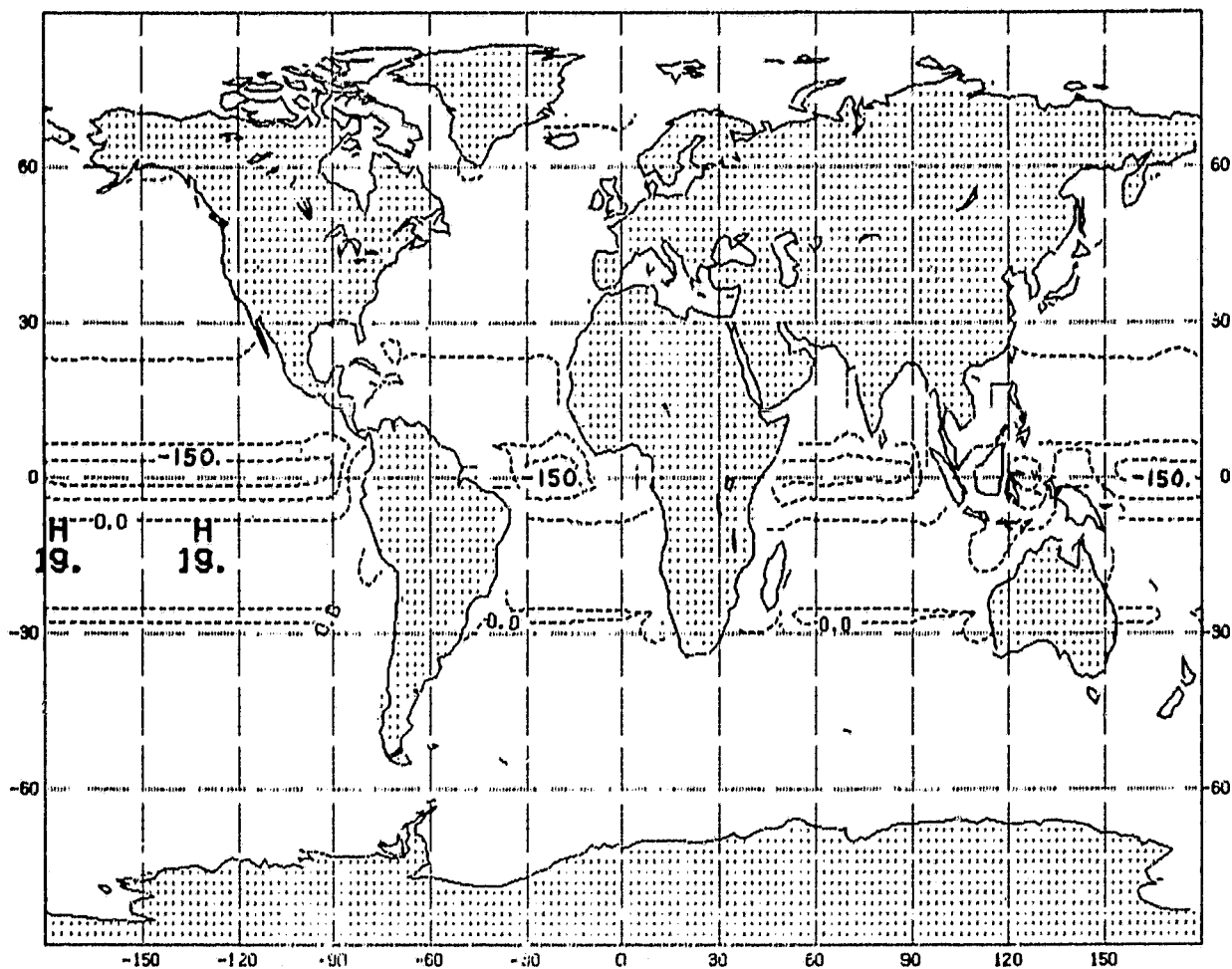
4.1.1 Weekly averaged ML depth changes after one week for the first case.
Contour interval of 10 m

ORIGINAL PAGE IS
OF POOR QUALITY



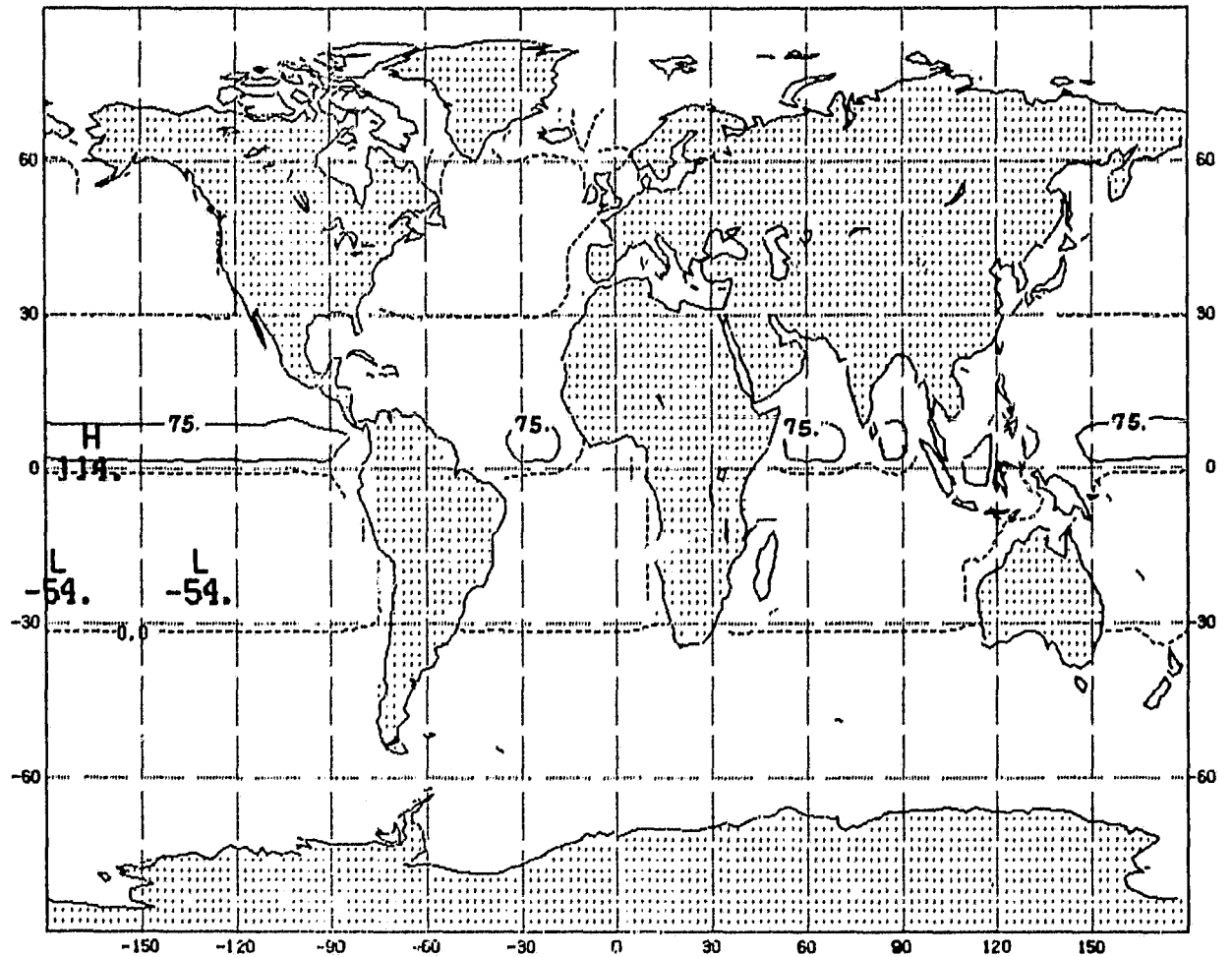
4.1.2 Weekly averaged ML temperature changes after one week for the first case. Contour interval of 1° C

ORIGINAL PAGE IS
OF POOR QUALITY



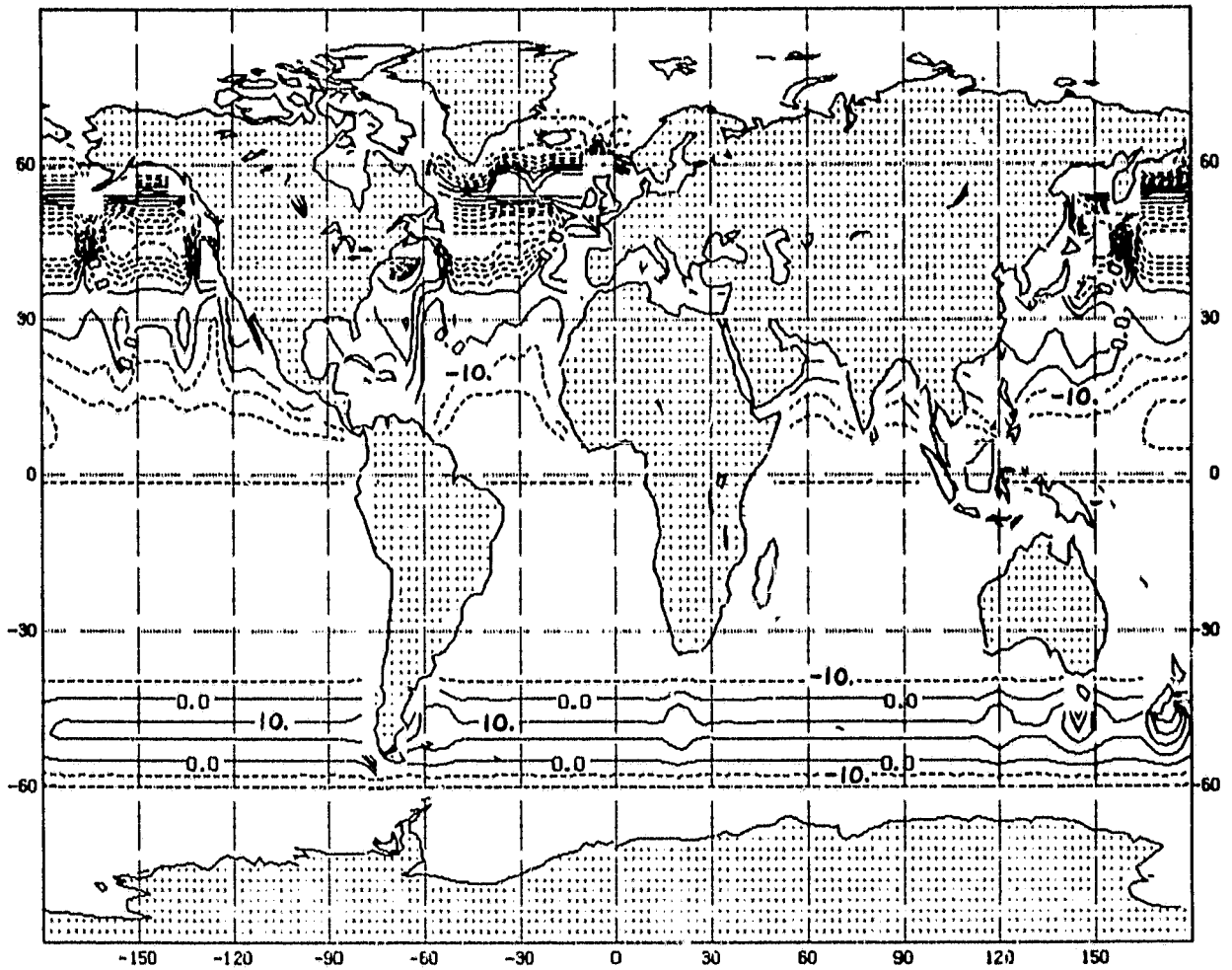
4.1.3 Weekly averaged value of the zonal velocity field, u , after one week for the first case. Contour interval of 75 mm/s

ORIGINAL PAGE IS
OF POOR QUALITY



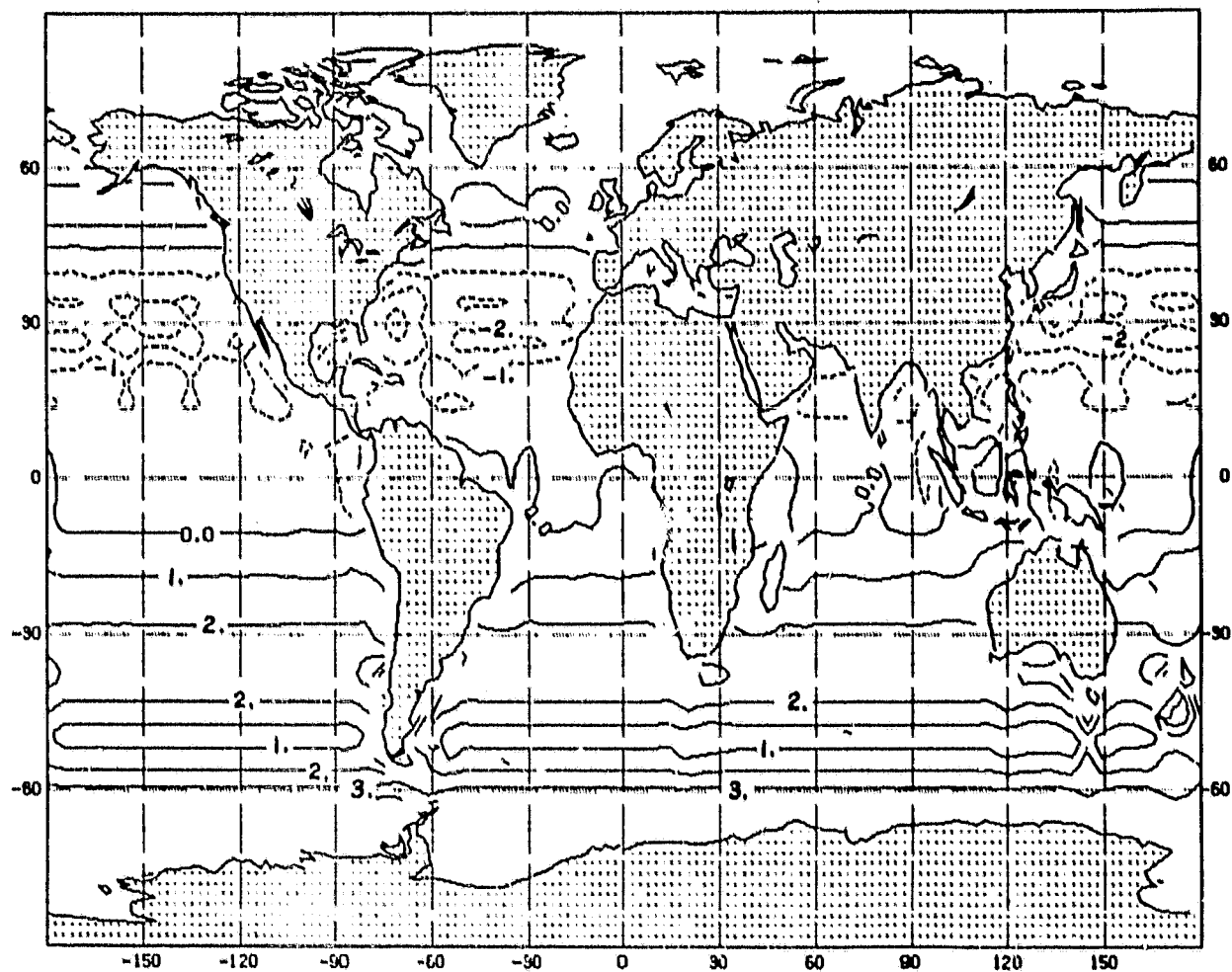
4.1.4 Weekly averaged value of the meridional velocity field, v , after one week for the first case. Contour interval of 75 mm/s

ORIGINAL PAGE IS
OF POOR QUALITY



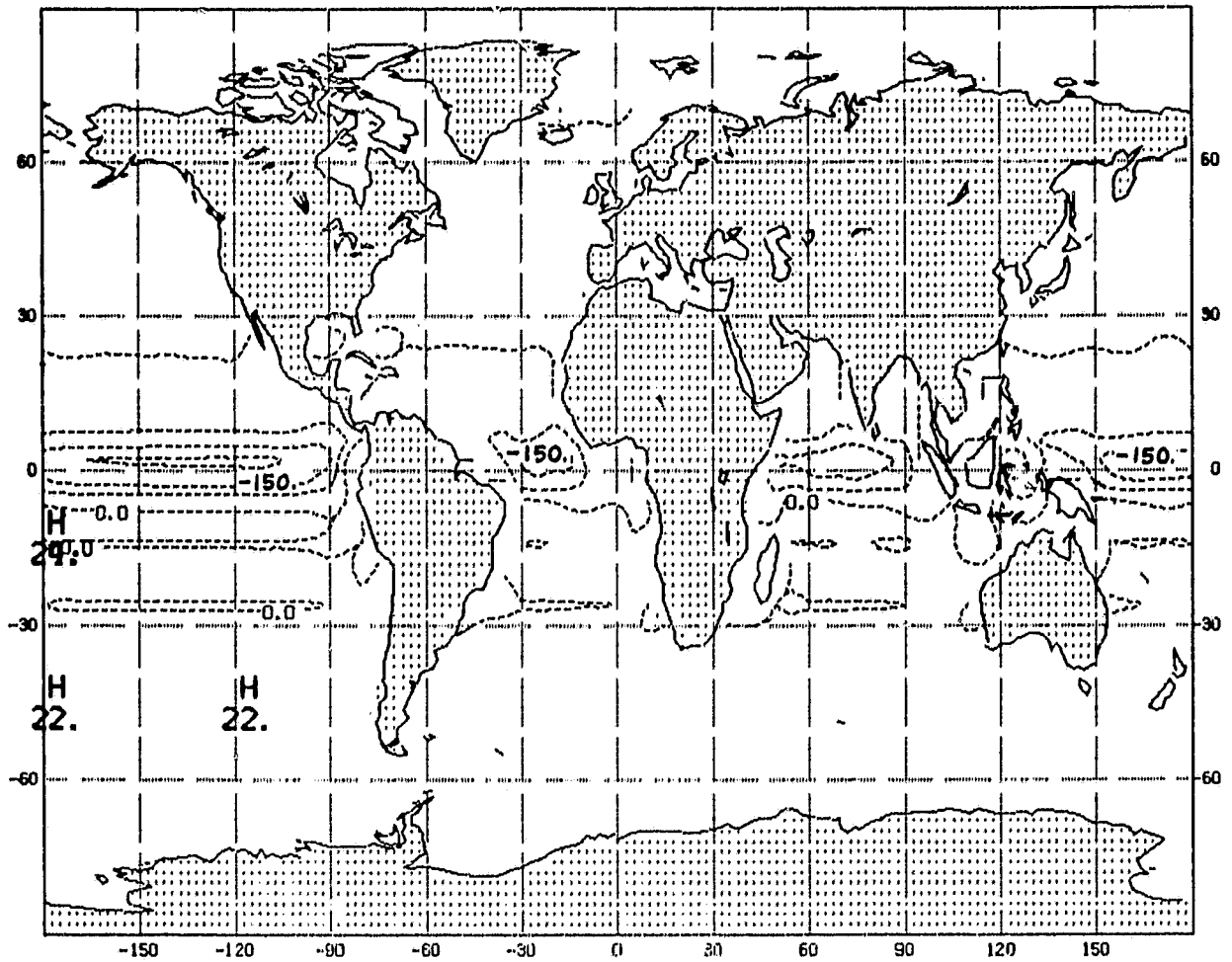
4.1.5 Weekly averaged ML depth changes after five weeks for the first case.
Contour interval of 10 m

ORIGINAL PAGE IS
OF POOR QUALITY



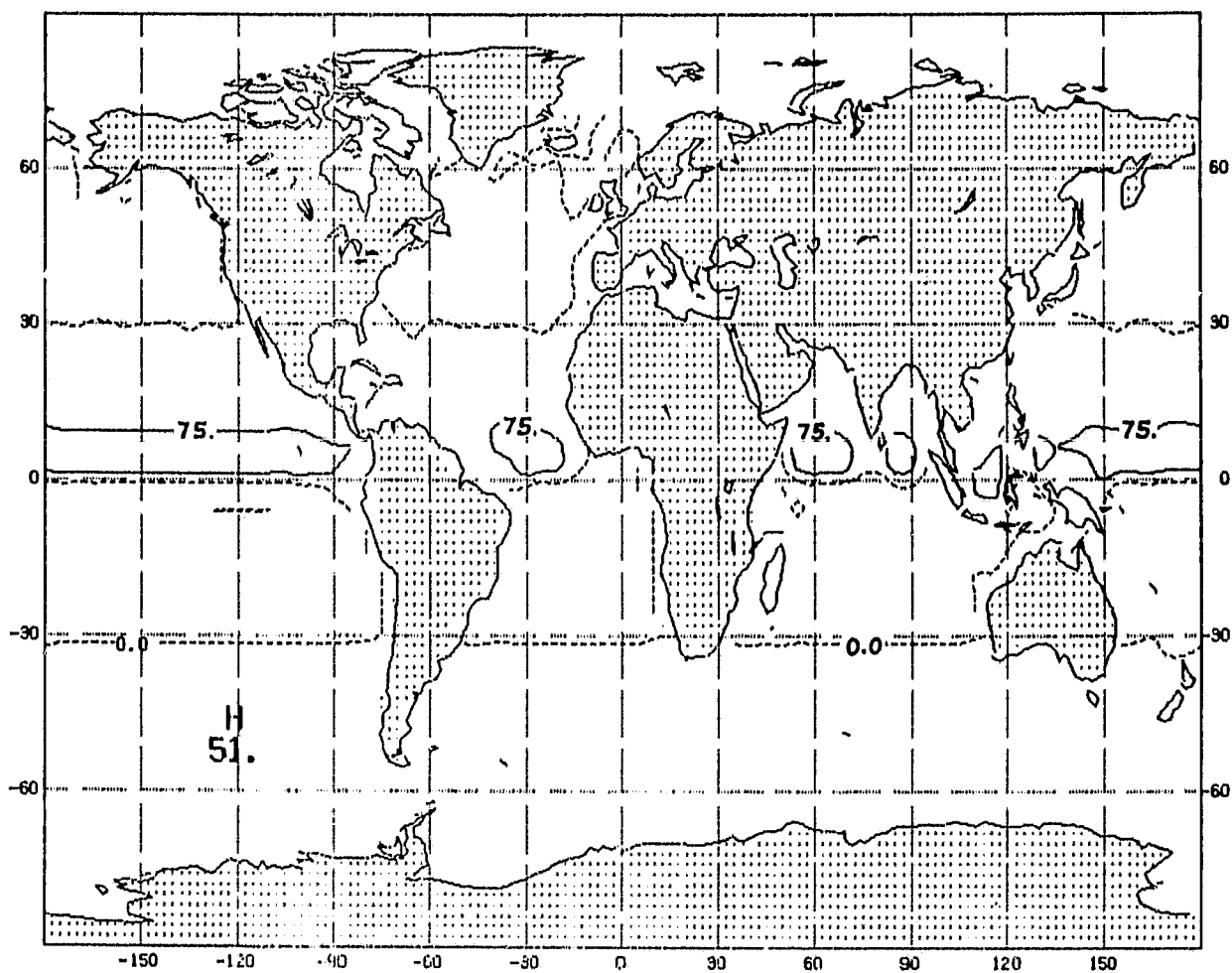
4.1.6 Weekly averaged the ML temperature changes after five weeks for the first case . Contour interval of 1° C

ORIGINAL PAGE IS
OF POOR QUALITY



4.1.7 Weekly averaged value of the zonal velocity field, u , after five weeks for the first case. Contour interval of 75 mm/s

ORIGINAL PAGE IS
OF POOR QUALITY



4.1.8 Weekly averaged value of the meridional velocity field, v , after five weeks for the first case. Contour interval of 75 mm/s

The weak winds north of 30°S are responsible for the shallowing of the mixed layer at those latitudes especially at high latitudes in the northern hemisphere (Figures 3.5 and 4.1.5). The deepening of the mixed layer in the belt between 40°S - 55°S is due to the westerly winds, which are stronger in the southern hemisphere.

Second Case: (zonally averaged initial conditions, zonally averaged wind stress and friction velocity, time averaged, but non zonally averaged heat flux)

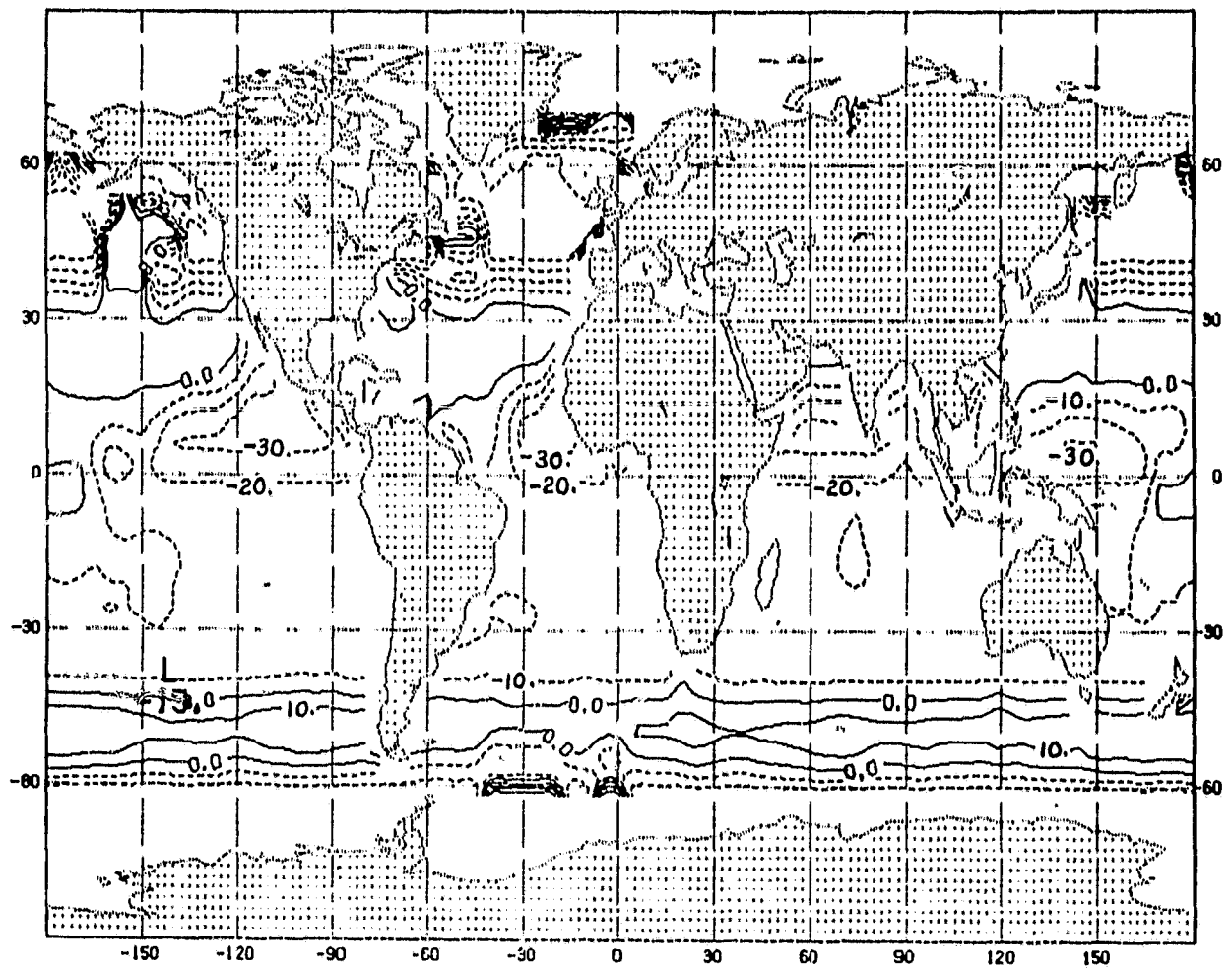
As in the previous case most of the changes in the height and in the horizontal velocity of the oceanic boundary layer model take place in the very first days (Figures 4.2.1, 4.2.3, 4.2.4, 4.2.5, 4.2.7 and 4.2.8). Again, from Figure 4.2.2 it is observed that the temperature field changes observed after one week are small.

There is a marked difference in the temperature field between this case and the previous one. From a comparison of Figures 3.6 and 4.2.6, we observe that whenever we have a deficit of surface heat balance, the ocean model responds by a decrease in the temperature field, and viceversa. The only exception is again north of 50°N .

In the northern hemisphere, where we have a maximum deficit of surface heat balance, we observe a deepening of the mixed layer (Figure 4.2.5). Therefore the deepening of the mixed layer observed in the belt of 15°N - 35°N in the sub-tropical Atlantic and Pacific Ocean is due to both the deficit of surface heat balance and the strength of the winds observed at those latitudes (Figures 3.5 and 3.6).

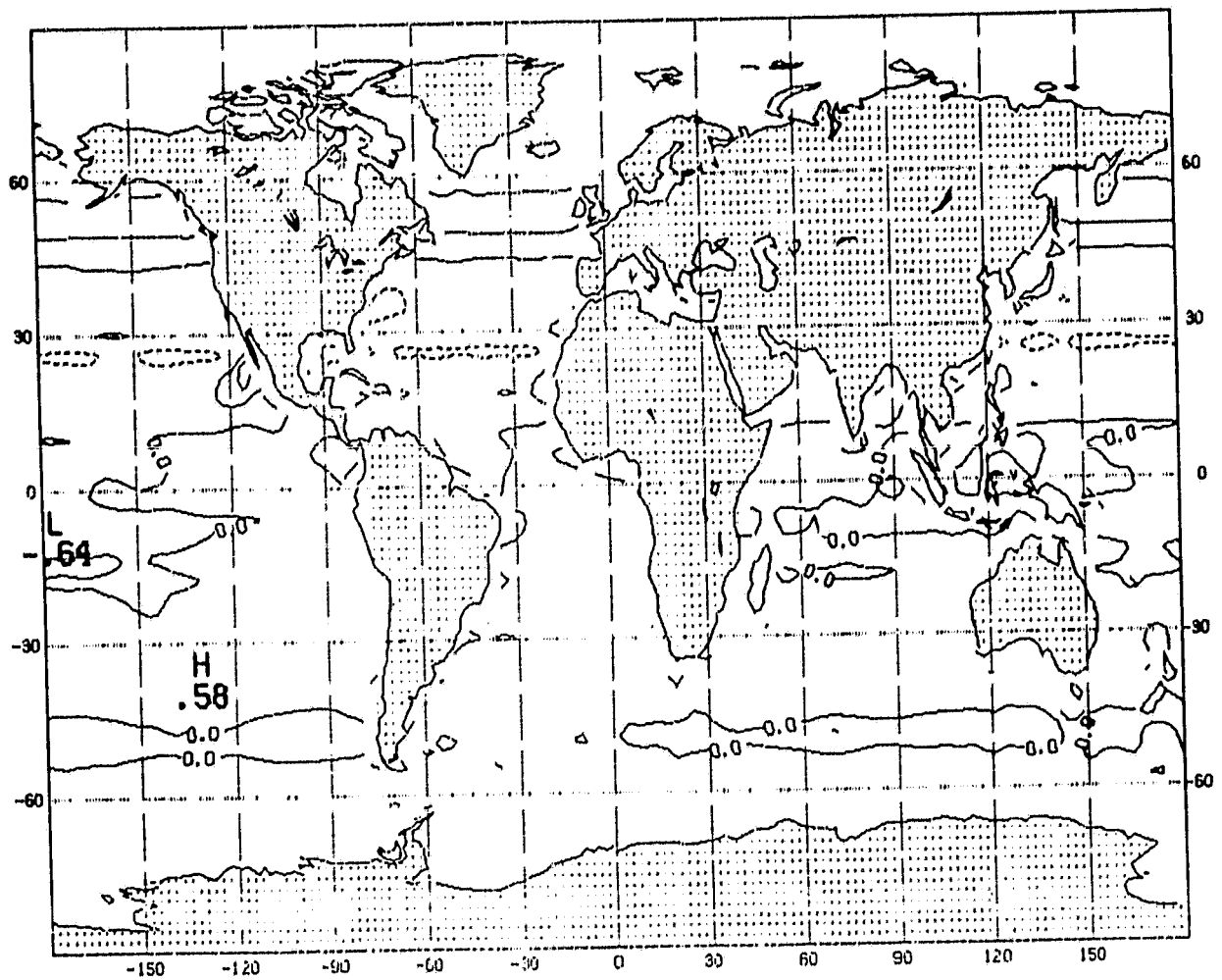
The analysis of these same figures demonstrates that the effects of the lighter winds north of 35°N are more important than the effects of the deficit

ORIGINAL PAGE IS
OF POOR QUALITY



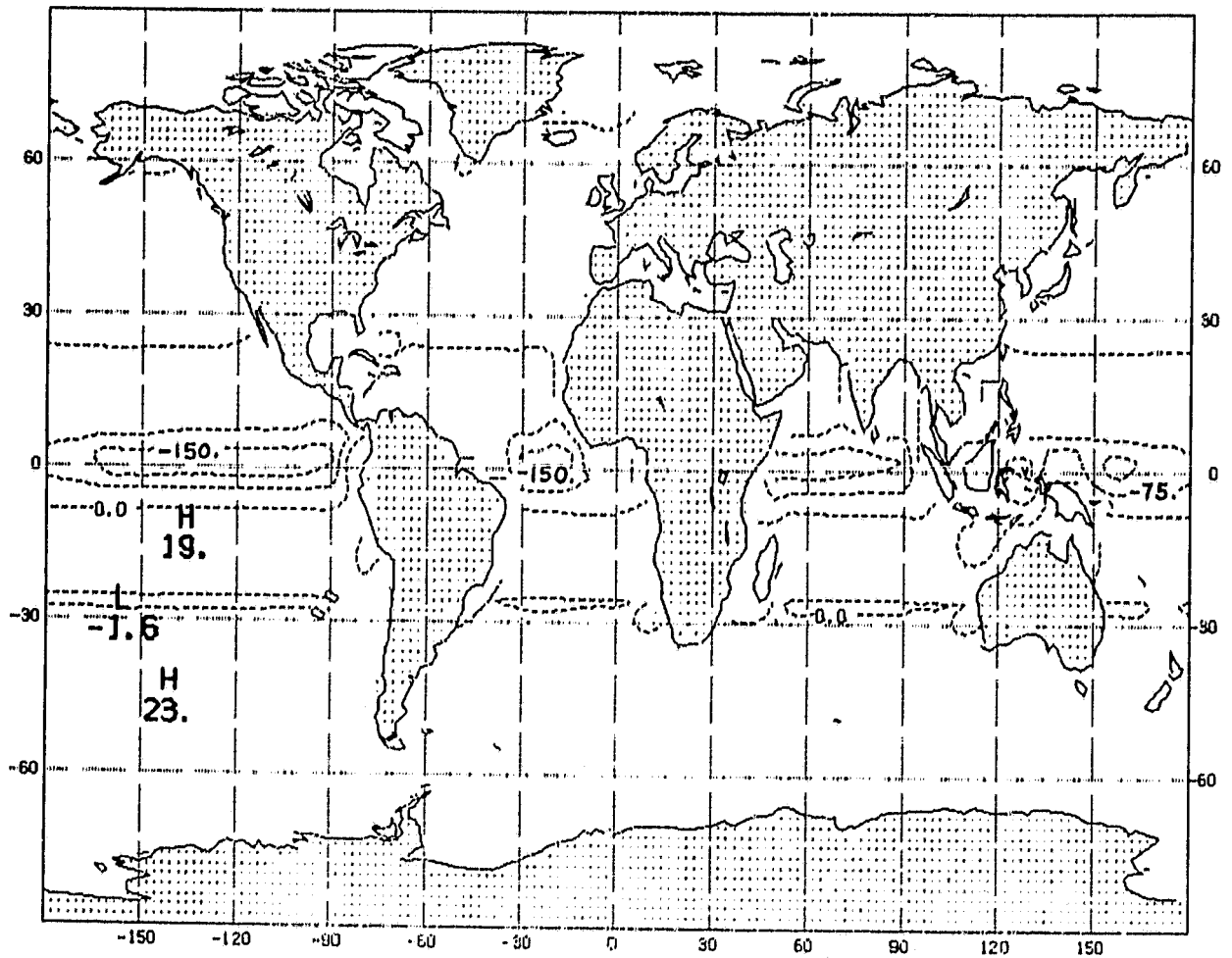
4.2.1 Weekly averaged ML depth changes after one week for the second case.
Contour interval of 10 m

ORIGINAL PAGE IS
OF POOR QUALITY



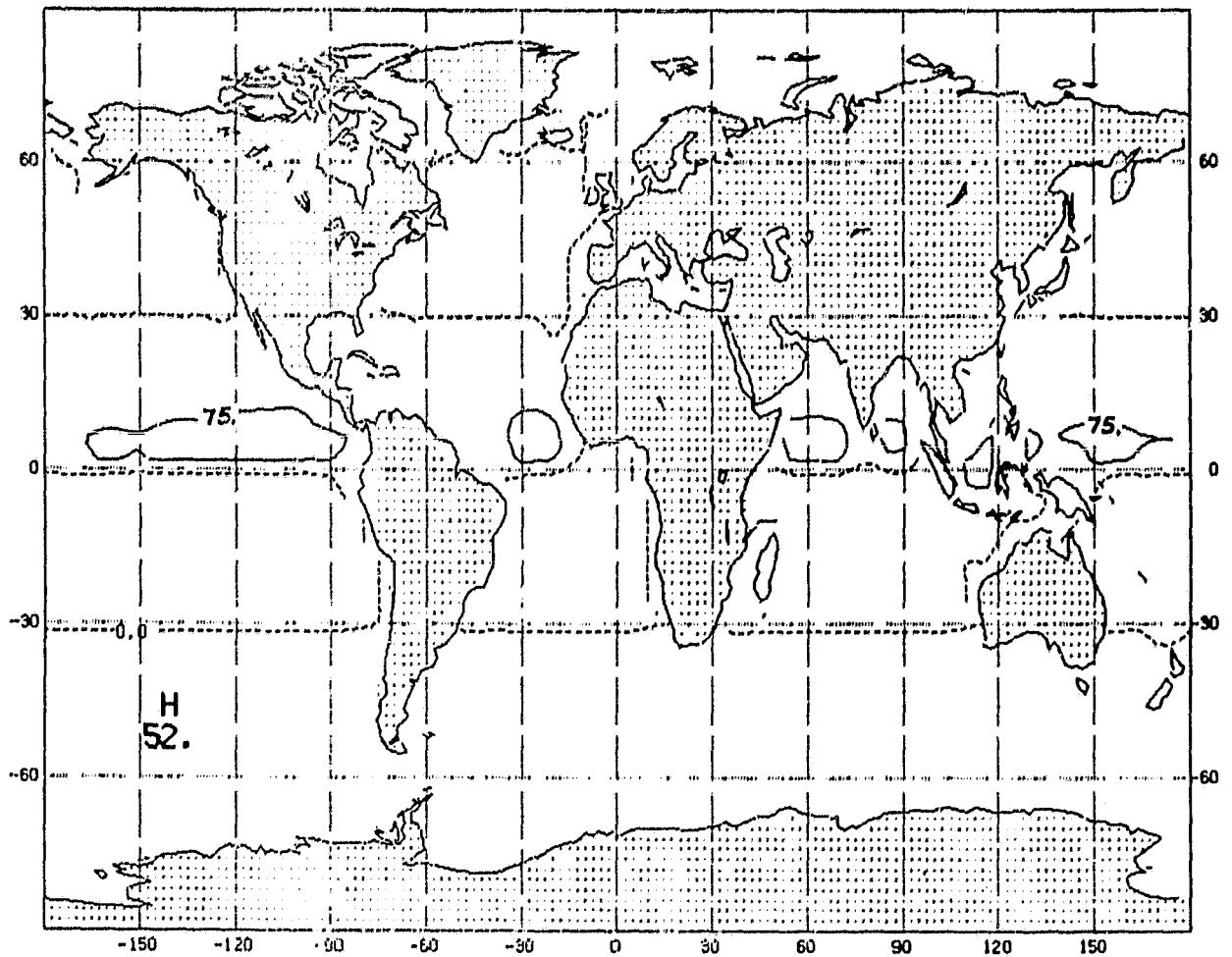
4.2.2 Weekly averaged ML temperature changes after one week for the second case. Contour interval of 1°C

ORIGINAL PAGE IS
OF POOR QUALITY



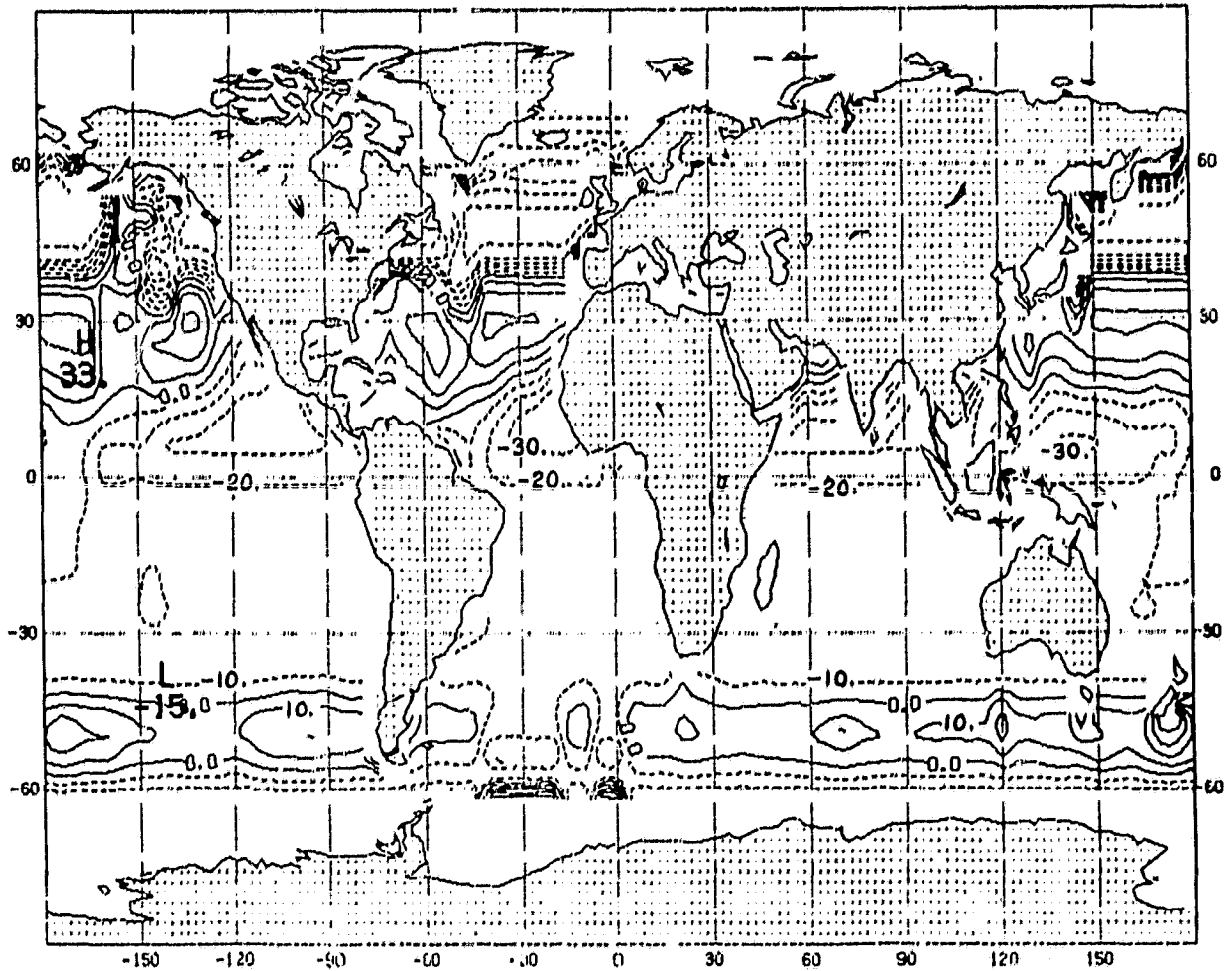
4.2.3 Weekly averaged value of the zonal velocity field, u , after one week for the second case. Contour interval of 75 mm/s

ORIGINAL PAGE IS
OF POOR QUALITY



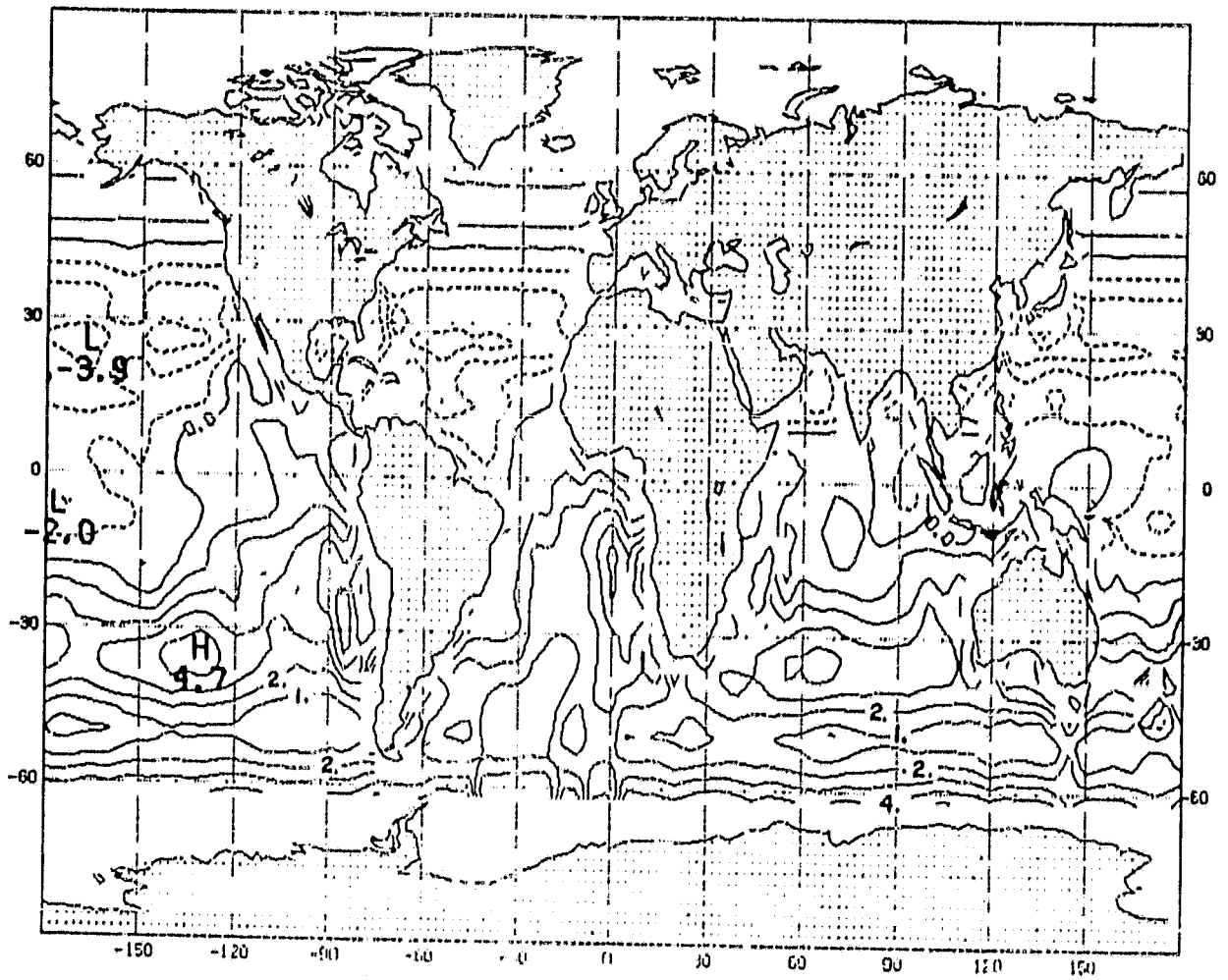
4.2.4 Weekly averaged value of the meridional velocity field, v , after one week for the second case. Contour interval of 75 mm/s

ORIGINAL PAGE IS
OF POOR QUALITY



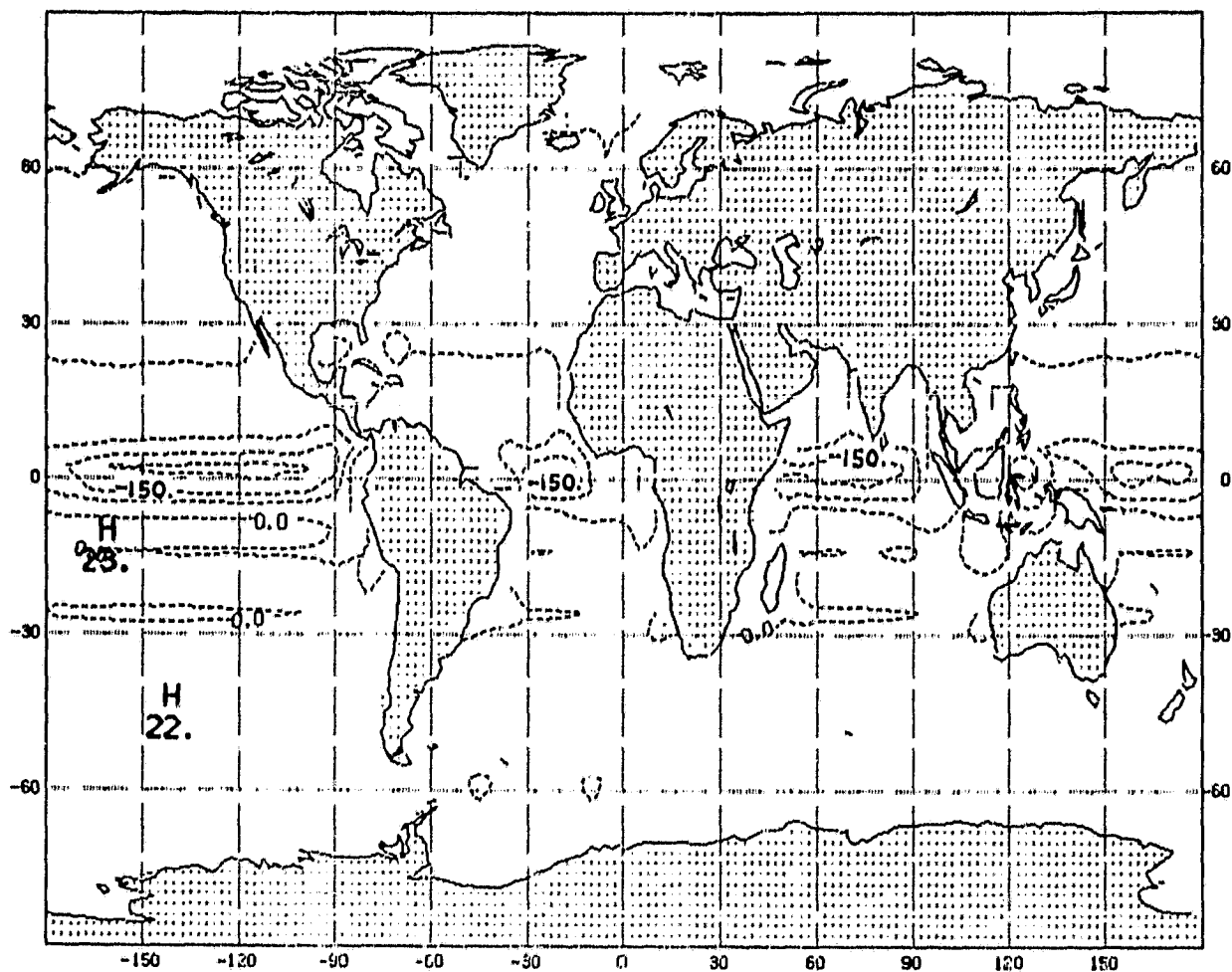
4.2.5 Weekly averaged ML depth changes after five weeks for the second case.
Contour interval of 10 m

ORIGINAL PAGE IS
OF POOR QUALITY



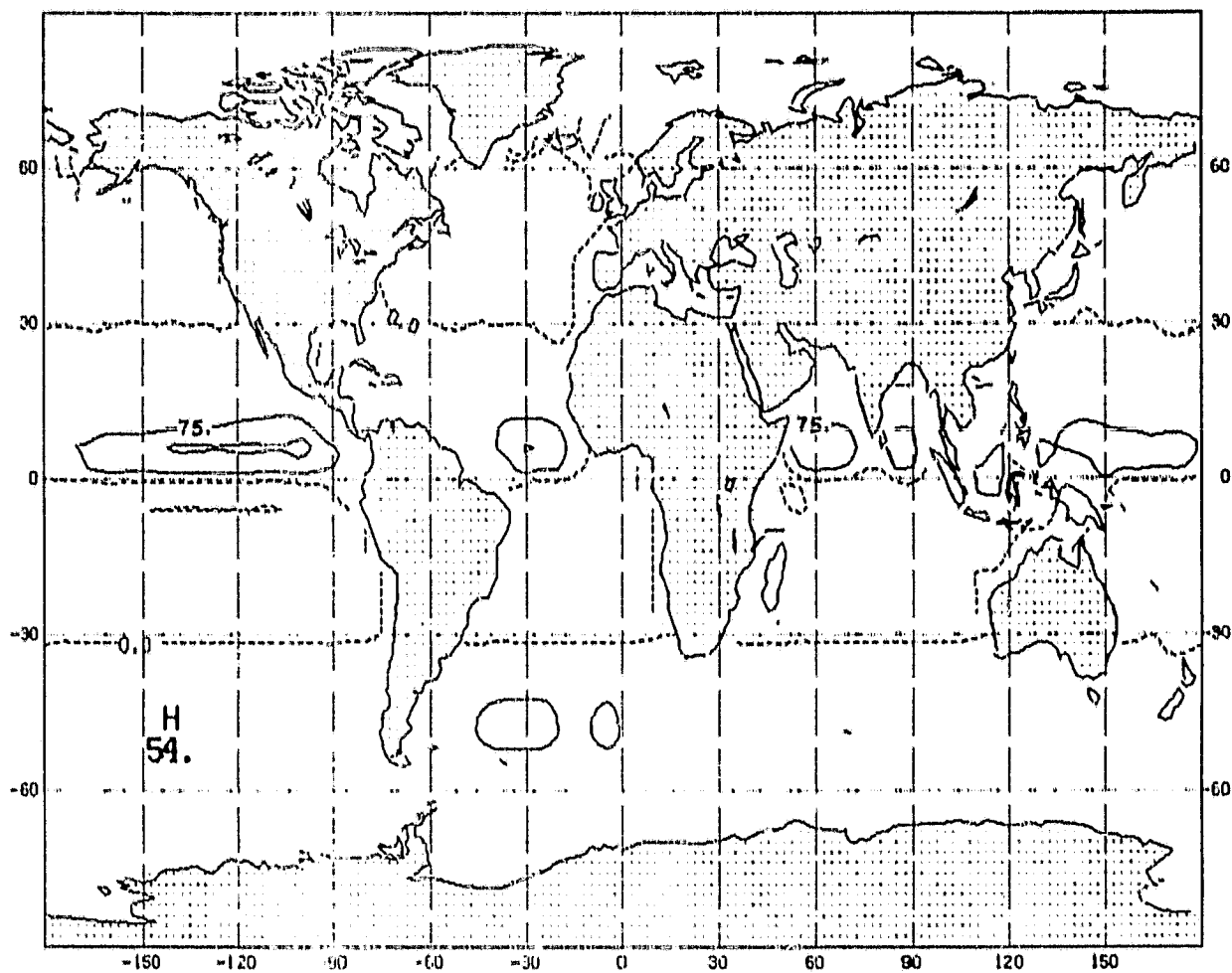
4.2.6 Weekly averaged ML temperature changes after five weeks for the second case. Contour interval of 1°C

ORIGINAL PAGE IS
OF POOR QUALITY



4.2.7 Weekly averaged value of the zonal velocity field, u , after five weeks for the second case. Contour interval of 75 mm/s

ORIGINAL PAGE IS
OF POOR QUALITY



4.2.8 Weekly averaged value of the meridional velocity field, v , after five weeks for the second case. Contour interval of 75 mm/s

of surface heat balance. This is reflected in the shallowing of the mixed layer observed north of 35°N (Figure 4.2.5). Similarly, the shallowing observed south of 15°N should be attributed to the very moderate winds in this region and warming by the surface heat flux. As in the previous case, the shallowing of the mixed layer is interrupted by a deepening observed between 40°S and 55°S . It is also observed that the increase in temperature in that belt is somewhat intense ($2\text{--}3^{\circ}\text{C}$) and it can be stated that in the belt of 40°S to 55°S the effects of the surplus of surface heat balance and the strong winds do not tend to balance each other as far as the temperature field is concerned.

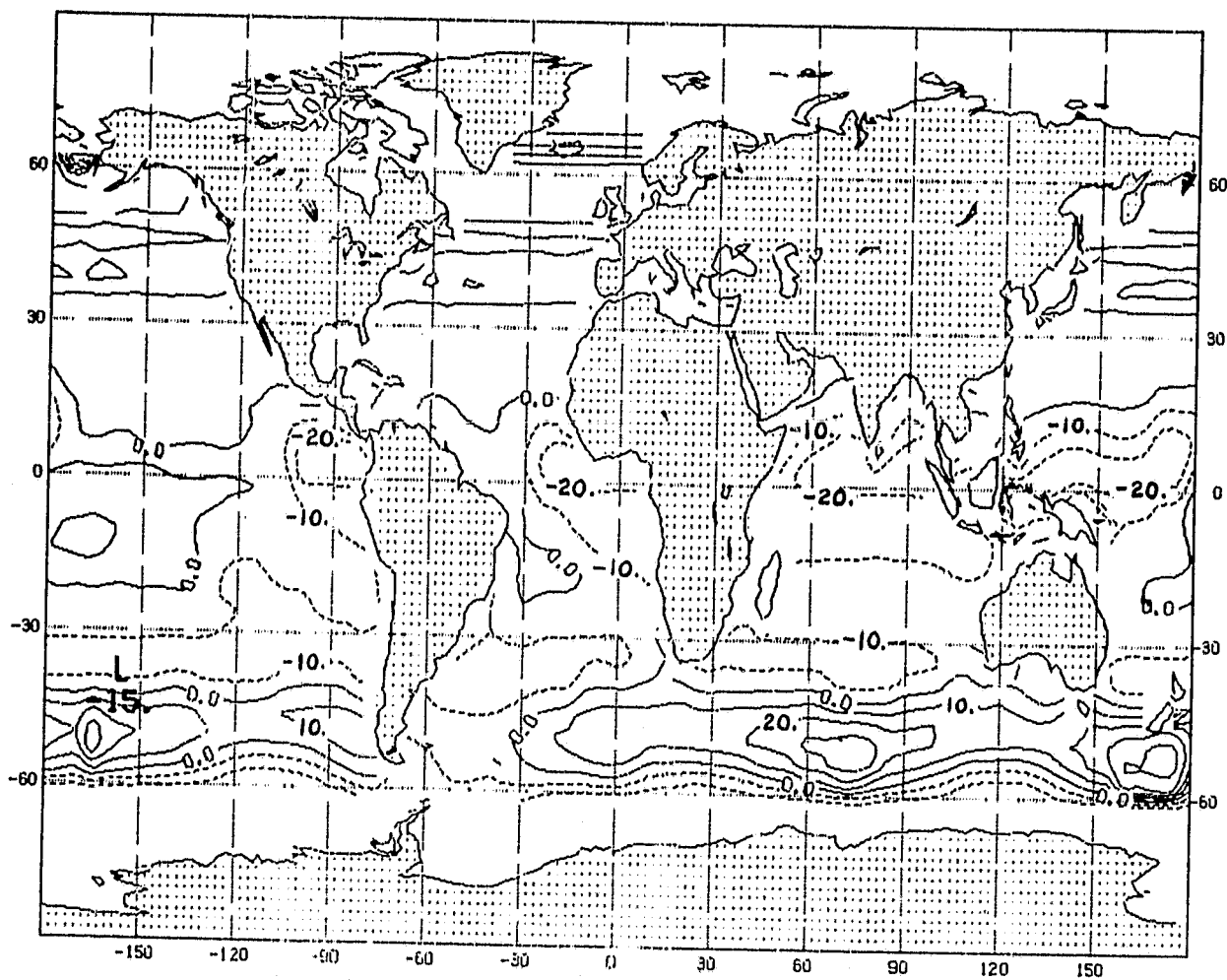
Third Case: (zonally averaged initial conditions, zonally averaged heat flux, time averaged, but not zonally averaged wind stress and friction velocity)

For the same reasons as before I will limit my analysis to the five week results. The results after one week (Figs. 4.3.1-4.3.4) are also included for reference.

In Figure 4.3.5, a deepening of the mixed layer in the north-central Pacific and extra-tropical northern Atlantic is observed. Thus the zonal asymmetry in the oceanic boundary layer height reflects the zonal asymmetry in the friction velocity (Figures 4.3.5 and 3.9).

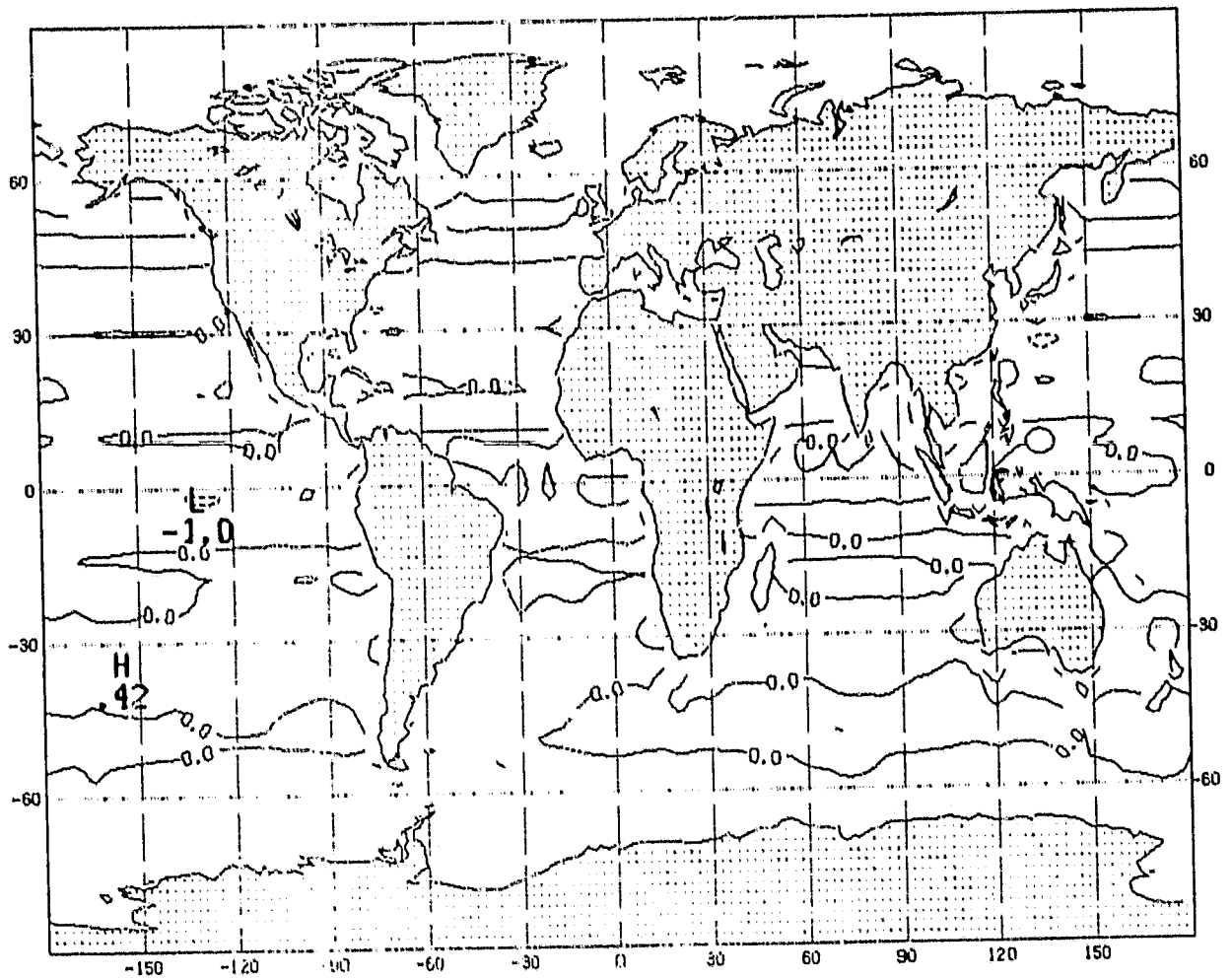
Since the deficit of solar radiation north of 40°N is weak (Figure 3.3), no net change in the deepening or shallowing of the mixed layer occurs. The shallowing of the mixed layer west of South and Central America is due to the presence of very light winds. The same effect is observed in most of the South Atlantic. In this particular case, in the belt between 40°S and 60°S , the deepening of the mixed layer is stronger than in the previous cases as a direct result of stronger westerly winds. The shallowing of the mixed layer observed in the northern and central Indian Ocean is due to the presence of very light to moderate easterly winds, combined with a surplus of solar radiation.

ORIGINAL PAGE IS
OF POOR QUALITY



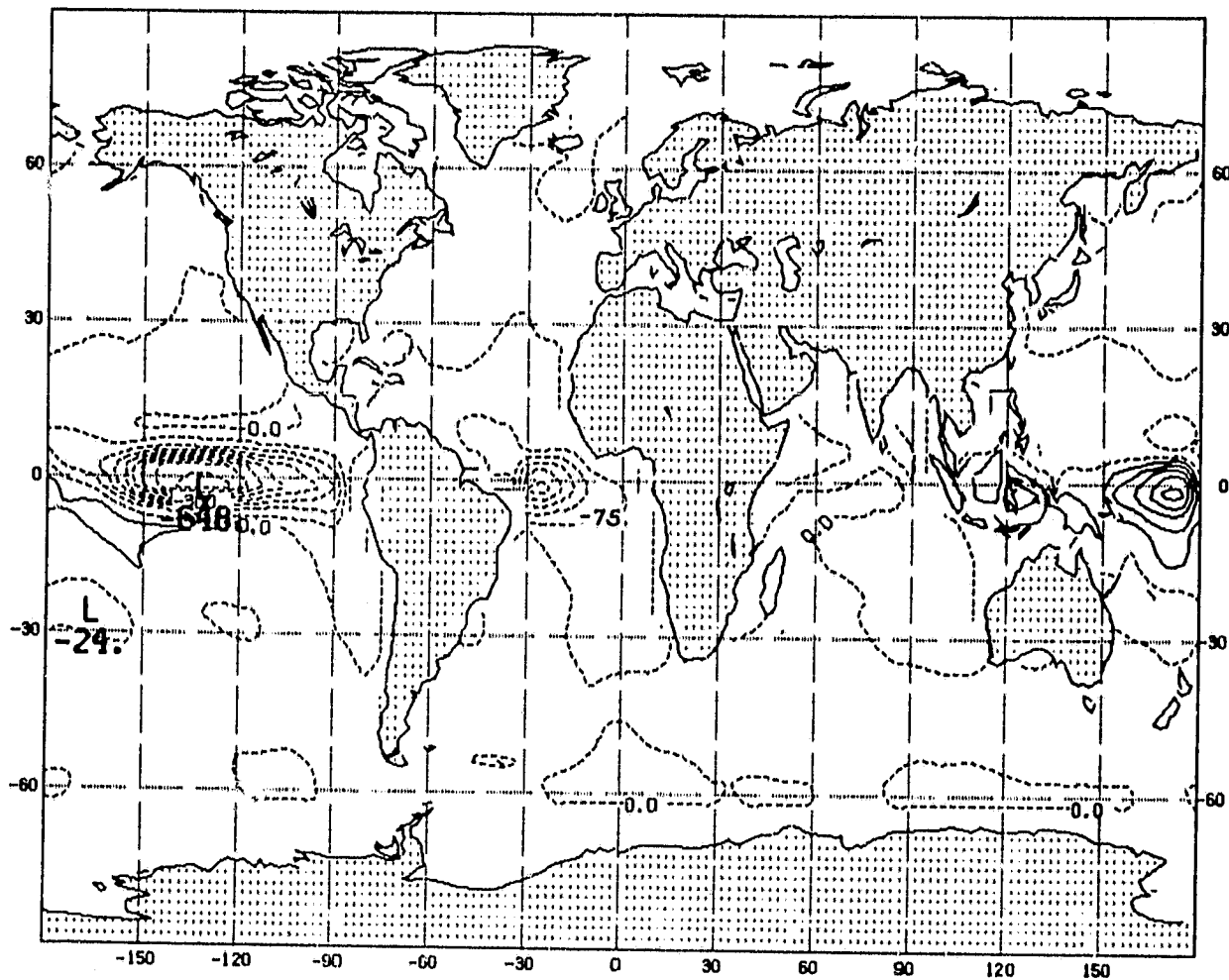
4.3.1 Weekly averaged ML depth changes after one week for the third case.
Contour interval of 10 m

ORIGINAL PAGE IS
OF POOR QUALITY



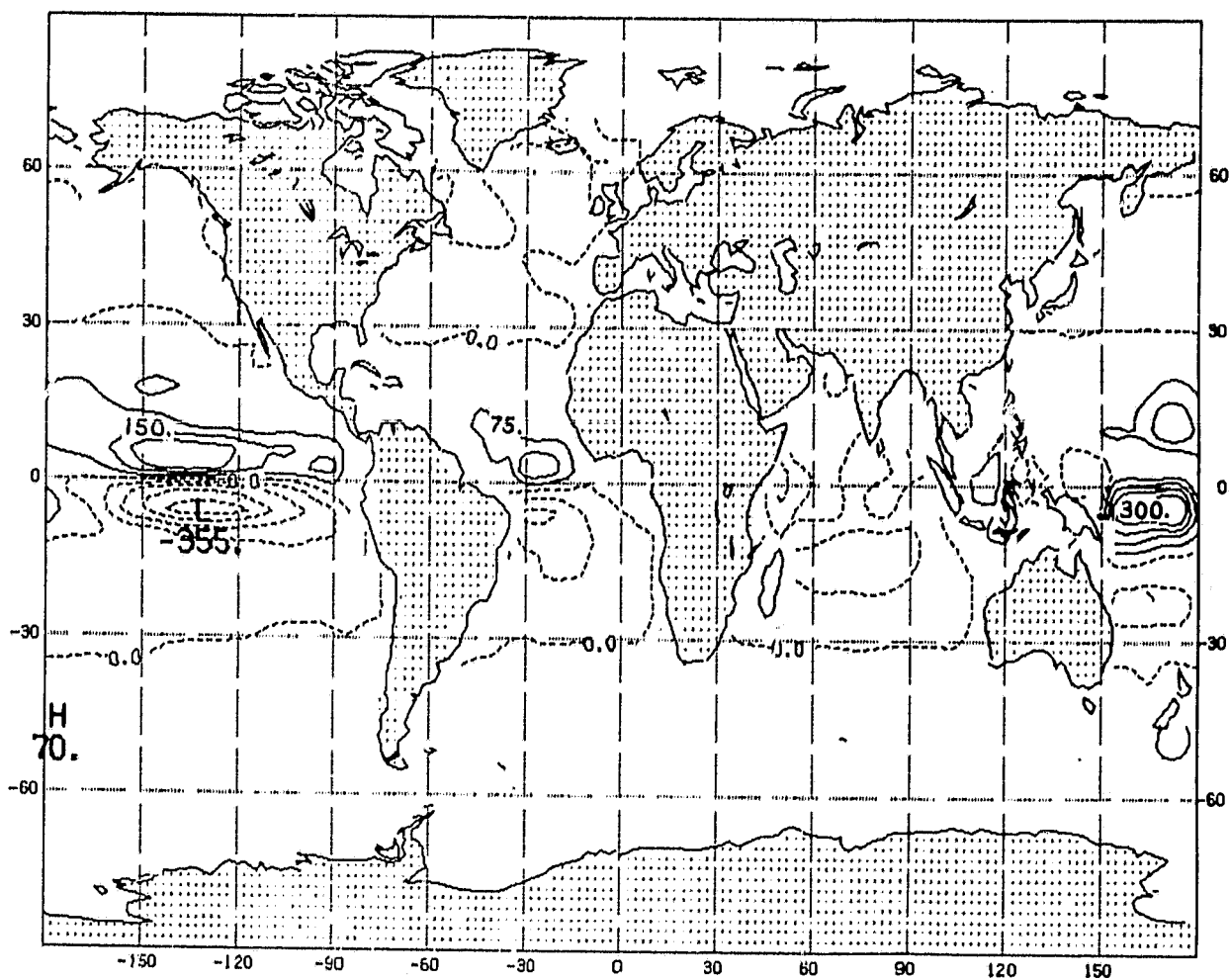
4.3.2 Weekly averaged ML temperature changes after one week for the third case. Contour interval of 1°C

ORIGINAL PAGE 19
OF POOR QUALITY



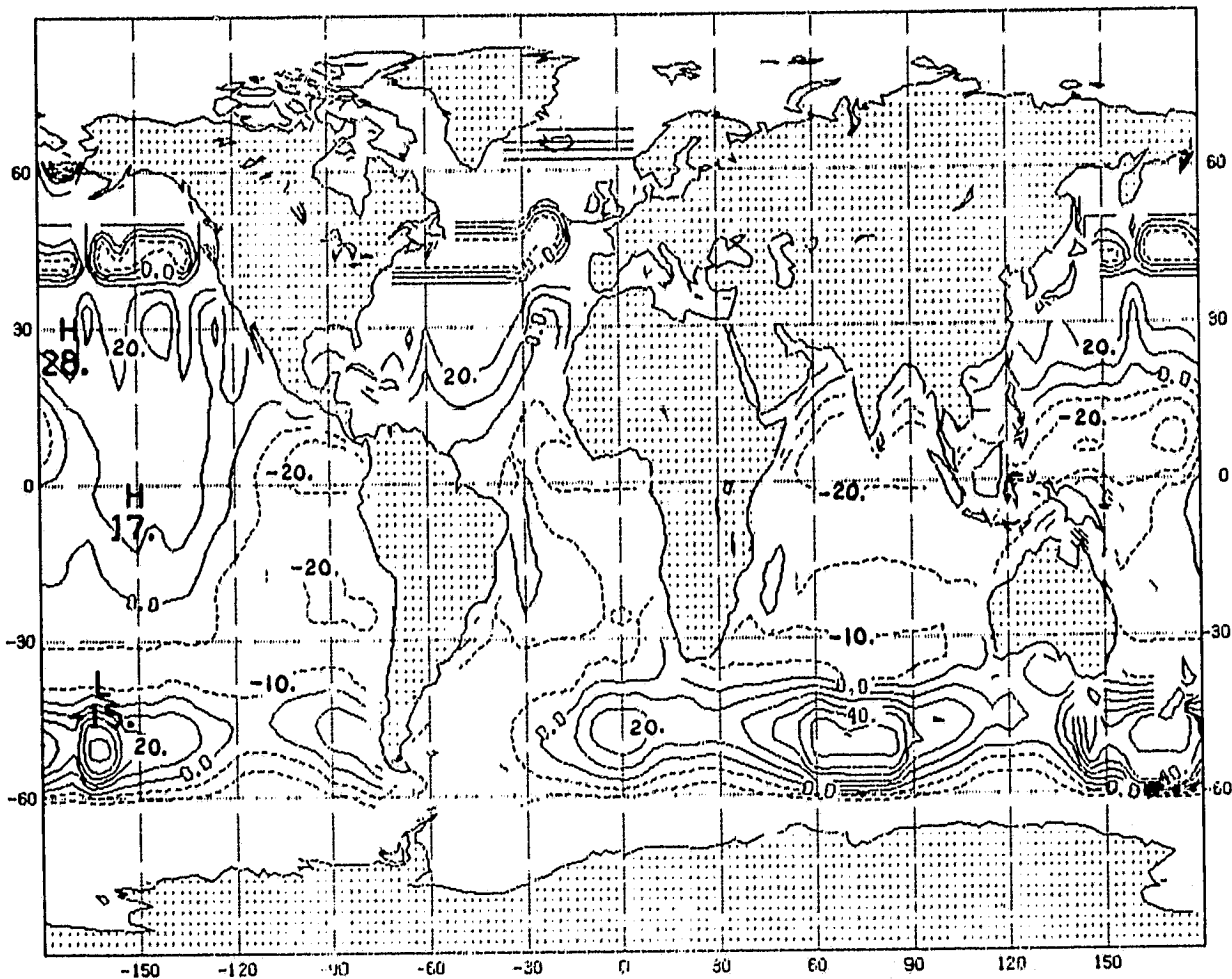
4.3.3 Weekly averaged value of the zonal velocity field, u , after one week for the third case. Contour interval of 75 mm/s

ORIGINAL PAGE IS
OF POOR QUALITY



4.3.4 Weekly averaged value of the meridional velocity field, v , after one week for the third case. Contour interval of 75 mm/s

ORIGINAL PAGE IS
OF POOR QUALITY



4.3.5 Weekly averaged ML depth changes after five weeks for the third case. Contour interval of 10 m

ORIGINAL PAGE IS
OF POOR QUALITY

The sharp decrease in temperature in the Atlantic and Pacific Oceans at the equator should be attributed to the equatorial upwelling (Figures 4.3.6, 4.3.7 and 4.3.8) and by advection by the meridional wind. The increase in temperature south of 30°S should be to the surplus of the surface heat balance, the effects of which outweigh the effect of the wind stress. On the other hand, in the Atlantic and Pacific the decrease in temperature observed in the northern hemisphere up to 45°N should be attributed to the deficit of surface heat balance (Figure 3.3).

Fourth Case: (Time averaged but not zonally averaged heat flux, wind stress and friction velocity)

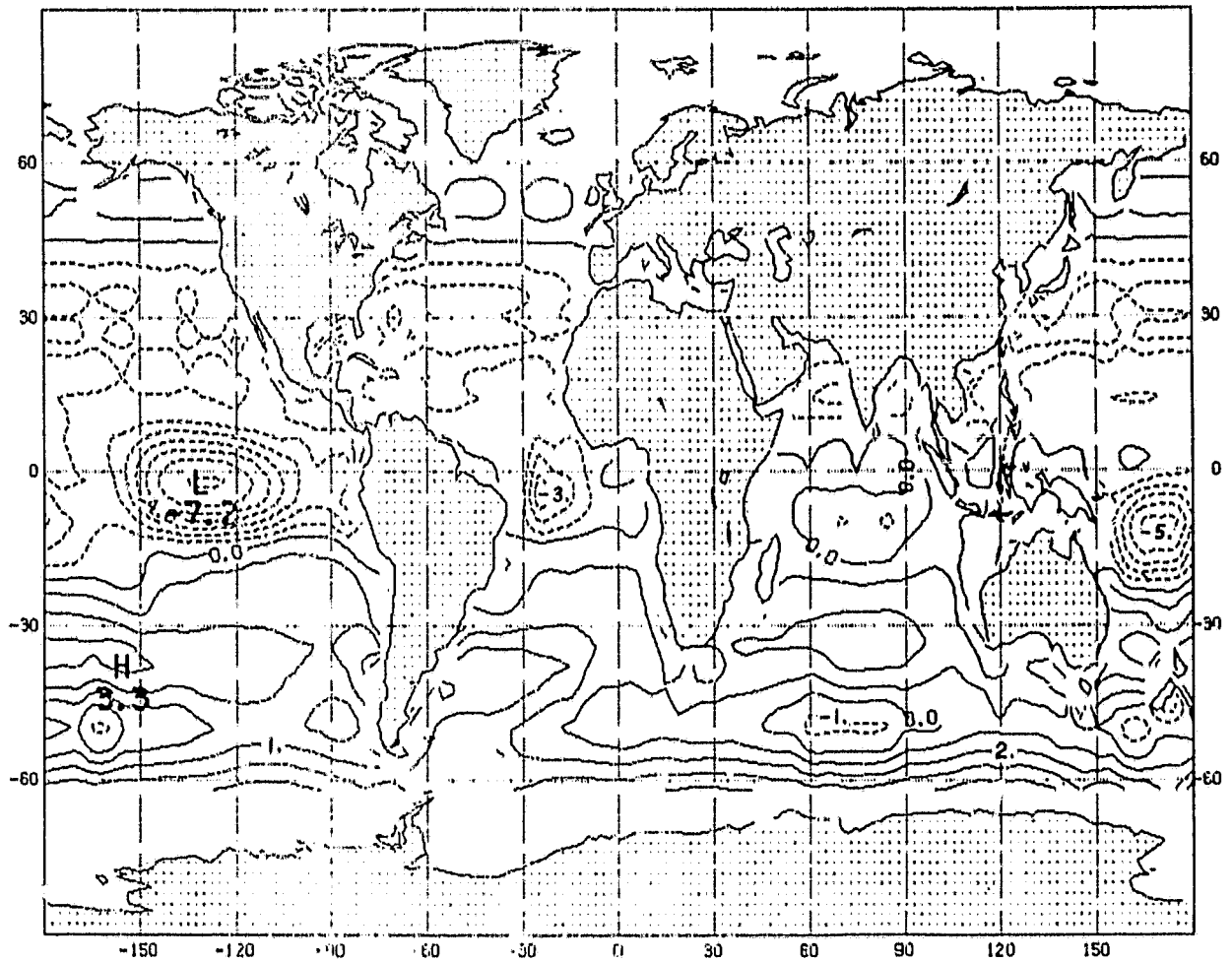
In these last two cases we will examine the differences between the first and fifth week results in more detail.

The first set of pictures we are going to analyze details the mixed layer depth and temperature fields after one week. Figure 4.4.1 shows a uniform global deepening of the mixed layer depth in the latitudes 40°S to 50°S . At the same time and in the same place, we can observe a slight cooling (Figure 4.4.2). In this region the effects of the strong westerly winds are almost balanced by the surplus of surface heat balance.

The shallowing of the mixed layer observed west of Central America and in the South Pacific is due to the combination of light winds and the surplus of surface heating. An increase in the SST is also observed. The deepening of the mixed layer observed in the central tropical Pacific can be explained by the stronger and more persistent easterlies (Figure 3.10). No net change of temperature is observed in that region, since the effects of the surplus of surface heat balance tend to counterbalance the effects of the stronger easterly winds.

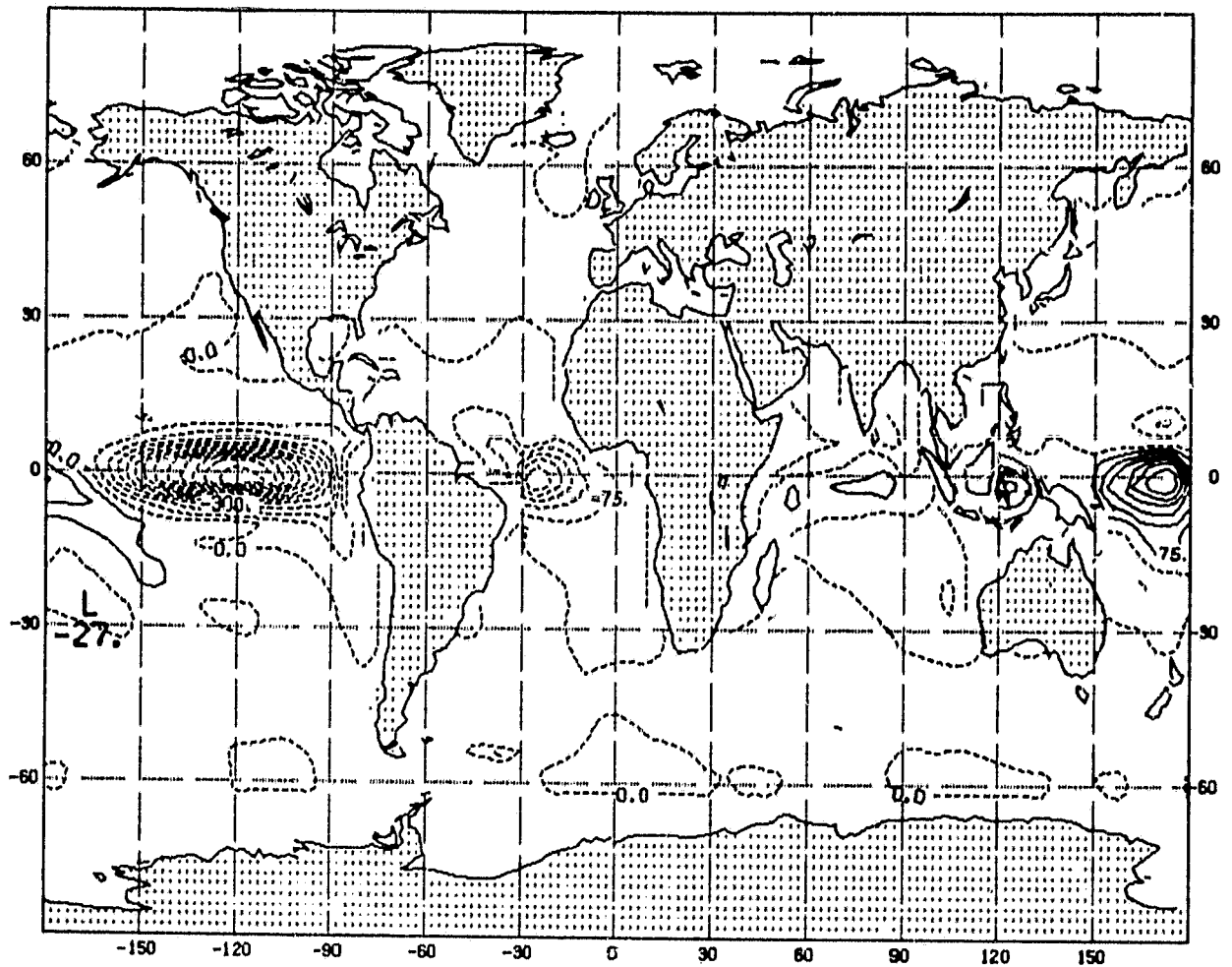
A shallowing of the mixed layer in the north and central Indian Ocean is caused by the effects of the light and variable winds, and the surplus of

ORIGINAL PAGE 13
OF POOR QUALITY



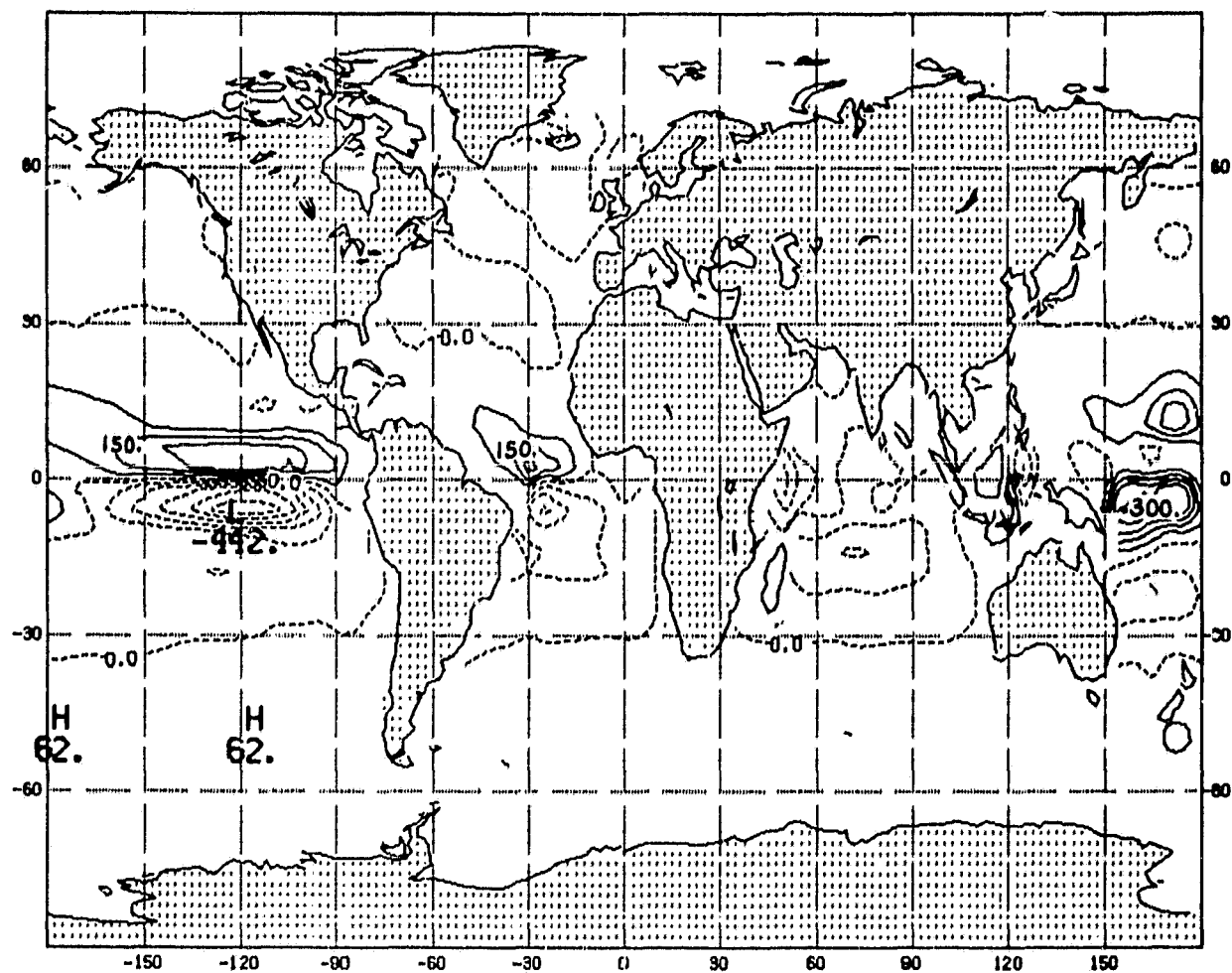
4.3.6 Weekly averaged ML temperature changes after five weeks for third case. Contour interval of 1°C

ORIGINAL PAGE IS
OF POOR QUALITY



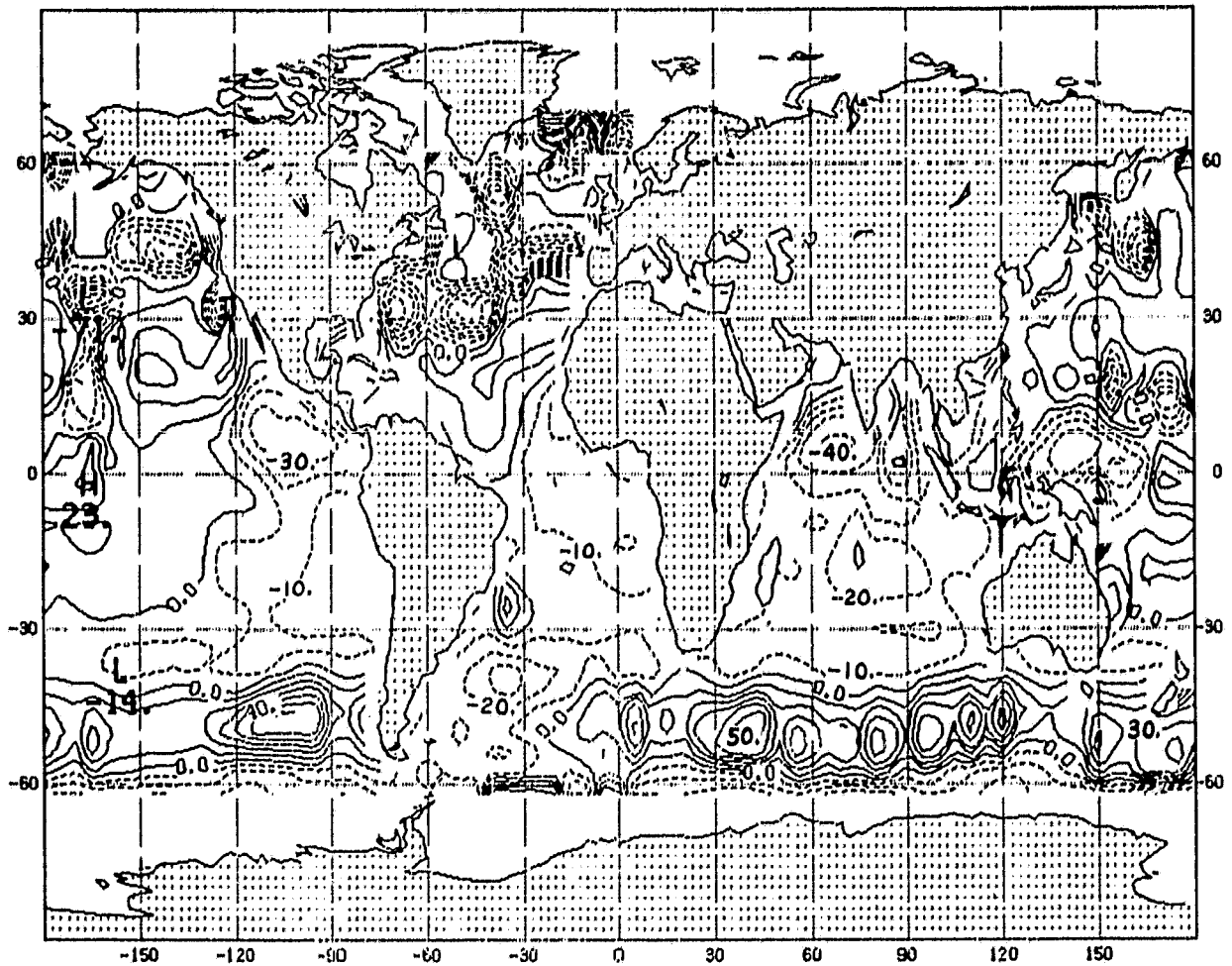
4.3.7 Weekly averaged value of the zonal velocity field, u , after five weeks for the third case. Contour interval of 75 mm/s

ORIGINAL PAGE IS
OF POOR QUALITY



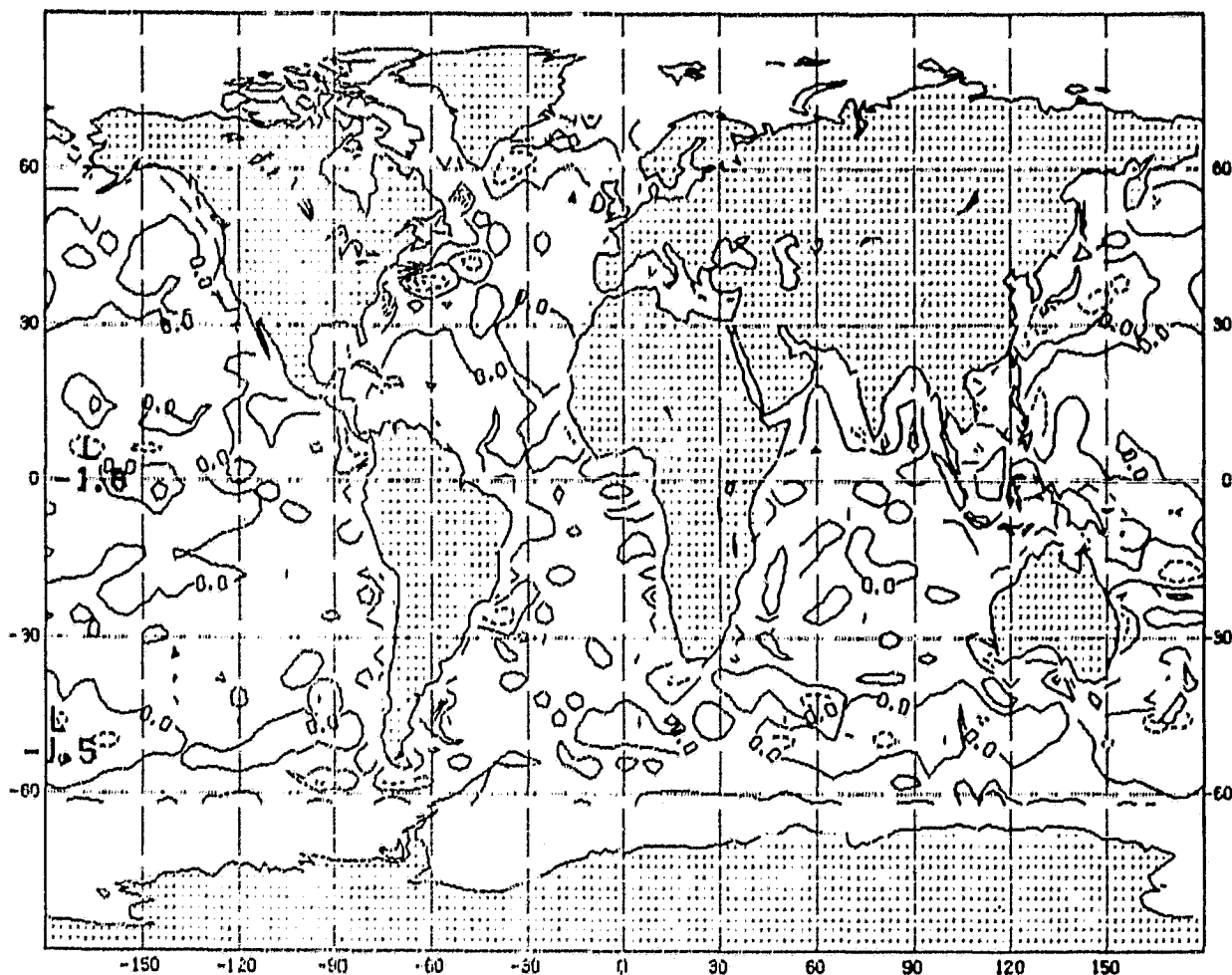
4.3.8 Weekly averaged value of the meridional velocity field, v , after five weeks for the third case. Contour interval 75 mm/s

ORIGINAL PAGE 13
OF POOR QUALITY



4.4.1 Weekly averaged ML depth changes after one week for the fourth case. Contour interval of 10 m

ORIGINAL PAGE IS
OF POOR QUALITY



4.4.2 Weekly averaged ML temperature changes after one week for the fourth case. Contour interval of 1°C

surface heat balance. These two factors also contribute to the slight increase in temperature observed in that region. Similar results can be found for most of the south Atlantic.

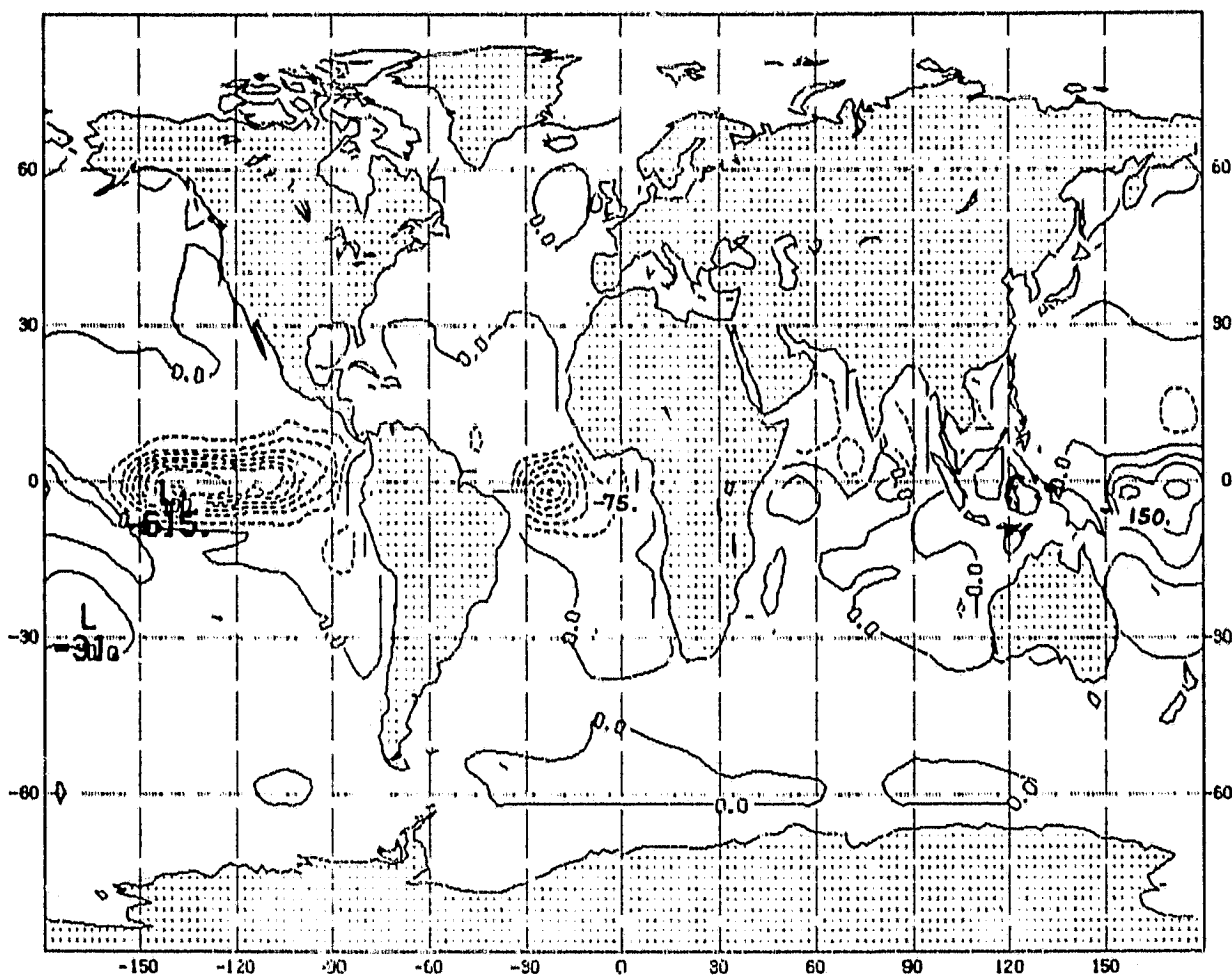
An analysis of the second set of pictures indicates no demonstrable differences in the mixed layer depth between the first and fifth weeks (Figures 4.4.1 and 4.4.5). The decrease in temperature observed in the equatorial Pacific is due to the strength of the local equatorial upwelling and the strong easterlies (Figures 4.4.6 and 4.4.8). Because of the surplus of surface heat balance, we observe a significant increase in the temperature field both in the south Atlantic and in the extra-tropical latitudes of the South Pacific, as well as along the western coast of South America. The results after one week are depicted in Figs. 4.4.1-4.4.4; and after five weeks in 4.4.5-4.4.8.

Because the effects of the westerlies are compensated by the surplus of solar heating, which is very strong at these latitudes, the decrease in temperature in the southern belt between 40°S and 50°S is marginal. The decrease in temperature observed both in the tropical Atlantic and Pacific Oceans in the northern hemisphere can be explained by the deficit of surface heat balance and the light and persistent easterlies.

Fifth Case: (Instantaneous values for all atmospheric forcing)

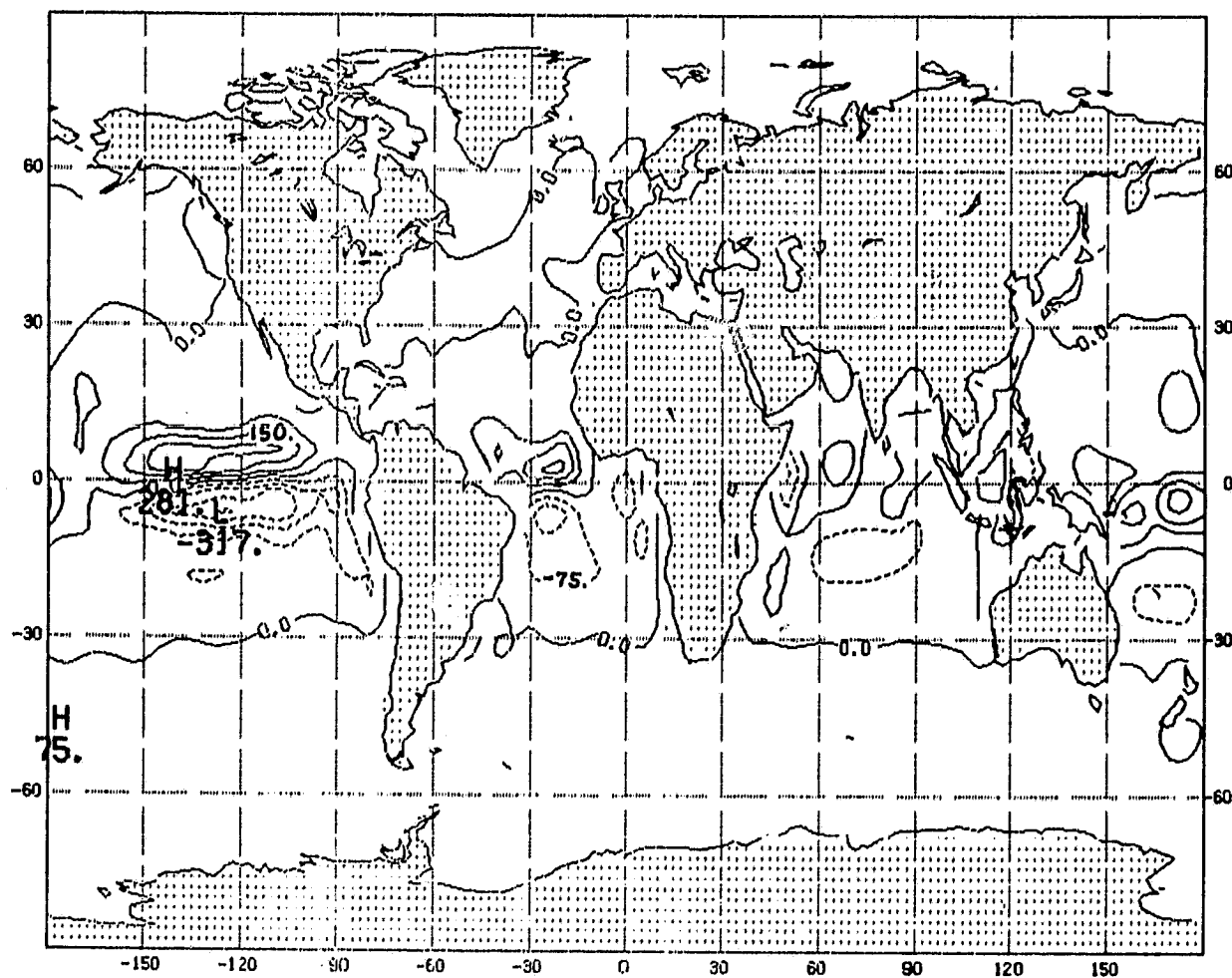
We will begin with an analysis of the one week results (Figs. 4.5.1-4.5.8). In this case, in the belt between 35°S and 60°S the deepening of the mixed layer is well organized globally, (Figures 4.5.5). The changes in temperature after one week are (Fig. 4.5.6) are generally smaller than 1°C . The main exception is near the East coast of North America. It is interesting to notice that the use of time varying wind stress and friction results in smaller changes in ML depth (Fig. 4.4.1). A discontinuous temperature front can be observed to the Southeast of Africa. This front is stronger than in the previous cases.

ORIGINAL PAGE IS
OF POOR QUALITY



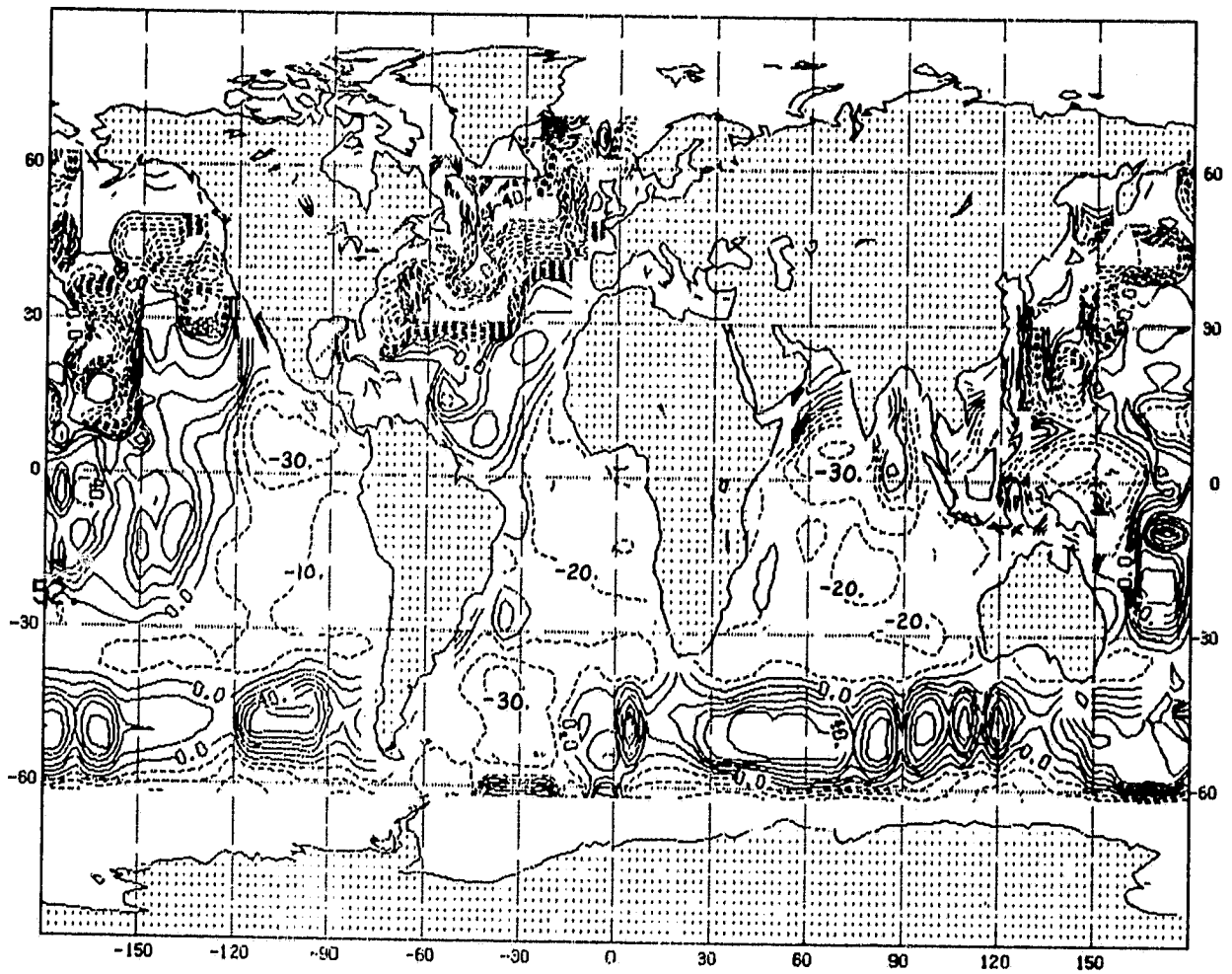
4.4.3 Weekly averaged value of the zonal velocity field, u , after one week for the fourth case. Contour interval of 75 mm/s

ORIGINAL PAGE IS
OF POOR QUALITY



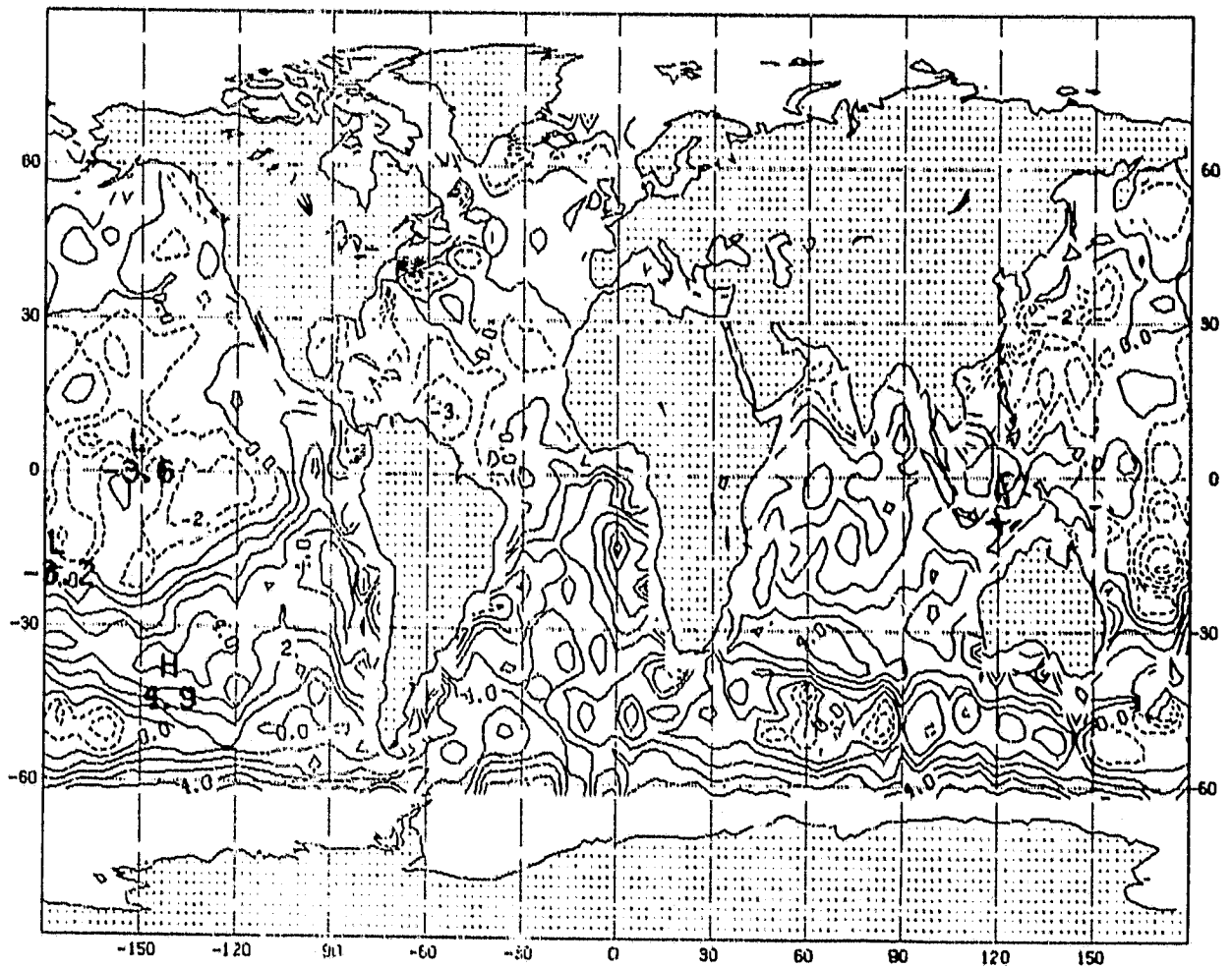
4.4.4 Weekly averaged value of the meridional velocity field, v , after one week for the fourth case. Contour interval of 75 mm/s

ORIGINAL PAGE IS
OF POOR QUALITY



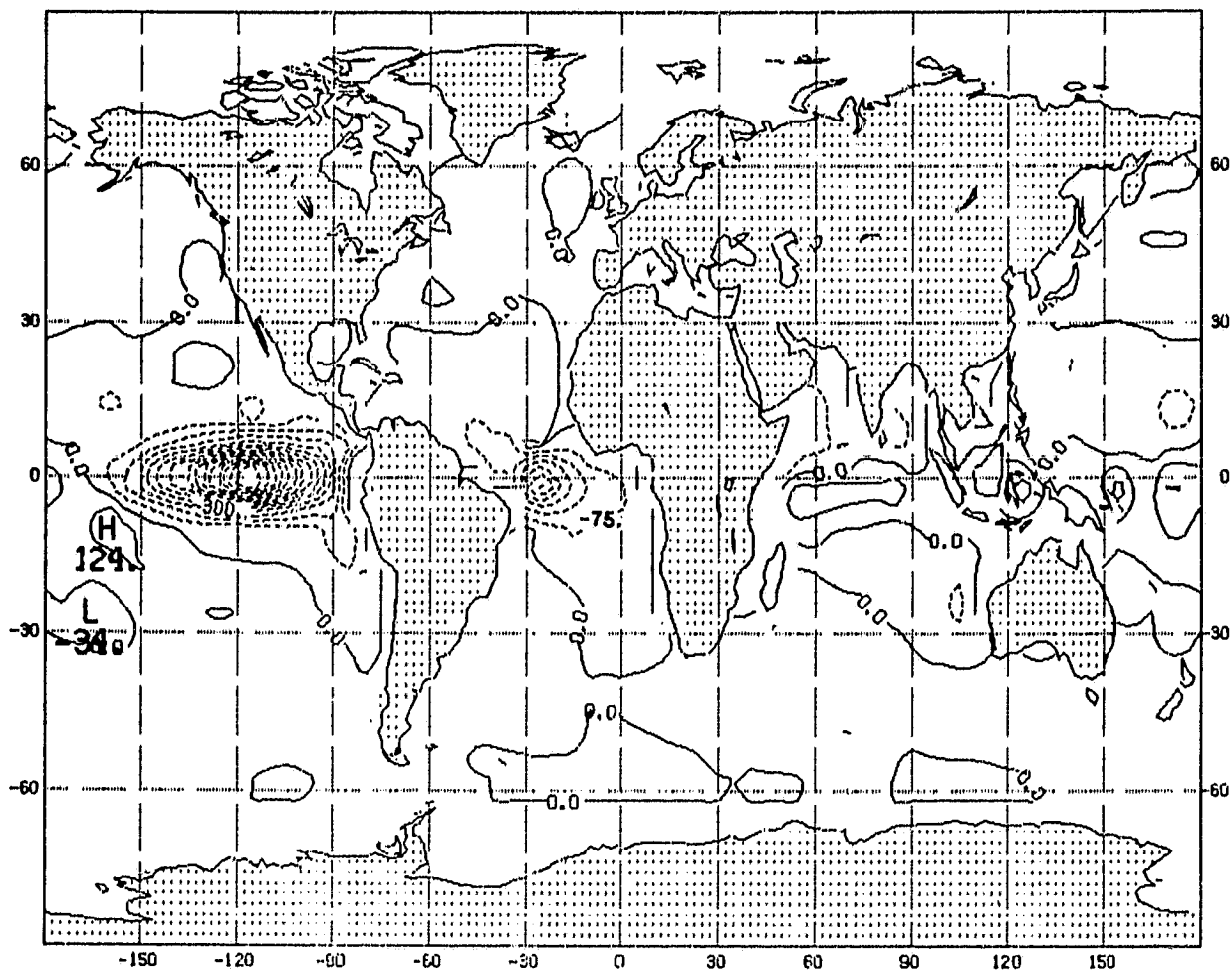
4.4.5 Weekly averaged ML depth changes after five weeks for the fourth case. Contour interval of 10 m

ORIGINAL PAGE 15
OF POOR QUALITY



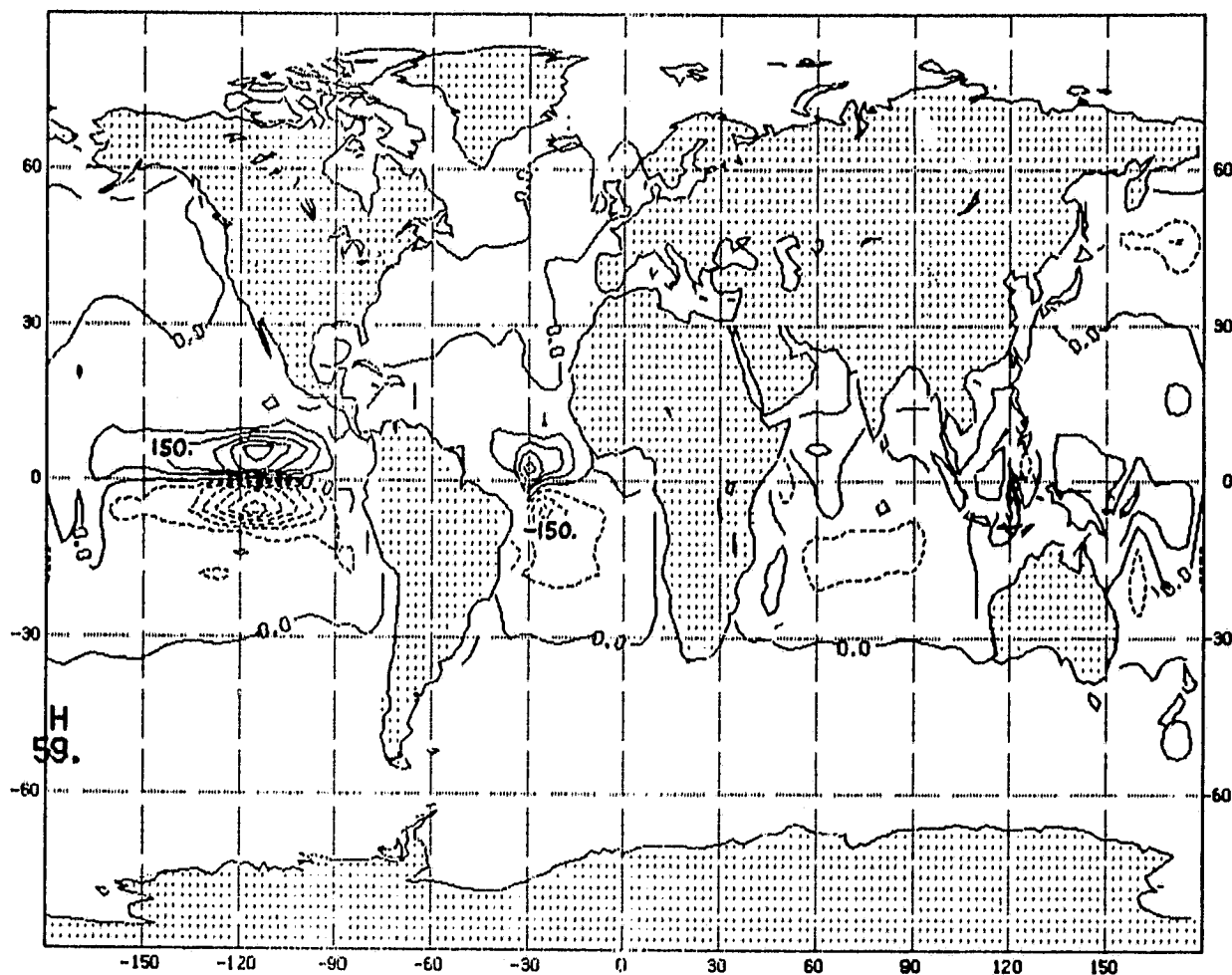
4.4.6 Weekly averaged value ML temperature changes after five weeks for the fourth case. Contour interval of 1° C

ORIGINAL PAGE IS
OF POOR QUALITY



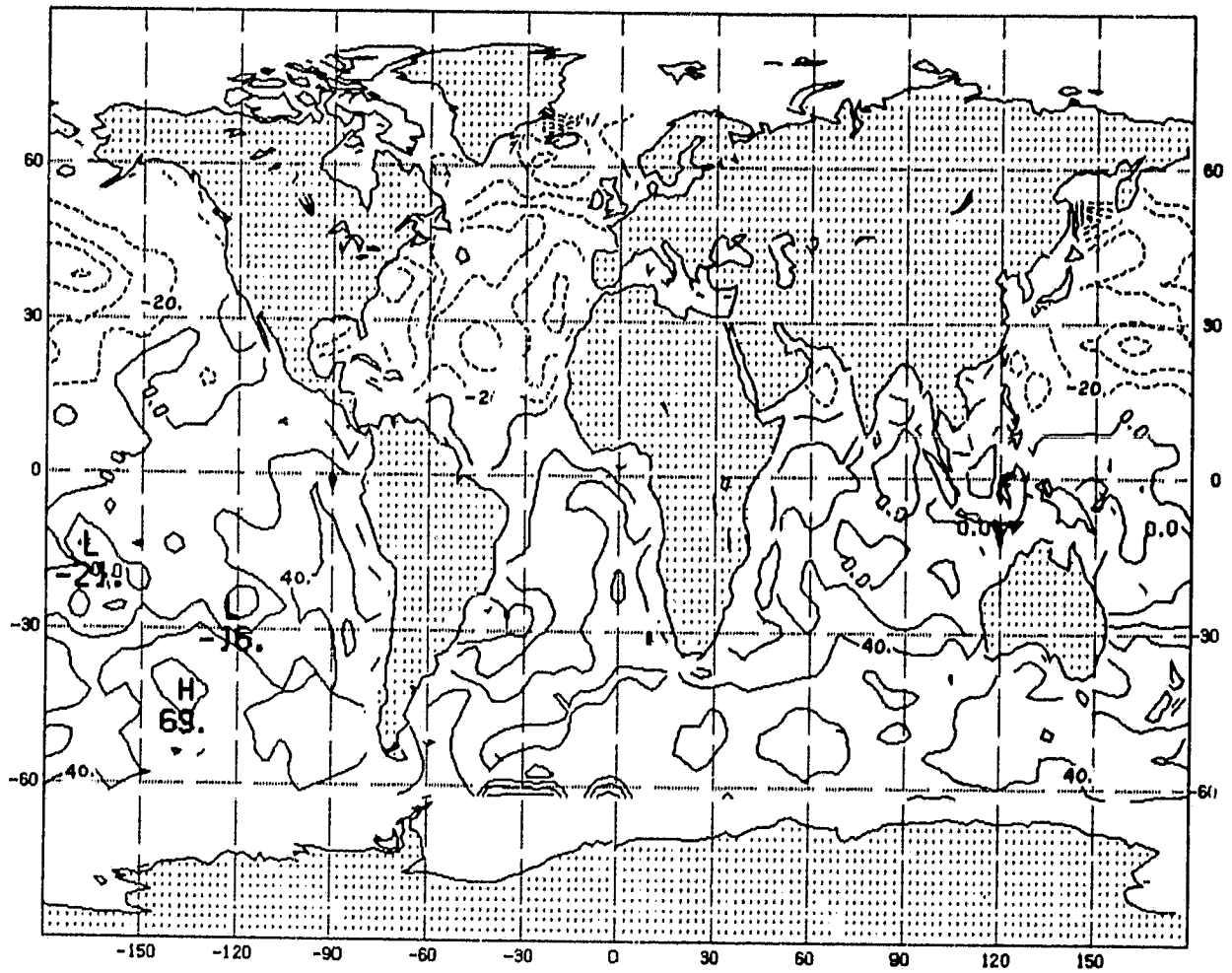
4.4.7 Weekly averaged value of the zonal velocity field, u , after five weeks for the fourth case. Contour interval of 75 mm/s

ORIGINAL PAGE IS
OF POOR QUALITY



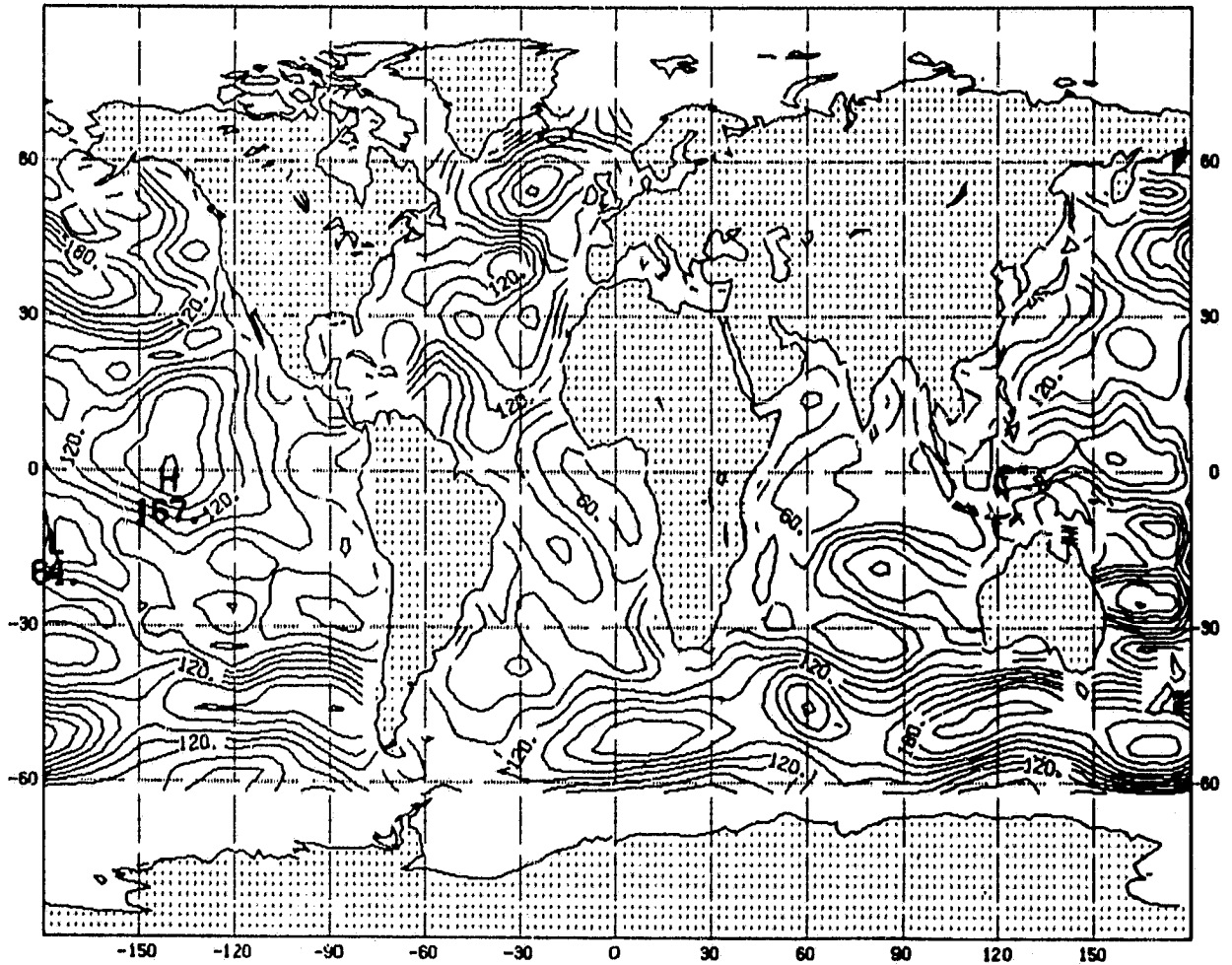
4.4.8 Weekly averaged value for the meridional velocity field, v , after five weeks for the fourth case. Contour interval of 75 mm/s

ORIGINAL PAGE IS
OF POOR QUALITY



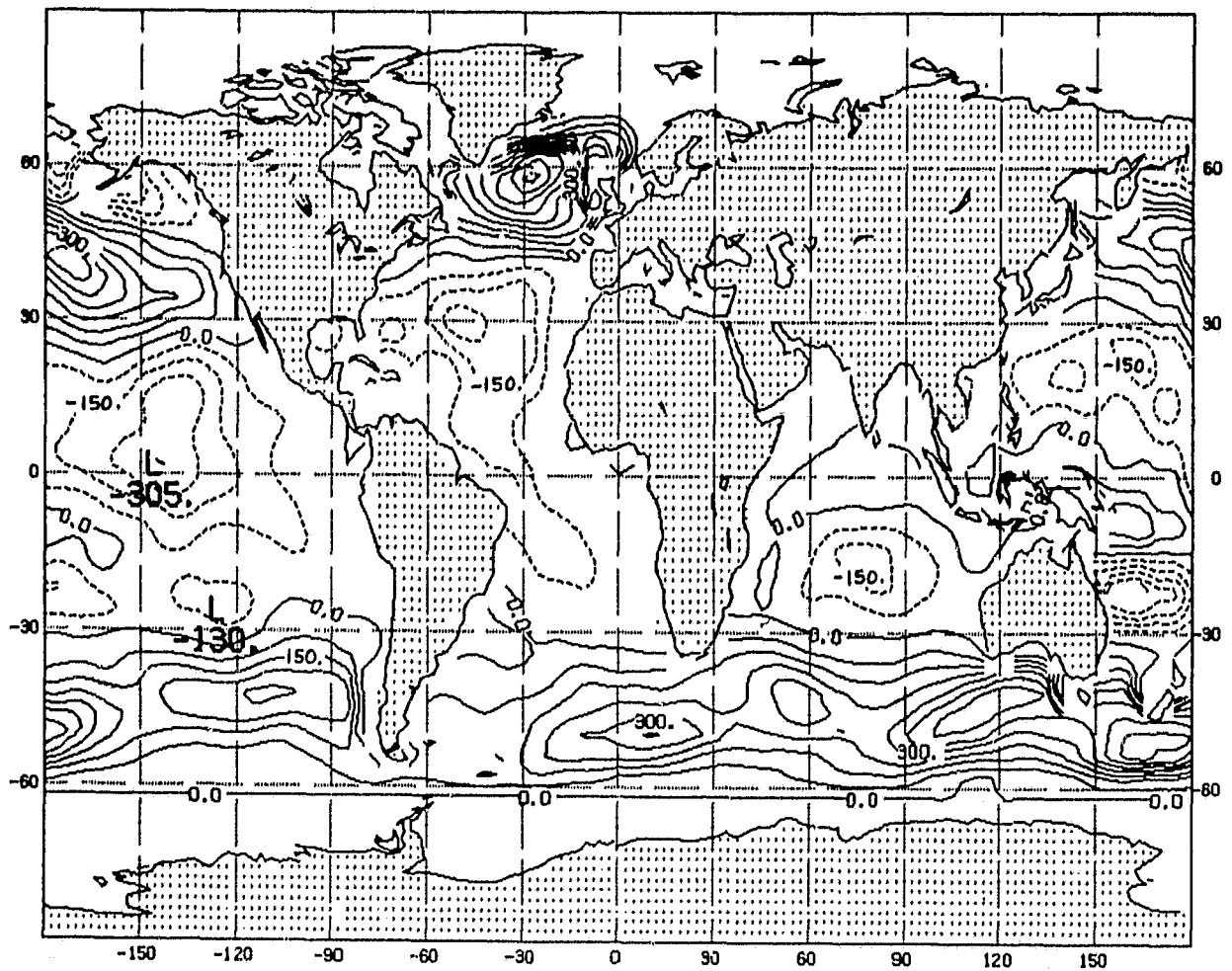
4.5.1 Weekly averaged value of the surface heat balance after one week.
Contour interval of 20 Watts/m²

ORIGINAL PAGE IS
OF POOR QUALITY



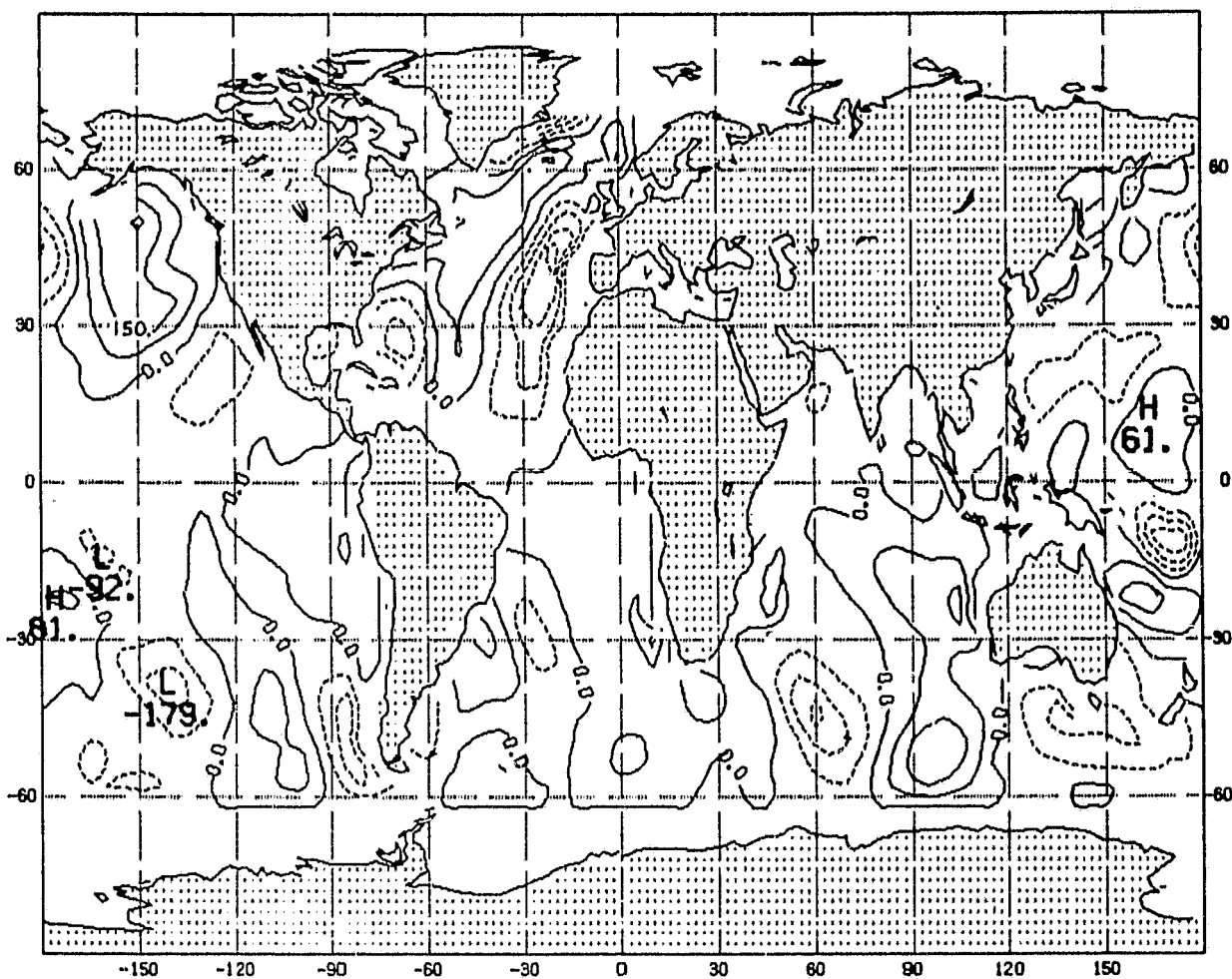
4.5.2 Weekly averaged value of friction velocity after one week.
Contour interval of $15 \cdot 10^{-1} \text{ mm/s}$

ORIGINAL PAGE 11
OF POOR QUALITY



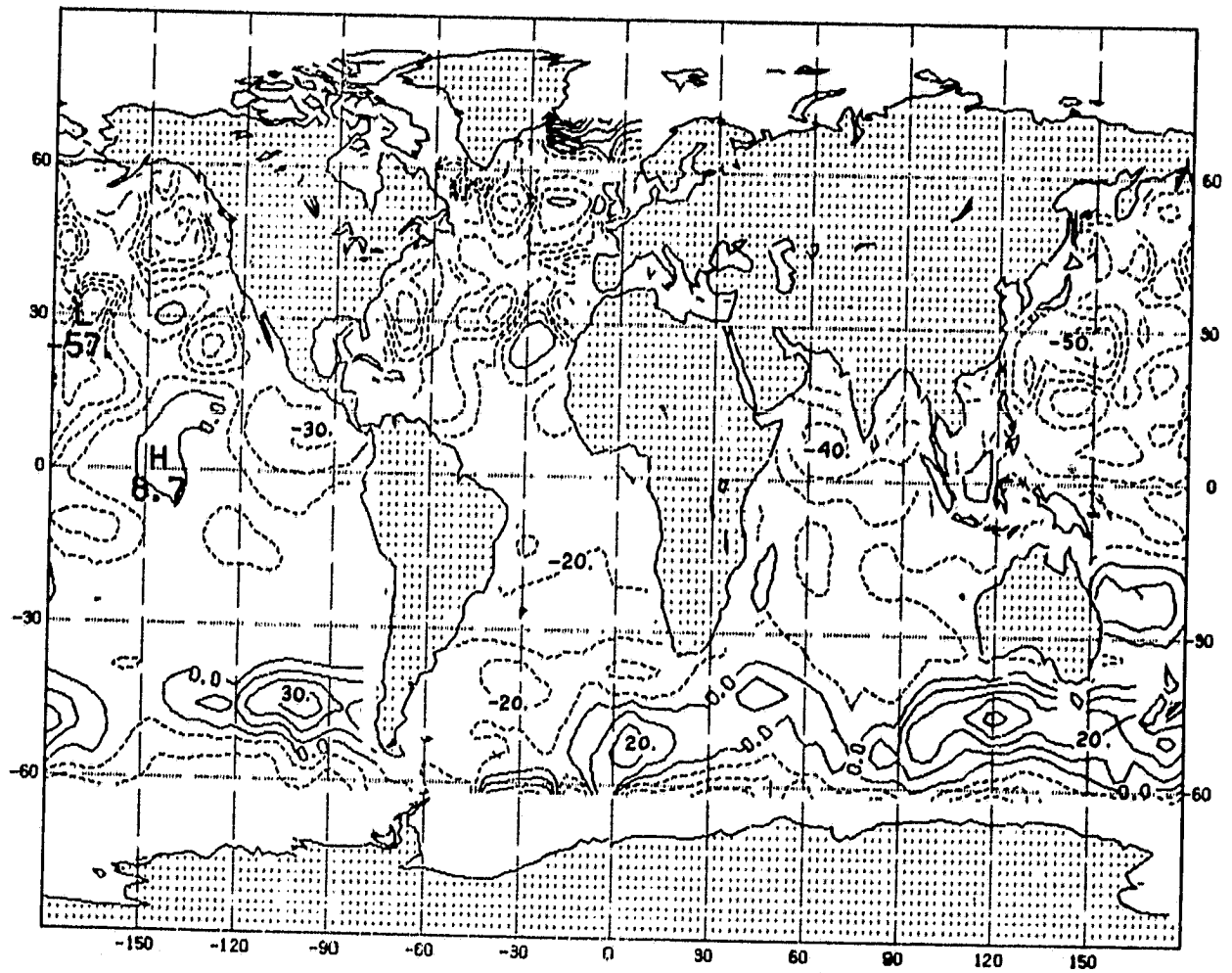
4.5.3 Weekly averaged value of the wind stress in the x direction after one week. Contour interval of $75 \cdot 10^{-3} \text{ N/m}^2$

ORIGINAL PAGE IS
OF POOR QUALITY



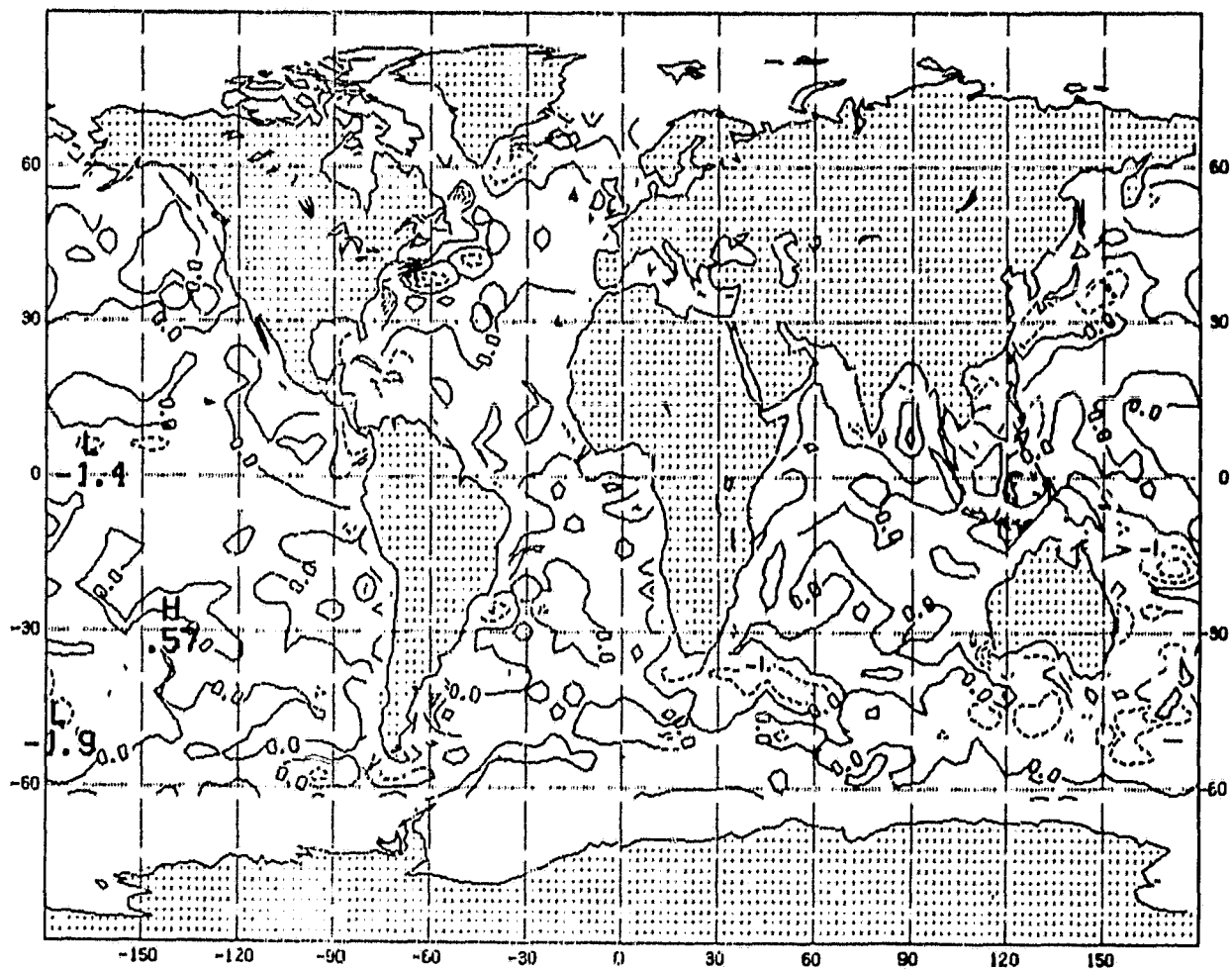
4.5.4 Weekly averaged value of the wind stress in the y direction after one week. Contour interval of $75 \cdot 10^{-3} \text{N/m}^2$

ORIGINAL PAGE IS
OF POOR QUALITY



4.5.5 Weekly averaged ML height changes after one week for the fifth case. Contour interval of 10 m

ORIGINAL PAGE IS
OF POOR QUALITY



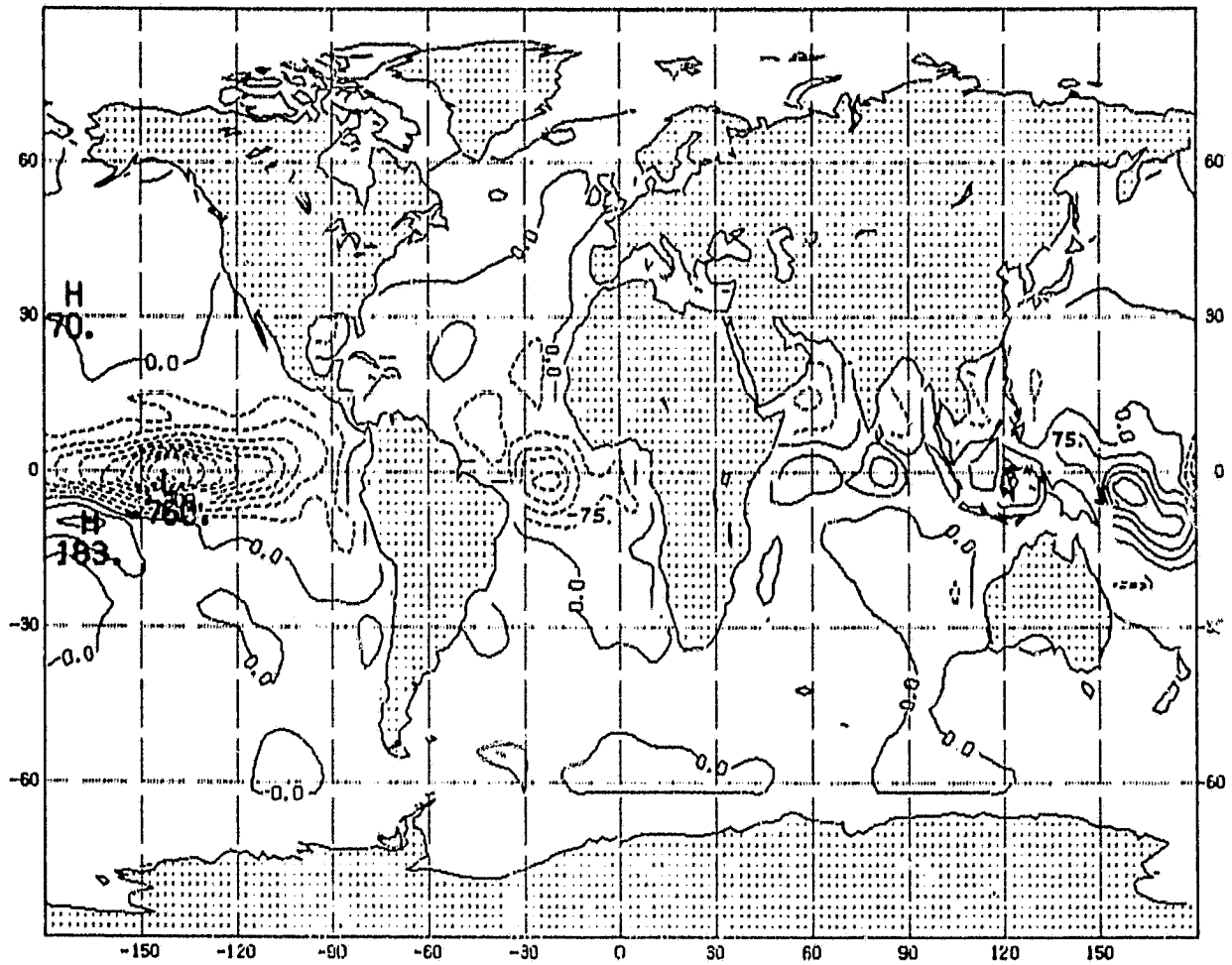
4.5.6 Weekly averaged ML temperature changes after one week for the fifth case. Contour interval of 1°C

After five weeks the deepening at the ML observed in most of the south Atlantic may be explained by the deficit of surface heat balance which counterbalances the effects of the very light easterlies observed in the region. Opposite reasons are valid for the shallowing of the ML observed in the south Pacific down to 40°S (Figures 4.5.9 and 4.5.13). Also very light easterly winds are observed in the south Pacific after five weeks (Figures 4.5.11). As far as the temperature in the north and central Indian Ocean is concerned, the deficit of a strong surface heating balance, combined with the minimal balancing effects of the light winds, produces a decrease in the temperature fields. The light winds do not balance the deficit of a strong surface heating balance, thus decrease in the temperature fields (Figures 4.5.14). Because of the absence of easterly winds west of southern Africa, we observe a great increase in the SST. The same is true of the west of South America. Furthermore, north of 10°S the deficit of heat balance produces a decrease in the SST in the Atlantic Ocean up to 35°N . Results for the fifth week are depicted in Figs. 4.5.8-4.5.14.

This decrease in temperature is not as remarkable in the Pacific Ocean because of a strong surplus of surface heat balance. The presence of moderate easterly winds tends to counterbalance the effects of the surplus of surface heat balance in the belt between 10°N and 30°N in the Central Pacific, explaining the slight decrease in the SST observed in that area. North of 30°N , in the same Pacific Ocean, the surplus of surface heating tends to counterbalance the effects of the westerlies, thus generating no net change in the temperature fields.

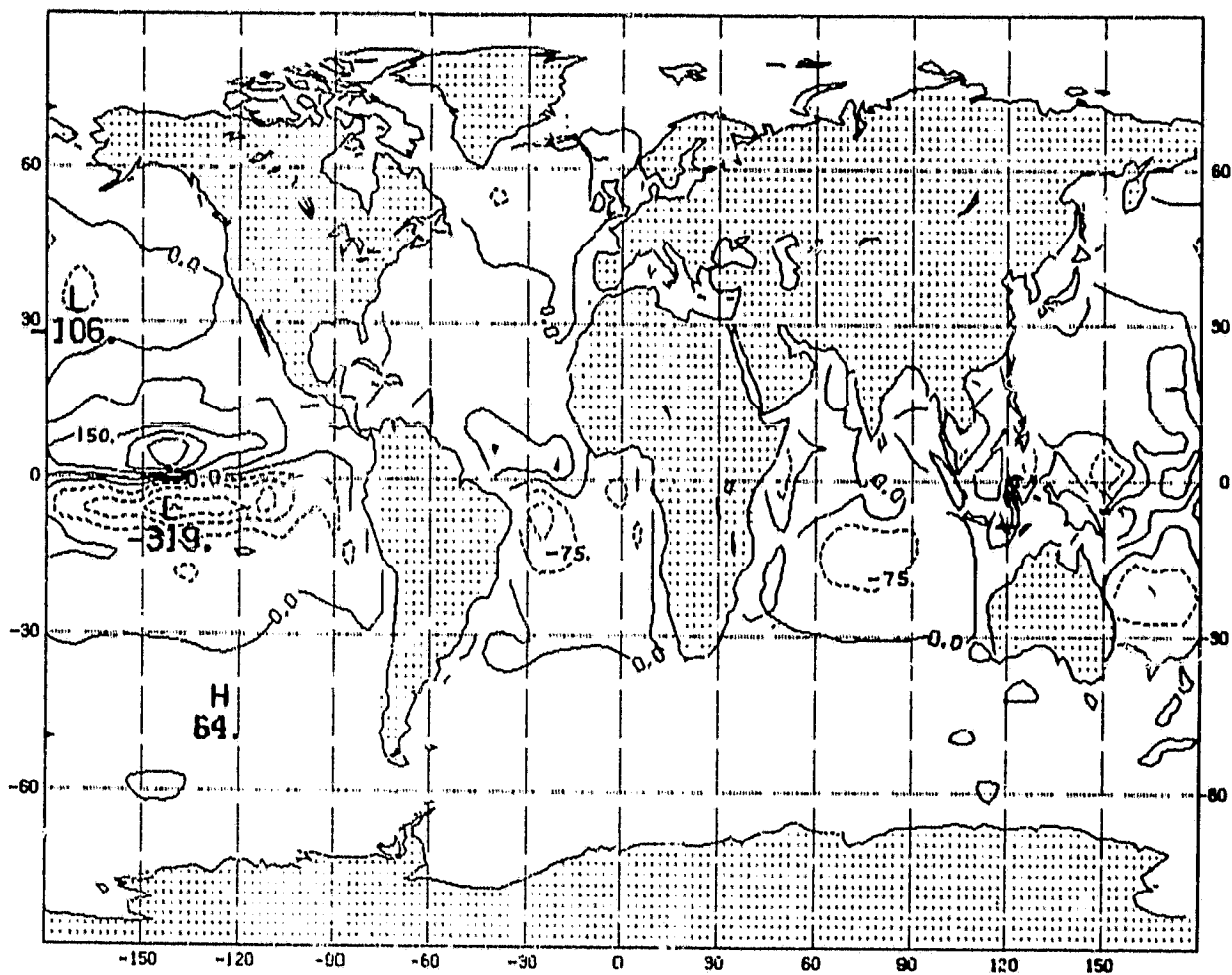
Because the time scale of response of the mixed layer temperature to the atmospheric wind forcing is a matter of hours, the instantaneous effects of the stronger wind stress will have a greater impact than in the time averaged case.

ORIGINAL PAGE IS
OF POOR QUALITY



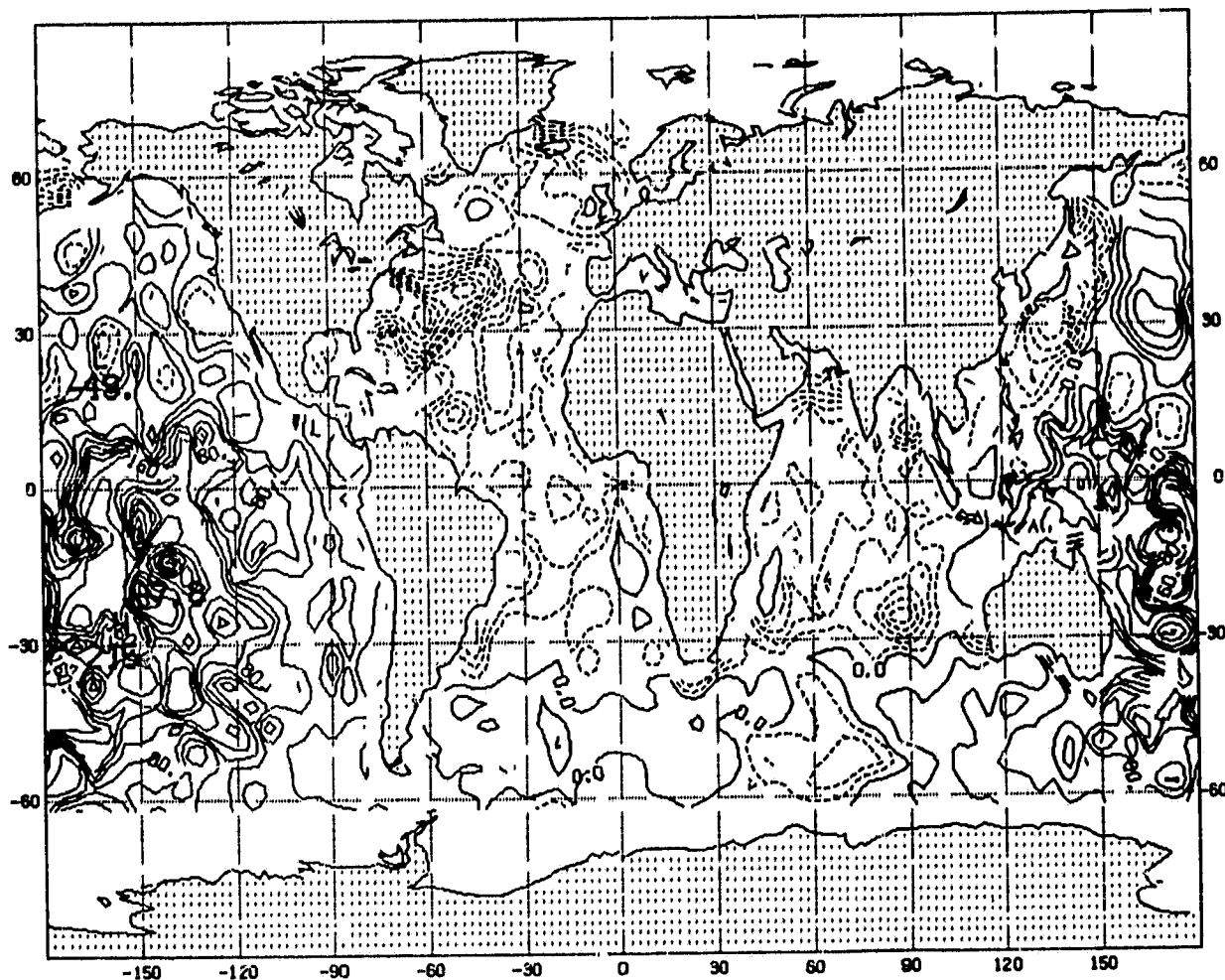
4.5.7 Weekly averaged value of the zonal velocity, u , after one week for the fifth case. Contour interval of 75 mm/s

ORIGINAL PAGE IS
OF POOR QUALITY



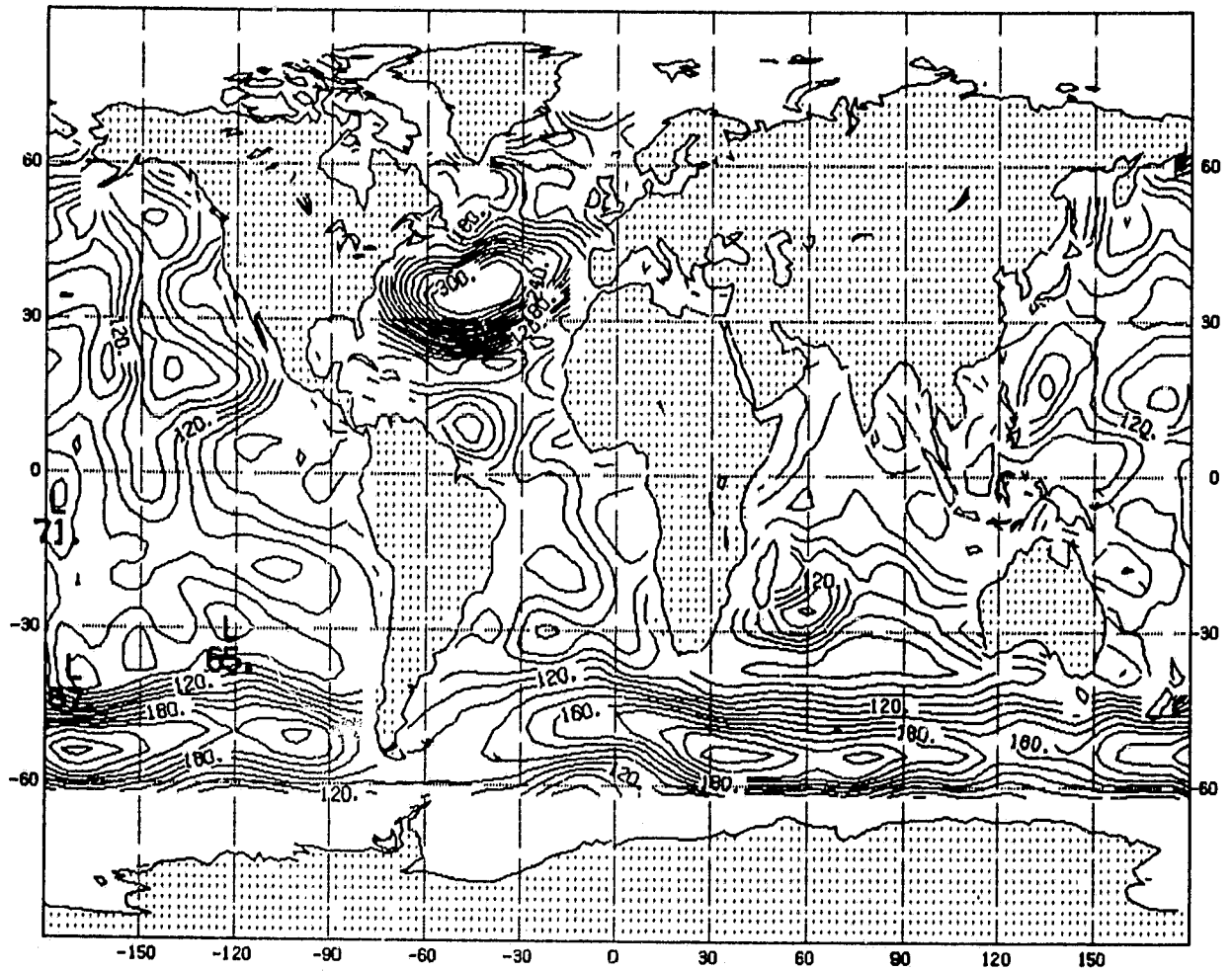
4.5.8 Weekly averaged value of the meridional velocity, v , after one week for the fifth case. Contour interval of 75 mm/s

ORIGINAL IMAGE IS
OF POOR QUALITY



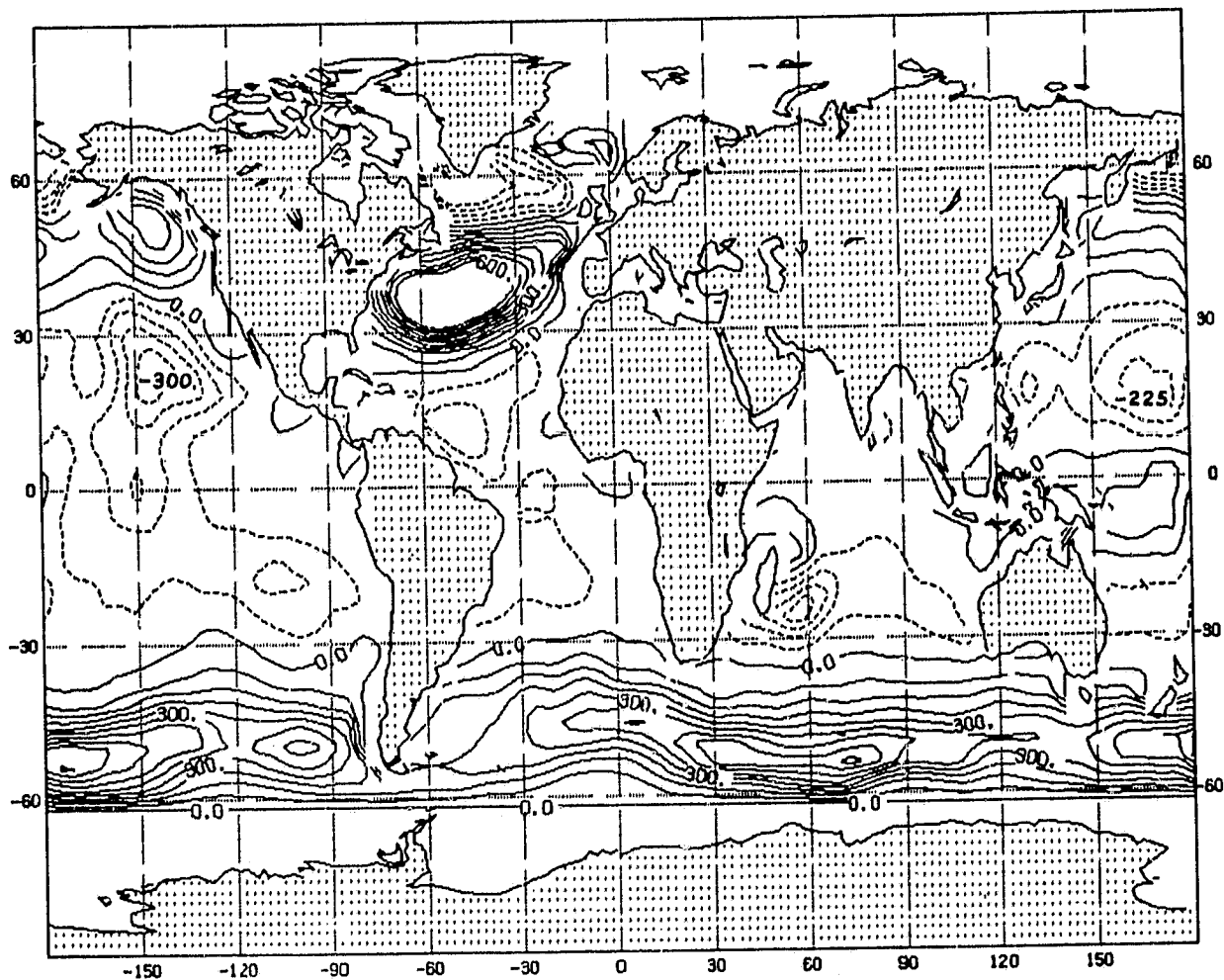
4.5.9 Weekly averaged value of surface heat balance for the fifth week
Contour interval of 20 Watts/m²

ORIGINAL PAGE IS
OF POOR QUALITY.



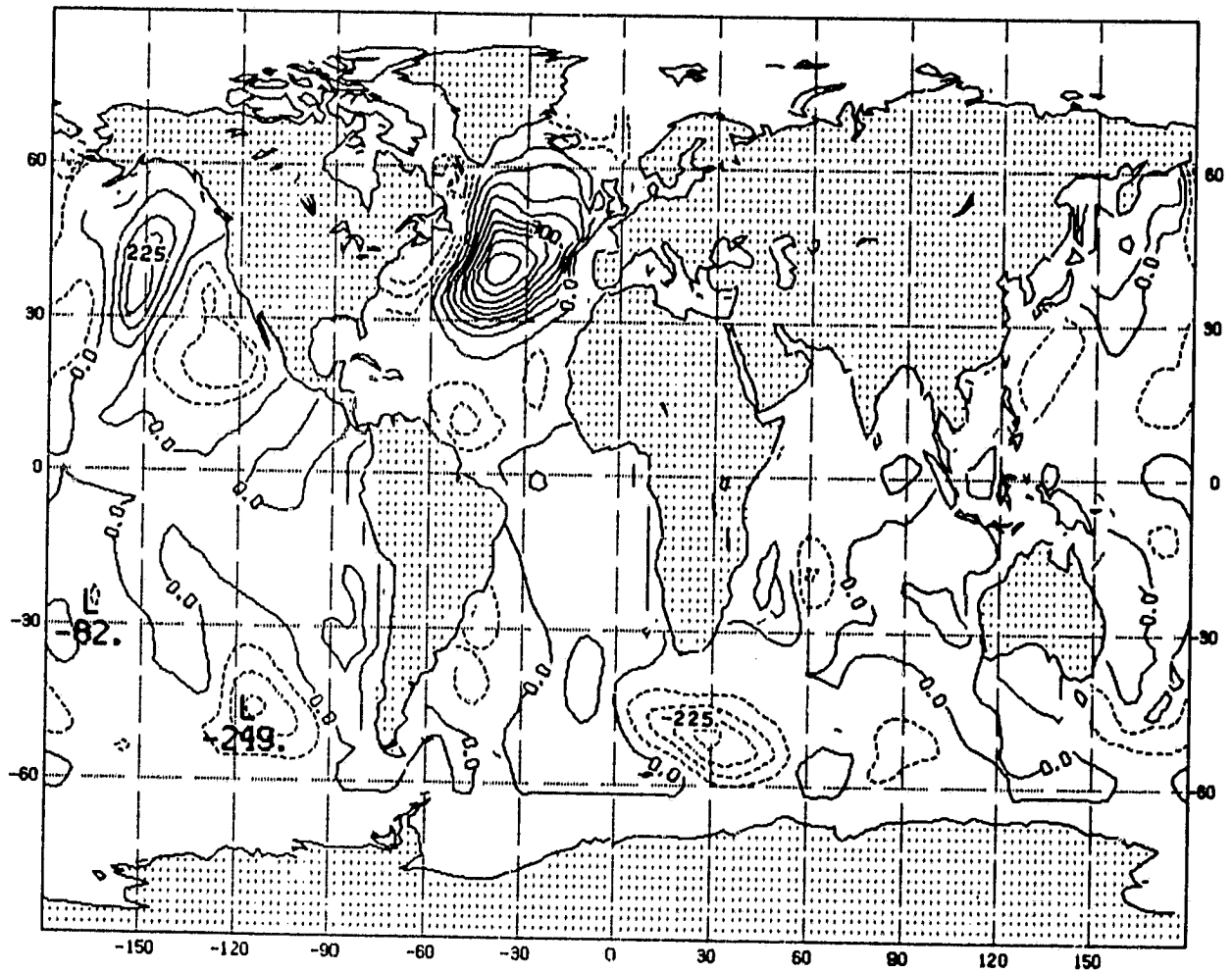
4.5.10 Weekly averaged value of friction velocity for the fifth week
Contour interval of $15 \cdot 10^{-1} \text{ mm/s}$

ORIGINAL PAGE IS
OF POOR QUALITY



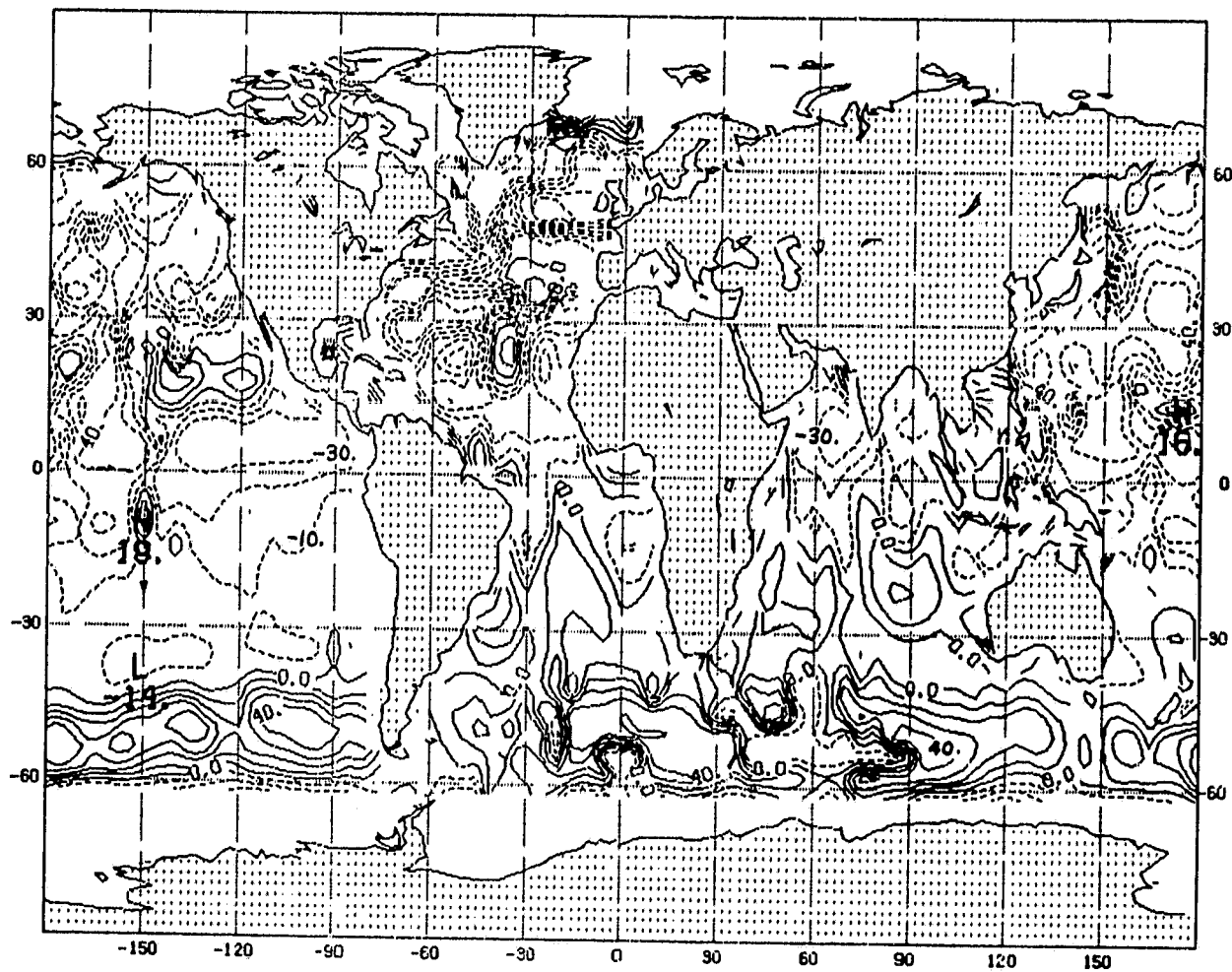
4.5.11 Weekly averaged value of the wind stress in the x direction for the fifth week. Contour interval of $75 \cdot 10^{-3} \text{N/m}^2$

ORIGINAL PAGE IS
OF POOR QUALITY



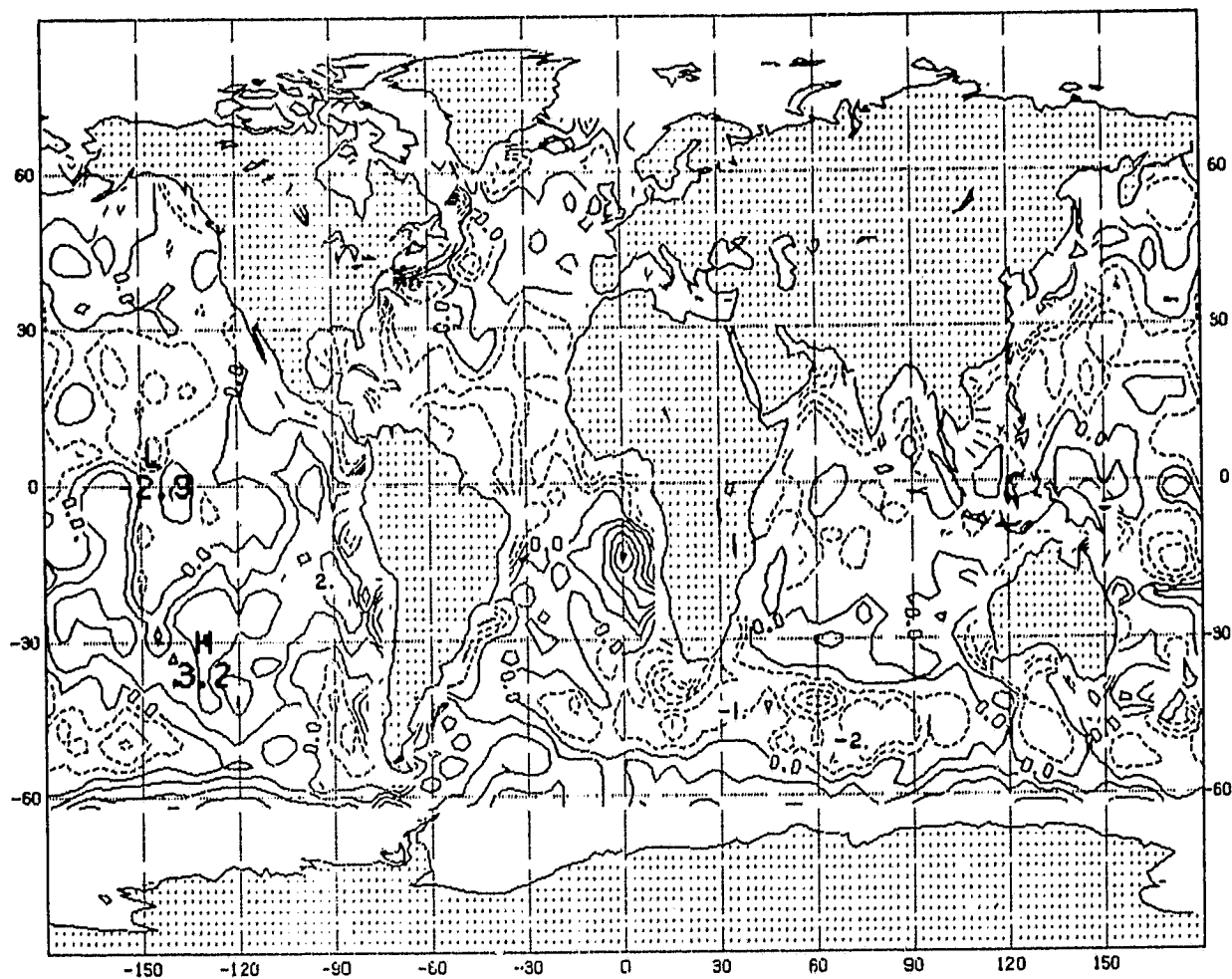
4.5.12 Weekly average value of the wind stress in the y direction for the fifth week. Contour interval of $75 \cdot 10^{-3} \text{N/m}^2$

ORIGINAL PAGE 13
OF POOR QUALITY



4.5.13 Weekly averaged ML height changes after five weeks for the fifth case. Contour interval of 10 m

ORIGINAL PAGE IS
OF POOR QUALITY



4.5.14 Weekly averaged ML temperature changes after five weeks for the fifth case. Contour interval 1° C

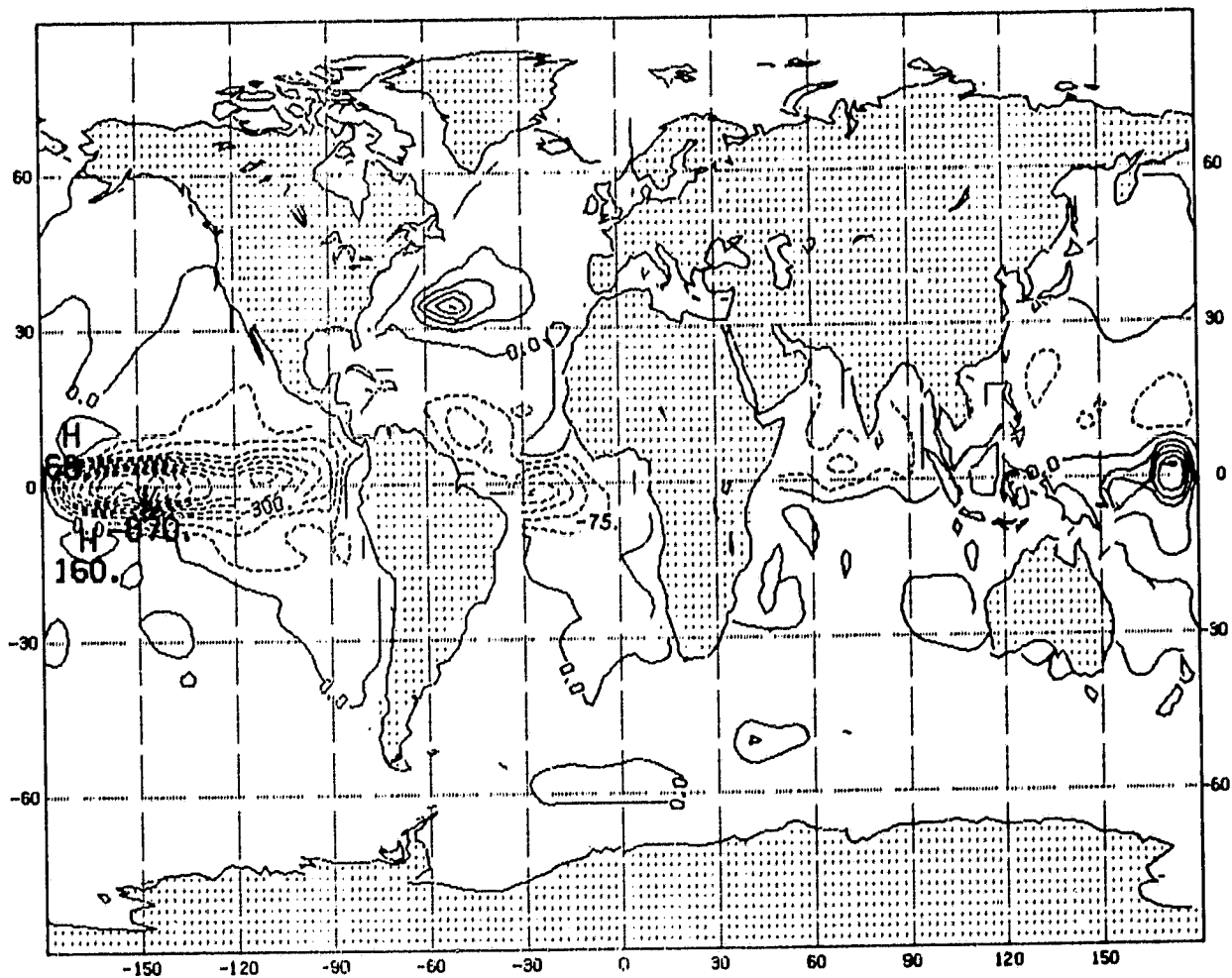
Then, after five weeks the temperature front observed in the Indian Ocean at 35°S is stronger than after one week. Simultaneously, the decrease in temperature observed after five weeks in the belt between 40°S and 60°S is even greater than after one week. East of Asia, the decrease in SST can be explained by the deficit of surface heating in that area.

We now compare the five week temperature changes predicted by the model (Fig. 4.5.14) with the actual observed changes from January to February 1979, (Fig. 3.13). First of all we should point out the model has less skill in predicting the changes than climatology (Fig. 3.14). Although there is some skill in predicting the sign of the change, their magnitudes are generally overpredicted. The model has correctly predicted cooling in the North Atlantic and North Pacific. The observed warming west of South America and South Africa are also predicted, but larger than observed. The cooling in the South Indian Ocean and in the Australian region is well predicted, but the model predicted cooling in the Arabian Sea and Bay of Bengal, whereas warming was observed. Similarly, the model overpredicted the cooling northeast of South America. A major failure occurred in the belt between 30°S to 60°S, where there was generally observed warming, with some small regions with cooling. Here the model predicted strong cooling, presumably through excessive deepening of the mixed layer by the roaring forties. Results after five weeks are depicted in Figs. 4.5.15 and 4.5.16.

It is interesting to note that, of all five experiments, the first two have the best agreement with the climatological changes (Fig. 4.1.6 and 4.2.6). The second one (in which surface friction and wind stress were zonally and time averaged and the surface heat flux was only time averaged) has the best skill in predicting the observed changes (cf Fig. 4.2.6 with Fig. 3.13).

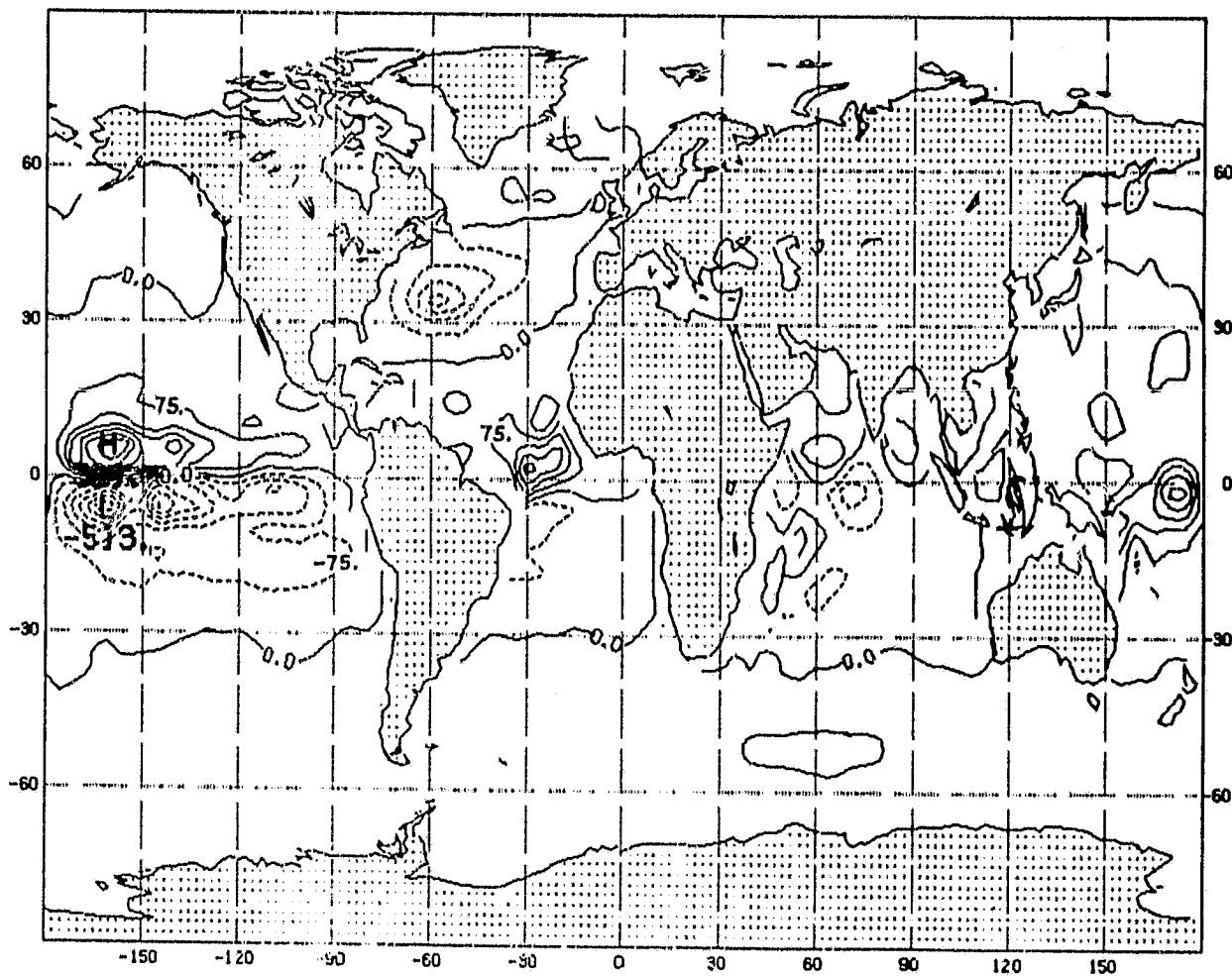
ORIGINAL PAGE IS
OF POOR QUALITY

ORIGINAL PAGE IS
OF POOR QUALITY



4.5.15 Weekly averaged value of the zonal velocity, u , after five weeks for the fifth case. Contour interval 75 mm/s

ORIGINAL PAGE IS
OF POOR QUALITY



4.5.16 Weekly averaged value of the meridional velocity, v , after five weeks for the fifth case. Contour interval 75 mm/s

5. Conclusions

We have performed a series of experiments with the Schopf and Cane (1983) upper ocean model driven by surface fluxes derived from the GLAS atmospheric analysis for January 1979, with SST's derived for January 1979 by Susskind et al. (1982), and starting from a state of rest.

The model results are generally qualitatively reasonable. Namely, that whenever we have strong winds a deepening of the oceanic boundary layer is observed, and viceversa. Conversely, the opposite is also true. Furthermore, the temperature changes respond to the surface heat budget. Whenever an upward heat flux is observed, the boundary layer model responds by a decrease of temperature and viceversa.

The model results show that most changes in the mixed layer height and horizontal velocity occur in the first days. On the other hand, changes in the temperature field take a longer time to develop. The best forecast was obtained in the experiment where the driving surface stress and friction velocity were zonally and time averaged, and the surface heat flux was time averaged. In the most realistic case (real initial conditions, instantaneous forcing fields from the atmospheric analysis), the resulting changes in temperature were larger than observed and the correlation between observed and predicted changes was poor.

The deficiency in the forecast of SST changes may be due to several factors: lack of sufficient ocean resolution, improper initialization, lack of feedback between the ocean and the atmosphere and the absence of transports by the strong boundary currents and perhaps unrealistic surface fluxes of heat and momentum. Unless these problems are alleviated it will not be reasonable to perform coupled atmospheric ocean forecasts.

Appendix: Computational implementation of the coupling

The initialization of the model is in the sub-routine CLIMIN. The sub-routine reads ocean data from a data file. The fields are as follows:

H1: Oceanic boundary layer depth;
H2: Subsurface layer depth;
T1: Mixed layer temperature
T2: Sublayer temperature
T200: Temperature at the base of the subsurface layer;
T300: Temperature at the pressure reference surface.

The atmospheric forcing is fed into the model in the subroutine FORCIN. These values are taken from a log 8 tape. The values are as follows:

TAU: Time in hours of data;
TS: Ground temperature;
U8, U9, V8, V9: Components of horizontal velocity at levels 8 and 9 in the GCM model;
Ev: Evaporative heat flux;
SH: Sensible heat flux;
SW: Solar radiation at ground level;
XW: Long-wave radiation at ground level;
WM: Wind magnitude;
ST: Total surface wind stress.

Also in this same subroutine the horizontal wind stresses are computed as TAUX and TAUY. The friction velocity and the surface heating budget are also computed as USTR and HEATNG, respectively.

The daily and weekly averages are computed in the main program. The average variables are preceded by the letters PR. For example, the averages of H1, H2, and T1 are PRU1, PRH2, and PRT1, respectively.

Figure Captions

Figures

- 3.1 Zonally averaged ML depth
 Contour interval of 5 m
- 3.2 Zonally averaged temperature
 Countour interval of 2°C
- 3.3 Zonally averaged surface heat balance
 Contour interval of 20 Watts/m²
- 3.4 Zonally averaged friction velocity
 Contour interval of 15 10⁻¹mm/s
- 3.5 Zonally averaged wind stress in the x direction
 Contour interval of 75 10⁻³N/m²
- 3.6 January 1979 average value of the surface heat balance
 Contour interval of 20 Watts/m²
- 3.7 Initial condition of ML depth (not zonally averaged)
 Contour interval of 5 m
- 3.8 Initial condition of ML temperature (not zonally averaged)
 (Susskind et al. 1982) Contour interval of 2° C
- 3.9 January 1979 average value of the friction velocity
 Contour interval of 15 10⁻¹mm/s
- 3.10 January 1979 average value of the wind stress in the x direction
 Contour interval of 75 10⁻³N/m²
- 3.11 January 1979 average value of the wind stress in the y direction
 Contour interval of 75 10⁻³N/m²
- 3.12 February 1979 average sea surface temperature (Susskind et al. 1982)
 Contour interval of 2° C
- 3.13 Observed sea surface temperature difference between February and
 January 1979 (Susskind et al. 1982) Contour interval of 0.5° C
- 3.14 Climatological sea surface temperature difference between February
 and January. Contour interval of 0.5° C.
- 4.1.1 Weekly averaged ML depth changes after one week for the first case.
 Contour interval of 10 m
- 4.1.2 Weekly averaged ML temperature changes after one week for the first
 case. Contour interval of 1° C
- 4.1.3 Weekly averaged value of the zonal velocity field, u, after one week
 for the first case. Contour interval of 75 mm/s

- 4.1.4 Weekly averaged value of the meridional velocity field, v , after one week for the first case. Contour interval of 75 mm/s
- 4.1.5 Weekly averaged ML depth changes after five weeks for the first case. Contour interval of 10 m
- 4.1.6 Weekly averaged the ML temperature changes after five weeks for the first case . Contour interval of 1° C
- 4.1.7 Weekly averaged value of the zonal velocity field, u , after five weeks for the first case. Contour interval of 75 mm/s
- 4.1.8 Weekly averaged value of the meridional velocity field, v , after five weeks for the first case. Contour interval of 75 mm/s
- 4.2.1 Weekly averaged ML depth changes after one week for the second case. Contour interval of 10 m
- 4.2.2 Weekly averaged ML temperature changes after one week for the second case. Contour interval of 1°C
- 4.2.3 Weekly averaged value of the zonal velocity field, u , after one week for the second case. Contour interval of 75 mm/s
- 4.2.4 Weekly averaged value of the meridional velocity field, v , after one week for the second case. Contour interval of 75 mm/s
- 4.2.5 Weekly averaged ML depth changes after five weeks for the second case. Contour interval of 10 m
- 4.2.6 Weekly averaged ML temperature changes after five weeks for the second case. Contour interval of 1°C
- 4.2.7 Weekly averaged value of the zonal velocity field, u , after five weeks for the second case. Contour interval of 75 mm/s
- 4.2.8 Weekly averaged value of the meridional velocity field, v , after five weeks for the second case. Contour interval of 75 mm/s
- 4.3.1 Weekly averaged ML depth changes after one week for the third case. Contour interval of 10 m
- 4.3.2 Weekly averaged ML temperature changes after one week for the third case. Contour interval of 1° C
- 4.3.3 Weekly averaged value of the zonal velocity field, u , after one week for the third case. Contour interval of 75 mm/s
- 4.3.4 Weekly averaged value of the meridional velocity field, v , after one week for the third case. Contour interval of 75 mm/s
- 4.3.5 Weekly averaged ML depth changes after five weeks for the third case. Contour interval of 10 m
- 4.3.6 Weekly averaged ML temperature changes after five weeks for third case. Contour interval of 1° C

- 4.3.7 Weekly averaged value of the zonal velocity field, u , after five weeks for the third case. Contour interval of 75 mm/s
- 4.3.8 Weekly averaged value of the meridional velocity field, v , after five weeks for the third case. Contour interval 75 mm/s
- 4.4.1 Weekly averaged ML depth changes after one week for the fourth case. Contour interval of 1.0 m
- 4.4.2 Weekly averaged ML temperature changes after one week for the fourth case. Contour interval of 1° C
- 4.4.3 Weekly averaged value of the zonal velocity field, u , after one week for the fourth case. Contour interval of 75 mm/s
- 4.4.4 Weekly averaged value of the meridional velocity field, v , after one week for the fourth case. Contour interval of 75 mm/s
- 4.4.5 Weekly averaged ML depth changes after five weeks for the fourth case. Contour interval of 10 m
- 4.4.6 Weekly averaged value ML temperature changes after five weeks for the fourth case. Contour interval of 1° C
- 4.4.7 Weekly averaged value of the zonal velocity field, u , after five weeks for the fourth case. Contour interval of 75 mm/s
- 4.4.8 Weekly averaged value for the meridional velocity field, v , after five weeks for the fourth case. Contour interval of 75 mm/s
- 4.5.1 Weekly averaged value of the surface heat balance after one week. Contour interval of 20 Watts/m²
- 4.5.2 Weekly averaged value of friction velocity after one week. Contour interval of $15 \cdot 10^{-1}$ mm/s
- 4.5.3 Weekly averaged value of the wind stress in the x direction after one week. Contour interval of $75 \cdot 10^{-3}$ N/m²
- 4.5.4 Weekly averaged value of the wind stress in the y direction after one week. Contour interval of $75 \cdot 10^{-3}$ N/m²
- 4.5.5 Weekly averaged ML height changes after one week for the fifth case. Contour interval of 10 m
- 4.5.6 Weekly averaged ML temperature changes after one week for the fifth case. Contour interval of 1° C
- 4.5.7 Weekly averaged value of the zonal velocity, u , after one week for the fifth case. Contour interval of 75 mm/s
- 4.5.8 Weekly averaged value of the meridional velocity, v , after one week for the fifth case. Contour interval of 75 mm/s

- 4.5.9 Weekly averaged value of surface heat balance for the fifth week
Contour interval of 20 Watts/m²
- 4.5.10 Weekly averaged value of friction velocity for the fifth week
Contour interval of 15 10⁻¹mm/s
- 4.5.11 Weekly averaged value of the wind stress in the x direction for the fifth week. Contour interval of 75 10⁻³N/m²
- 4.5.12 Weekly average value of the wind stress in the y direction for the fifth week. Contour interval of 75 10⁻³N/m²
- 4.5.13 Weekly averaged ML height changes after five weeks for the fifth case. Contour interval of 10 m
- 4.5.14 Weekly averaged ML temperature changes after five weeks for the fifth case. Contour interval 1° C
- 4.5.15 Weekly averaged value of the zonal velocity, u, after five weeks for the fifth case. Contour interval 75 mm/s
- 4.5.16 Weekly averaged value of the meridional velocity, v, after five weeks for the fifth case. Contour interval 75 mm/s

REFERENCES

- Baker, W. E., 1983: Objective analysis and assimilation of observational data from FGGE. Mon. Wea. Rev., 111, 328-342.
- Elsberry R. L. And N. T. Camp, 1978: Oceanic thermal response to strong atmospheric forcing. Part I. Characteristics of forcing events J. Phys. Oceanogr., 8, 206-214.
- Elsberry R. L. and S. D. Raney, 1978: Sea surface temperature response to variations in atmospheric wind forcing. J. Phys. Oceanogr., 8, 881-887.
- Halem, M., E. Kalnay, W. E. Baker, and R. Atlas, 1982: An assessment of the FGGE satellite observing system during SOP-1. Bull. Amer. Meteor. Soc. 63, 407-426.
- Kalnay-Rivas, E. and D. Hoitsma, 1979: The effect of accuracy, conservation, and filtering on numerical weather forecasting. Fourth Conference on Numerical Weather Prediction, Silver Springs, MD AMS Boston 302-312
- _____, A. Bayliss, and J. Storch, 1977: The 4th order GISS model of the global atmosphere. Beitr. Phys. Atmos., 50, 299-311.
- Kasahara, A., 1972: Simulation experiments for meteorological observing systems for GARP. Bull. Am. Meteorol. Soc., 53, 252-264.
- Kim, J. W. 1976: A generalized bulk model of the oceanic mixed layer, J. Phys. Oceanography, 6, 686-695.
- Leovy, C. B., 1981: Review of remote sensing of atmospheres and oceans A. Deepak (ed.), EOS, 62 (44), 732-733.
- Müller, P. P. and E. B. Kraus, 1977: One dimensional models of the upper ocean. Modelling and Prediction of the Upper Layers of the Ocean. E. B. Krauss, Ed. Pergamon Press. 143-172.
- O'Brien, J. J. 1981: The Future for satellite-derived surface winds, Oceanus, 24 (3), 27-31.
- Schopf, P. S. and M. A. Cane, 1983: On Equatorial Dynamics, Mixed Layer Physics and Sea Surface Temperature, Journal of Physical Oceanography. Submitted for publication.
- Sommerville, R. C., P. H. Stone, M. Halem, J. E. Hansen, J. S. Hogan, L. M. Druryan, G. Russell, A. A. Lacis, W. J. Quirk and J. Tenenbaum, 1974: The GISS model of the global atmosphere. J. Atmo. Sci. 31, 84-117.
- Susskind, J., J. Rosenfield, D. Reuter and M. T. Chahine, 1982: The GLAS Physical Inversion Method for Analysis of HIRS2/MSU Sounding Data. NASA Tech. Memo. 84936, Goddard Space Flight Center, Greenbelt, Md. 101pgs.